CHAPTER ONE

INTRODUCTION

1.1 Background of the Study

Heat is a form of energy and geothermal energy is, literally, the heat contained within the earth that generates geological phenomena on a planetary scale as plate tectonics, tectonic and volcanic activity in the earth crust (Dickson and Fanelli, 2004). 'Geothermal energy' is often used nowadays, however, to indicate that part of the earth's heat that can, or could, be recovered and exploited by man. The word "geothermal" comes from two Greek words geo (earth) and theme (heat). It originates from the formation of the earth (molten magma) and from the decay of long lived isotopes of Uranium, Thorium and Potassium found within the Precambrian basement rocks (Downing and Gray, 1986).

Understanding geothermal energy begins with an understanding of the source of this energy which is the earth's internal heat. The earth's temperature increases with depth, with the temperature at the centre reaching more than 4,200 ^{0}C (REPP Mission, 2010). A portion of this heat is a relic of the planet's formation about 4.5 billion years ago, and a portion is generated by the continuing decay of radioactive isotopes (REPP Mission, 2010). Heat energy naturally moves from hotter to cooler regions, so earth's heat flows from its interior toward the surface. Geothermal energy is generated in the earth's core, about 6,000 km below the surface. Temperatures hotter than the sun's surface are continuously produced inside the earth by slow decay of radioactive particles, a process that happens in all rocks. The earth has a number of different layers:

  i.   The core itself has two layers: a solid iron core and an outer core made up of very hot melted rock, called magma.

  ii.   The mantle which surrounds the core and is about 3,000 km thick. It is made up of magma and rock.

iii. The crust which is the outermost layer of the earth, the land that forms the continents and ocean floors. It may be 3 km to 8 km thick under the oceans and 24 km to 58 km thick on the continents (Blodgett, 2014).

The earth's crust is broken into pieces called plates. Magma comes close to the earth's surface near the edges of these plates. This is where the volcanoes occur. The lava that erupts from volcanoes is partly magma. Deep underground, the rocks and water absorb the heat from this magma. The temperature of the rocks and water get hotter and hotter as you go deeper underground (Ochieng, 2013). Although the earth's stored heat is theoretically finite, its large amount (12.6×10^{24}MJ) makes geothermal energy practically a renewable energy that can theoretically sustain the energy needs of mankind many times. Geothermal energy involves the science that deals with the theoretical study of the thermal regime of the earth as well as the engineering aspects to use the earth's heating/cooling and electric power generations.

Geothermal energy has become a viable alternative and sustainable source of energy in many countries. The energy is commonly manifested on the terrestrial surface in the form of volcanoes and fumaroles (holes where volcanic gases are released), hot springs, geysers, steaming grounds and altered grounds (Ochieng, 2013). The economically usable geothermal energy is that which occur close to the earth's surface where it can be tapped by drilling wells up to 3,000m below the earth's surface. Such shallow heat sources are in most cases attributed to volcanic activity which are commonly associated with plate boundaries, and other geodynamic environments (Ochieng, 2013). The essential components of a geothermal system include: heat source, permeable reservoir, cap rock and recharge regime. Multiple geoscientific disciplines such as geology, geophysics and geochemistry are commonly employed in the geothermal exploration in order to define the components mentioned earlier.

Some applications of geothermal energy use the earth's temperatures near the surface, while others require drilling some kilometres into the earth. The three main uses of geothermal energy are:

i.   Direct use and District Heating System - which use hot water from springs or reservoir near the surface.

ii. Electricity generation - in a power plant requires water or steam at a very high temperature (300^0F-700^0F). Geothermal power plants are generally built close to geothermal reservoirs.

iii. Geothermal heat pumps - use stable ground or water temperatures near the earth's surface to control building temperatures above ground.

The direct use of hot water as an energy source has been happening since ancient times. The Romans, Chinese, American and Africans used hot mineral springs for bathing, cooking and heating. Today, many hot springs are still used for bathing, and many people believe that the hot, mineral rich waters have natural healing powers (Dickson and Fanelli, 2004). There is great need for renewable energy sources in Nigeria, such as the geothermal energy, since other energy sources like petroleum and gas are fast depleting. Hence there is pressing need for renewable energy in the country. This informs the decision to investigate the geothermal energy potentials in Nigeria.

In the present study, we shall investigate the geothermal energy potentials of parts of the Middle Benue Trough using aeromagnetic and aeroradiometric data. The study area (the Middle Benue Trough) was chosen because of the evidence of hot springs in the study area. From several researches, it is found that one of the hottest springs (53.5^0C) in the area is located near Akiri, and another famous Nigerian warm spring is Wikki warm spring (32^0C), this flows from Gombe Sandstone in Yankari Game Reserve (Ikechukwu *et al.*, 2015; Abraham *et al.,* 2015; Abraham and Nkitnam, 2017). Another hot one is located in the

Northern part of Benue Trough, near the study area, within a huge tectonic structure–Lamurde anticline, near Numan and is called Ruwan Zafi (Garba *et al.*, 2012; Sedara and Joshua, 2013; Abraham, 2013; Ikechukwu *et al.,* 2015). The water of the spring is heated by geothermal gradient on its way from unknown depths, in unconfined sandstone aquifer.

1.2 Statement of the Problem

Nigeria being one of the biggest producers of oil and gas in the World, hydrocarbons are the major source for general energy production. The general problem within Nigerian energy sector is that the demand exceeds the energy generated. With a fast growing population, Nigeria needs an alternative renewable energy source since the oil and gas reserves are fast depleting. Geothermal energy is preferred because it is an abundant, cost effective, secure, unpolluted and clean source of energy. One of biggest advantages of geothermal energy is that it is constantly available. Geothermal investigations have not received enough attention across Nigeria as very few works have been documented; this was noted in the concluding statement of Nwankwo *et al*., (2011), where they acknowledged the fact that there is a missing gap in crustal temperature information of the central Nigeria. At present, there are no installed geothermal plants in Nigeria. Geothermal investigations in the study area are scarce; hence there are little or no records of crustal temperature studies. Curie temperature depth in conjunction with heat flow assessment would significantly compliment the geothermal information of the area to bridge the gap of lacking crustal temperature records. Hence, this study involves the interpretation of aeromagnetic and aeroradiometric data so as to determine the geothermal heat flow and radiometric heat production of the study area; and establish likely areas of geothermal energy potential in the study area. This will eventually improve the energy needs of Nigeria.

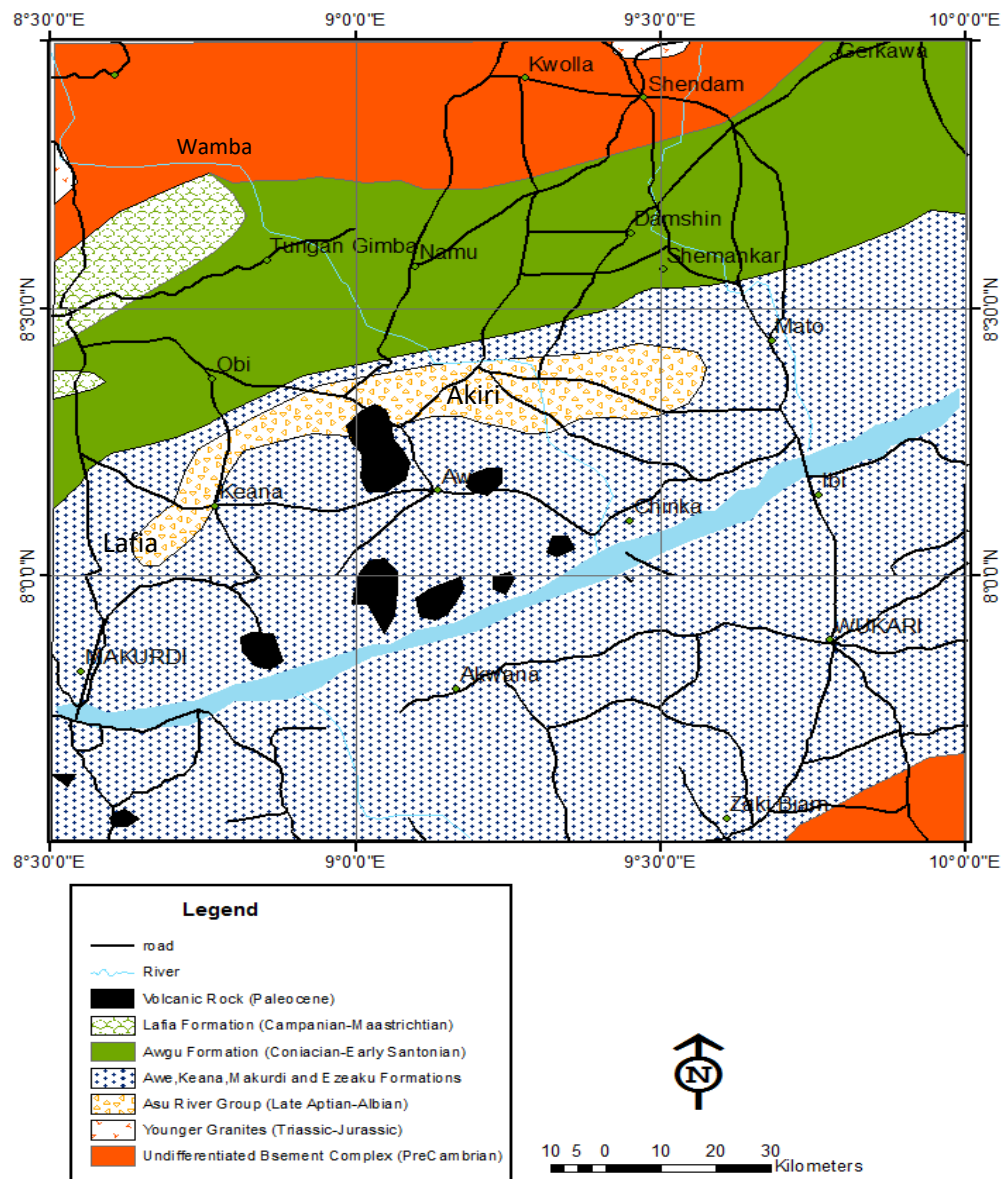## 1.3 Location of the Study Area

Figure 1.1: Location and Geological Map of the Study Area (Offodile, 1976; NGSA, 2009; Anudu *et al*., 2014)

Figure 1.1 shows the location and geological map of the study area (Offodile, 1976; NGSA, 2009; Anudu et al., 2014). The study area is located in the middle part of the Benue Trough of Nigeria. It is situated between latitudes 7^030^I N and 9^000^I N; and longitudes 8^030^I E and

$10^{0}00^{l}$ E (Figure 1.1). It is flanked by the Precambrian crystalline basement rocks. The area of coverage for the study area includes Plateau, Nassarawa, Benue and Taraba states. Various geological studies conducted across the area have reported the local occurrence of intra-sedimentary volcanic rocks and associated geological structures [especially folds, joints and veins] (Offodile, 1976, 1989; Ajayi and Ajakaiye, 1981).

1.4 Aim and Objectives of the Study

The aim of the study is to investigate geothermal energy potential of parts of the Middle Benue Trough, Nigeria using aeromagnetic and aeroradiometric data.

The specific objectives of the study include to:

a) determine the Curie Point Depths (CPDs) and succeeding geothermal parameters which include depth to top, depth to centroid and depth to bottom of magnetic sources; geothermal gradient and geothermal heat flow.

b) determine the Lineament trends in the study area and model the magnetic anomalies and geologic structures.

c) establish relationships between Curie Point Depths and geothermal heat flow; geothermal gradients and geothermal heat flow; radiometric heat and geothermal heat flow in the study area.

d) produce radiometric heat map and identify areas of high and low radiometric concentrations in the study area.

e) compare the radiometric heat and the geothermal heat flow (calculated from Spectral method) in the study area.

f) delineate areas with geothermal energy potential

1.5 Scope of the Study

The study is limited to two methods; the use of spectral analysis to interpret aeromagnetic data and the analysis of radiometric data, to investigate the geothermal

energy potential over part of the Middle Benue Trough, Nigeria. The work involves the determination of Curie Point Depths and succeeding geothermal parameters in the study area. The geothermal parameters estimated were depths to top, centroid and bottom of magnetic sources; geothermal gradient and geothermal heat flow. Areas with high geothermal potential were delineated through the magnetic and radiometric analyses.

1.6 Significance of the Study

The expected benefits of the study are as follows:

- The study will aid in identifying the geothermal energy potentials in the study area which are manifested in hot springs at the surface. This will be of help to companies who wish to explore for geothermal energy sources.

- The findings of the study will be useful in determining the possibility to explore for new geothermal resources potentials in Nigeria, since there is pressing need for renewable energy in the country. This will be of benefit to Nigerians (the geosciences community, government and indigenes) as the exploitation of possible geothermal resource areas in the country could be a vital alternative to an industrializing nation like Nigeria.

- The depth to the basement provides the knowledge of the sedimentary thickness in the basin, this in turn is a key indicator in determining whether the deeper parts of the study area have been buried to sufficient depth to reach Hydrocarbon maturation window.

- The study will be used to identify and delineate areas of high radioactive heat in the study area and compare with areas of high geothermal heat.

- This research will be a great guide to researchers in the area of geothermal energy and thermal structures investigation.

- Finally, the study will impact positively on International and Local investors in geothermal energy, researchers and geoscience organisations.

CHAPTER TWO

LITERATURE REVIEW

2.1 Brief Geothermal History

The presence of volcanoes, hot springs, and other thermal phenomena must have led our ancestors to surmise that parts of the interior of the earth were hot. However, it was not until a period between the sixteenth and seventeenth century, when the first mines were excavated to a few hundred metres below ground level that man deduced, from simple physical sensations that the earth's temperature increased with depth. The first measurements by thermometer were probably performed in 1740 by De Gensanne, in a mine near Belfort, in France (Bullard, 1965). By 1870, modern scientific methods were being used to study the thermal regime of the earth (Bullard, 1965), but it was not until the twentieth century, and the discovery of the role played by radiogenic heat, that we could fully comprehend such phenomena as heat balance and the earth's thermal history. All modern thermal models of the Earth, in fact, must take into account the heat continually generated by the decay of the long-lived radioactive isotopes of uranium (U^{238}, U^{235}), thorium (Th^{232}) and potassium (K^{40}), which are present in the earth (Lubimova, 1968). Added to radiogenic heat, in uncertain proportions, are other potential sources of heat such as the primordial energy of planetary accretion. Realistic theories on these models were not available until the 1980s, when it was demonstrated that there was no equilibrium between the radiogenic heat generated in the earth's interior and the heat dissipated into space from the earth, and that our planet is slowly cooling down. To give some idea of the phenomenon involved and its scale, we will cite a heat balance from Stacey and Loper (1988), in which the total flow of heat from the earth is estimated at 42 x 10^{12} W (conduction, convection and radiation). Of this figure, 8 x 10^{12} W come from the crust, which represents only 2% of the total volume of the earth but is rich in radioactive isotopes, 32.3 x 10^{12} W come from the mantle, which represents 82% of the total

volume of the earth, and 1.7 x 10^{12} W come from the core, which accounts for 16% of the total volume and contains no radioactive isotopes. Since the radiogenic heat of the mantle is estimated at 22 x 10^{12} W, the cooling rate of this part of the Earth is 10.3 x 10^{12} W (Armstead, 1983).

In more recent estimates, based on a greater number of data, the total flow of heat from the earth is about 6 % higher than the figure utilized by Stacey and Loper in 1988. Even so, the cooling process is still very slow. The temperature of the mantle has decreased no more than 300 to 350 °C in three billion years, remaining at about 4000 °C at its base. It has been estimated that the total heat content of the earth, reckoned above an assumed average surface temperature of 15 °C, is of the order of 12.6 x 10^{24} MJ, and that of the crust is of the order of 5.4 x 10^{21} MJ (Armstead, 1983).

The thermal energy of the earth is therefore immense, but only a fraction could be utilized by mankind. So far our utilization of this energy has been limited to areas in which geological conditions permit a carrier (water in the liquid phase or steam) to 'transfer' the heat from deep hot zones to or near the surface, thus giving rise to geothermal resources; innovative techniques in the near future, however, may offer new perspectives in this sector. In many areas of life, practical applications precede scientific research and technological developments, and the geothermal sector is a good example of this. In the early part of the nineteenth century the geothermal fluids were already being exploited for their energy content. A chemical industry was set up in that period in Italy (in the zone now known as Larderello); to extract boric acid from the boric hot waters emerging naturally or from specially drilled shallow boreholes. The boric acid was obtained by evaporating the boric waters in iron boilers, using the wood from nearby forests as fuel. In 1827 Francesco Larderel, founder of this industry, developed a system for utilising the heat of the boric fluids in the evaporation process, rather than burning wood from the rapidly depleting forests. The

"covered lagoon" was used in the first half of the 19th century in the Larderello area, Italy, to collect the hot boric waters and extract the boric acid (Armstead, 1983).

Exploitation of the natural steam for its mechanical energy began at much the same time. The geothermal steam was used to raise liquids in primitive gas lifts and later in reciprocating and centrifugal pumps and winches, all of which were used in drilling or the local boric acid industry. Between 1850 and 1875 the factory at Larderello held the monopoly in Europe for boric acid production. Between 1910 and 1940 the low - pressure steam in this part of Tuscany was brought into use to heat the industrial and residential buildings and greenhouses. Other countries also began developing their geothermal resources on an industrial scale. In 1892 the first geothermal district heating system began operations in Boise, Idaho (USA). In 1928 Iceland, another pioneer in the utilization of geothermal energy also began exploiting its geothermal fluids (mainly hot waters) for domestic heating purposes (Stacey and Loper, 1988).

By 1904 the first attempt was being made at generating electricity from geothermal steam; it took take place at Larderello. The engine used at Larderello in 1904 in the first experiment in generating electric energy from geothermal steam, along with its inventor, Prince Piero Ginori Conti. The success of this experiment was a clear indication of the industrial value of geothermal energy and marked the beginning of a form of exploitation that was to develop significantly from then on. Electricity generation at Larderello was a commercial success. By 1942 the installed geothermoelectric capacity had reached 127, 650 kWe. Several countries were soon to follow the example set by Italy. In 1919 the first geothermal wells in Japan were drilled at Beppu, followed in 1921 by wells drilled at The Geysers, California, USA. In 1958 a small geothermal power plant began operating in New Zealand, in 1959 another began in Mexico, in 1960 in the USA, followed by many other countries in the years to come (Stacey and Loper, 1988).

After the Second World War many countries were attracted by geothermal energy, considering it to be economically competitive with other forms of energy. It did not have to be imported, and in some cases, it was the only energy source available locally. The installed geothermal electric capacity in 1995 and 2000 were given as 6,833 MWe and 7,972 MWe respectively; and the increase between 1995 and the year 2000 was 16% (Huttrer, 2001). The total installed capacity at the end of 2003 was 8,402 MWe. The geothermal power installed in the developing countries in 1995 and 2000 represents 38 and 47% of the world total, respectively. The utilization of geothermal energy in developing countries has exhibited an interesting trend over the years. In the five years between 1975 and 1979 the geothermal electric capacity installed in these countries increased from 75 to 462 MWe; by the end of the next five-year period (1984) this figure had reached 1,495 MWe, showing a rate of increase during these two periods of 500% and 223%, respectively (Dickson and Fanelli, 1988). In the next sixteen years, from 1984 to 2000, there was a further increase of almost 150%. Geothermal power plays a fairly significant role in the energy balance of some areas; for example, in 2001 the electric energy produced from geothermal resources represented 27% of the total electricity generated in the Philippines, 12.4% in Kenya, 11.4% in Costa Rica, and 4.3% in El Salvador (Huttrer, 2001).

As regards non-electric applications of geothermal energy, the installed capacity and energy use world-wide for the year 2000 were given as 15,145 MWe and (190,699 TJ/yr) respectively (Huttrer, 2001). During that year 58 countries reported direct uses, compared to 28 in 1995 and 24 in 1985. The number of countries with direct uses has very likely increased since then, as well as the total installed capacity and energy use. The most common non-electric use world-wide (in terms of installed capacity) is heat pumps (34.80%), followed by bathing (26.20%), space-heating (21.62%), greenhouses (8.22%), aquaculture (3.93%), and industrial processes (3.13%) (Lund and Freeston, 2001).

2.2 Geothermal Energy Potential of Nigeria

Nigeria's challenging energy needs is overwhelming, with demand exceeding generation. There is inequitable access by the populace to the meagre and unstable electricity services in the country. With the main power generating source being gas-fired thermal power stations and despite her increasing population of over 170 million, Nigeria energy generation capacity dwindle to as low as 2,800 MW in the year 2016 (Akinsoji, 2016). Alternative energy sources (preferably renewable sources) would provide some relief to the current energy challenge.

Energy plays the most vital role in economic growth, progress and development, poverty eradication and security of any country (Abraham and Nkitnam, 2017). Uninterrupted energy supply is a vital issue for all countries today and future economic growth depends crucially on the long – term availability of energy from sources that are affordable, accessible and environmentally friendly. A lack of access to energy can contribute to economic decline. Availability of energy sources would give rise to good productivity, income growth, education and health (Bhattacharyya and Leu, 1975). In the African continent, Nigeria has one of the lowest consumption rates of electricity per capita (Abraham and Nkitnam, 2017).

In 2015, Nigeria produced about 4,000 Megawatts (MW) for her population of over 170 million; with a similar population, Brazil generates 24 times as much. These challenges emphasize the need to explore all available energy resources (especially renewable energy sources) to chart a new energy future for Nigeria. Geothermal energy is important in the long–term vision of providing secure, abundant, cost effective and clean sources of energy for Nigeria. Electricity consumption from residential and commercial sectors in Nigeria represents 80% of total electricity demand. As a result of high economic growth and demographic pressure in 2008, the Energy Commission of Nigeria (ECN) in conjunction with the International Atomic Energy Agency (IAEA) projected a demand of 15,730 MW for 2010 and 119,200 MW for 2030 under the reference scenario (7% yearly economic growth)

(Abraham and Nkitnam, 2017). However, recent evaluation indicates that Nigeria has generation capability of 5,700 MW; 86% of the capability comes from gas-fired thermal power stations. The remaining 14% is from the three large hydroelectric power stations in the country (Akinsoji, 2016). At present, there are no installed geothermal plants in Nigeria. However, the Renewable Energy Master Plan (REMP) in its second draft of November 2012 as prepared by the Energy Commission of Nigeria (ECN) planned to increase the supply of renewable electricity from 13% of total electricity in 2015 to 23% in 2025 and 36% by 2030. Renewable electricity would then account for 10% of Nigerian total energy consumption 2025 (ECN, 2012).

Expressions of subsurface heat as manifested in the springs and lava flow have been documented largely in the Benue Trough and the Precambrian basement. Benue Trough houses 8 out of the 10 well known warm springs in Nigeria. These springs are populated in the northern and central portions of the trough. The warm springs in Nigeria includes Ikogosi warm spring, Kerang spring, Ngeji warm spring, Nike Lake and Wikki warm spring. Other warm or thermal springs are Keana–Awe thermal spring, Akiri warm spring, Lamurde Hot Spring, also known as Ruwan Zafi Hot Spring, and the Rafin Rewa Warm Spring. In the study area, the warm springs that serve as indicators for geothermal energy potential are Akiri warm spring, found at the centre of the study area; Wikki warm spring and Ruwan Zafi found in the northern part of Benue Trough, near the study area (Ajibade and Fitches, 1988; ECN, 2012).

2.3 Regional Geology and Tectonic Setting

The Benue Trough of Nigeria (Figure 2.1) is an intra-continental basin in Central West Africa that extends NE to SW. It is over 1000 km in length and exceeds 150 km in width. Its southern outcrop limit is the northern boundary of the Niger Delta Basin, while the northern out-cropping limit is the southern boundary of the Chad Basin separated from the Benue

Trough by an anticlinal structure termed the "Dumbulwa-Bage High" (Osazuwa et al., 1981; Zaborski et al., 1997). The Benue Trough is filled with up to 6000 m of Cretaceous sediments associated with some volcanics. The Benue Trough is a major geological Formation underlying a large part of Nigeria and extending about 1,000 km northeast from the Bight of Benin to Lake Chad. It is part of a mega-rift system termed the West and Central Africa Rift System (WCARS) (Figure 2.1). The WCARS includes the Termit Basin of Niger and western Chad, the Bongor, Doba and Doseo Basins of southern Chad, the Salamat Basin of Central African Republic and the Muglad Basin of Sudan.

The Benue Trough is geographically subdivided into southern, central and northern parts (Figure 2.1). The origin and tectonic history of the Benue Trough and the entire WCARS is associated with the separation of Africa and South America (break-up of Gondwanaland) during the early Cretaceous time (Burke and Whiteman, 1973; Benkhelil, 1989). This break-up was followed by the drifting apart of these continents, the opening of the South Atlantic and the growth of the Mid- Atlantic ridge (Burke and Whiteman, 1973; Benkhelil, 1989). The mechanism responsible for the origin and evolution of the Benue Trough is controversial. However, there are basically two models: the rift system models and the pull-apart model. Several mechanisms have been proposed based on the rift system. The trough is considered to be a third arm of a triple junction beneath the present Niger Delta. The earliest model was given by King (1950) and subsequently supported by Cratchley, et al., (1984) who proposed tensional movements resulting in a rift as the controlling factor. They interpreted an observed axial zone of positive gravity anomalies flanked by linear negative anomalies on both sides as an arrangement typical of rift valleys in general, and resulted from crustal thinning and elevation of crust-mantle boundary beneath the central parts of the rift. The weakness of this model is the lack of conspicuous rift faults at the margins of the trough (Ajibade and Fitches, 1988) and a generalized folding of the Cretaceous sediments. Except in the Abakaliki area,

Cretaceous magmatic activity associated with rift structures is very scarce; it is only found close to, or along major faults. Cratchley and Jones (1965), however, argued that the main boundary rift faults are now concealed by the Cretaceous sediments overlying the margins of the Trough.

Burke *et al*., (1972), suggested the existence below the Niger Delta and the Southern Benue Trough of a triple junction of the RRR type which indicates the existence of a spreading ridge active from Albian to Santonian. An unstable RRF triple junction model leading to plate dilation and the opening of the Gulf of Guinea was proposed by Burke and Whiteman, 1973. Olade (1975) and Wright (1981), considered the Benue Trough as the third failed arm of a three-armed rift system related to the development of hot spots. Most recent models based on pull-apart system revealed that wrenching was a dominant tectonic process during the Benue Trough evolution. Benkhelil, 1989, defined the Benue Trough as a set of juxtaposed pull-apart basins generated along pre-existing N60˚E strike-slip faults during the Lower Cretaceous. The strike-slip (transcurrent) faults are believed to be connected to the oceanic fracture zones and reactivated during the separation of the South American and African plates. This model originated from the fact that most of the major faults identified in the Benue Trough are transcurrent faults rather than normal faults of rift systems. Identified normal faults (mostly N120˚E trending) in the Benue Trough are seen to control the grabens but are always linked to major sinistral N60˚E strike-slip faults. During the mid-Santonian, N155˚E trending compression reactivated the sinistral faults as reverse faults, while the N120˚E normal faults acted as dextral strike-slip faults (Abubakar, 2014).
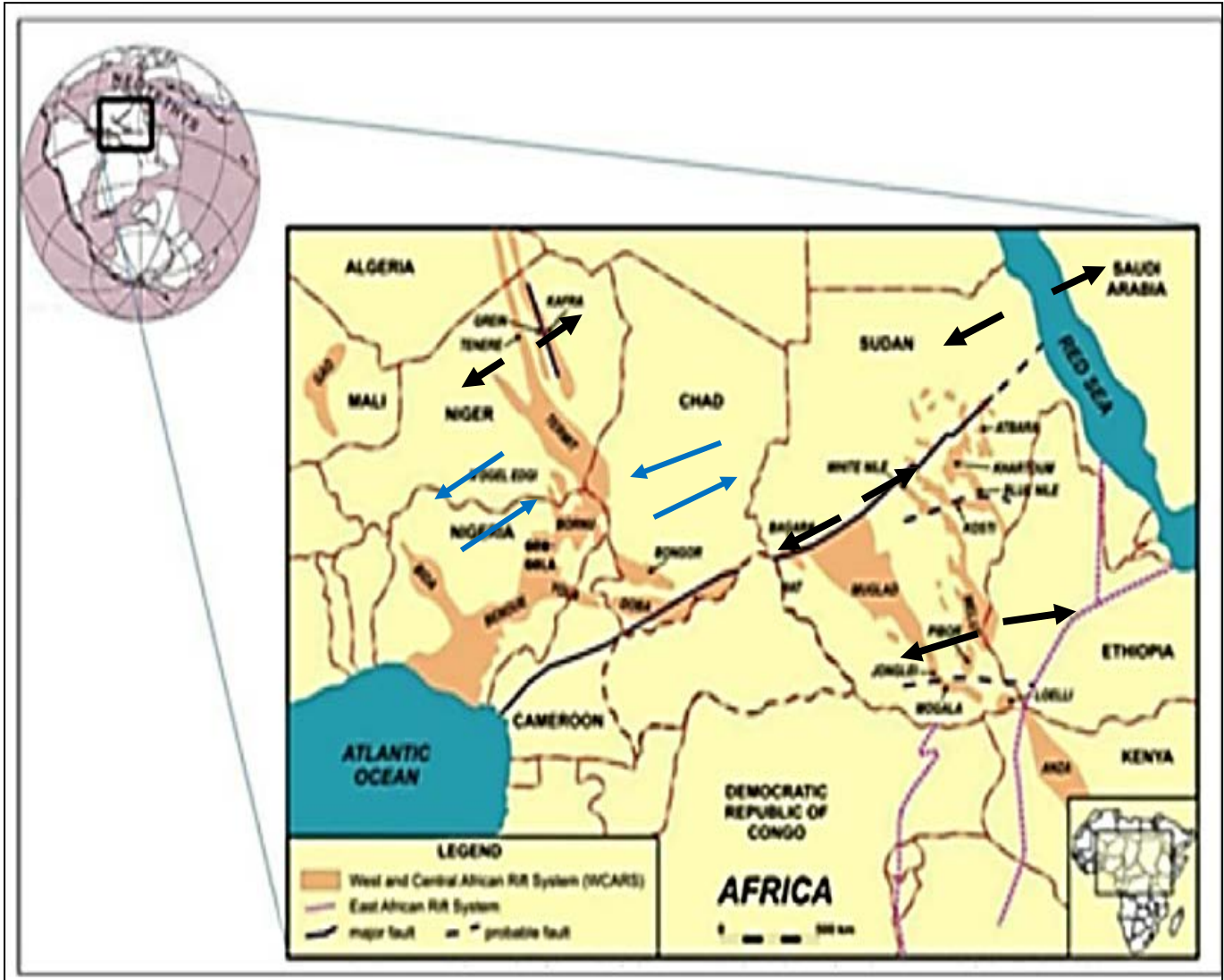
Figure 2.1: West and Central African Rift System showing the Benue Trough (Anudu et al., 2014) **Blue Arrows** = Regional shear zones**; Black Arrows =** Major Extension zones

In the Northern Benue Trough however, there is a controversy as to the existence of the Santonian event. Ajayi and Ajakaiye (1981), favour the Maastrichtian compression as the only Late Cretaceous event that affected the Northern Benue Trough; while several workers such as (Offodile, 1976; 1989 and Zaborski, 1979) suggested the presence of both the mid-Santonian and the Maastrichtian events in the trough. The Middle Benue Trough which is of particular interest in this research work has six sedimentary formations. The six formations include the Asu River Group, Awe Formation, Keana Formation, Ezeaku Formation, Awgu Formation and finally the youngest which is the Lafia Formation (Offodile, 1976, 1989; Obaje, 2009; NGSA, 2009; Anudu *et al*., 2014) (Figure 2.2). Tectonic activity remained localized along the major fault zones but also resulting in sub-meridian mineralized fractures. Ofoegbu (1984); Offodile (1976, 1989); Ajayi and Ajakaiye (1981); Ofoegbu and Odigi (1990) recognised that structural lineaments in the Benue Trough are dominantly N-S, NE-SW and NW-SE, often crossing one another forming a strong network of shearing fissures and fractures. Fault bounded basins filled with alluvial to fan delta deposits are common in the lower Benue Trough but few data are available on their tectono-sedimentary evolution (Ofoegbu and Odigi, 1990). Magmatic activity was contemporaneous with the opening and infilling of the Benue Trough. Various types of Volcanic occurrences especially dolerite intrusions transect the area. These igneous intrusions are associated with both pre and post-Turonian tectonic episodes (Nwachukwu, 1972).

2.4 Geology of the Study Area

The study area is underlain by the crystalline basement rocks, younger granites, sedimentary rocks and volcanic rocks (Offodile, 1976, 1989; Ajayi and Ajakaiye, 1981; Obaje, 2009; NGSA, 2009; Figure 2.2). Crystalline basement rocks of the Northern Nigerian Basement Complex and Eastern Nigerian Basement Complex underlie the northern and south-eastern parts of the area, respectively. The Middle Benue Trough links the upper and lower arms of the Benue Trough sedimentary basin in Nigeria. It is part of the long stretch arm of the Central African Rift System and one of the seven inland sedimentary basins in Nigeria originating from the early Cretaceous rifting of the Central West African basement uplift (Obaje, 2009; NGSA, 2009; Offodile, 1976). The Benue Trough is a linear Northeast - Southwest (NE-SW) trending structure characterized by the presence of thick sedimentary cover of varied composition whose age ranges from Albian to Maastrichtian (Obaje, 2009).

2.4.1 The Basement Complex

These crystalline basement rocks are grouped into two kinds, namely Migmatite-Gneiss Complex and the Older Granites.

The Migmatite-Gneiss Complex is Meso-Archean to Neo-Proterozoic (3200 Ma - 542 Ma) in age and composed migmatites, gneisses and schists. The Older Granites are Pan-African (800-400 Ma, i.e. Neo-Proterozoic to Early Palaeozoic) in age and consist mainly of granites, diorites and dolerites. The Migmatite-Gneiss Complex was deformed and intruded by the Older Granites during the Pan-African tectonic episodes (800-400 Ma). The Younger Granites of the Mada and Afu ring complexes (210-145 Ma, i.e. Triassic-Jurassic in age) occur close to margin of the Trough in the north-western part of the study area and are high level, anorogenic granites; they mainly consist of micro-granites and biotite granites.

2.4.2 The Sedimentary Formations

The Cretaceous sedimentary rocks underlie much of the study area and consist of the Asu River Group, the Awe Formation, Keana Formation, Makurdi Formation, Ezeaku Formation, Awgu Formation and Lafia Formation (Figure 2.2). The marine Asu-River group of Albian age commenced the sedimentation in the Middle Benue Trough (Obaje, 2009). Cretaceous sedimentary rocks older than the Santonian were deformed during the Santonian tectonic event (about 86 Ma) to produce several uplifts, faults and numerous folds, generally trending in a NE-SW direction, parallel to the trough margin (Burke *et al*., 1972; Benkhelil, 1989).

In the Palaeocene, the Cretaceous Middle Benue Trough experienced the same volcanic activity. The intra-sedimentary rocks emplaced are basic to intermediate in composition (Offodile, 1980) and are mainly basalts, phenolites and trachytes. They occur as small cones, plugs, lava sheets and tuffs that may exceed a few square kilometres in extent and appear to be to be widely distributed in the region (Wright, 1989). They are located mostly around Awe, Arufu and Makurdi areas (Offodile, 1976, 1989; Figure 2.2). Basaltic lava and dolerite sills are inter-bedded in shales around Otukpo area and in the Turonian shales and sandstone in the Makurdi area (Benkhelil, 1989). Stratigraphically, the Middle Benue Trough consists of the following Formations;

The Asu River Group (Aptian–Albian)

The oldest outcropping beds occurring in the core of the Keana Anticline are Micaceous siltstone, shale, mudstone, clays and fine grained sandstones which Cratchley and Jones (1965) and Offodile (1976) referred to as the Asu River Group. This constitutes the oldest sediments in the Lower Benue Basins. Sediments of the Asu River Group consist of alternating shales and siltstones with occurrences of limestone and arkosic sandstones in these basins. Maximum thickness of the group was put at 1500m in the Abakaliki Basin. They are frequently exposed on the core of anticlinal structures and lateral facies variations.

These sediments are composed of fine grained sandstones and siltstones interbedded with shales in the Middle Benue Keana anticline where a thickness of 3000m was reported (Offodile, 1976). Stratigraphic studies suggest that sediments belonging to the Asu River were deposited mostly during the Albian in view of the prevalence of the Middle Albian Ammonites in the marine limestone facies.

The terrain of the Asu River Group directly overlies the Pre-Cambrian to Lower Paleozoic basement rocks and the lithofacies and their lateral equivalents were derived from the weathering and erosion of the crystalline basement. The continental deposits were succeeded by marine shales of the first marine flooding into the Benue Trough in the Albian times during which the shales, limestone and the interbedded siltstone facies of the Asu River were deposited. Variation in thicknesses of the successions is indicative of the accommodation space created due to differential subsidence within the block faulted basins. The Asu River Group is interpreted as sediments of the first transgressive cycle into the Lower and Middle Benue Basins (Offodile, 1976).

Awe/Keana/ Makurdi / Ezeaku Formations (Late Cenomanian –Turonian)

In the Middle Benue Trough, a regressive phase, the Awe Formation consisting of transitional beds of sandstones and carbonaceous shales overlies the Asu River Group (Benkhelil, 1989). This is overlain by continental fluvial sands of the Keana Formation. Both the Awe and the Keana Formations are succeeded by the marine strata of the Ezeaku Formation consisting of calcareous shales, micaceous fine to medium grained sandstones and shelly limestones in the Middle Benue Basin. Locally, the shales grade into the predominantly fluvial cross bedded sandstones of the Makurdi Formation (Figures 2.2 and 2.3).

Awgu Formation (Cenomanian-Santonian)

The Ezeaku Formation is overlain by the Awgu Formation in the Lower and Middle Benue basins. The Awgu Formation consists of a sequence of fossiliferous black shales and limestones in the Abakiliki Basin. In the Middle Benue Basin, the shales are interbedded with siltstone, sandstones, coals and subordinate limestone. The top parts of the Ezeaku Formation and the marine successions of the Awgu Formation were deposited during the Late Cenomanian to Coniacian transgressive cycle. The Santonian was a period of non-deposition, folding and faulting. This was followed by uplift and erosion of the sediments (Burke and Whiteman, 1973).

Lafia Formation (Campanian-Maastrichtian)

The Lafia Formation comprises the youngest sediments in the southern part of the Middle Benue Trough. It is confined to the Kadarko sub-basin. A thickness of 500-1500m was quoted by Offodile (1976) though only about 50m was reported east of Lafia where wedging out is apparent. It consists of red, poorly consolidated, commonly cross-bedded frequently ferruginous sandstones, flaggy mudstones and clays, with palaesol horizon identified just south of Lafia (Offodile, 1976). Carbonized plant remains are the only fossils in the area. Although not precisely dated, the formation is generally regarded as Maastrichtian. Offodile (1976) suggested an origin within a south-westerly flowing fluviatile system discharging into the Anambra Basin.
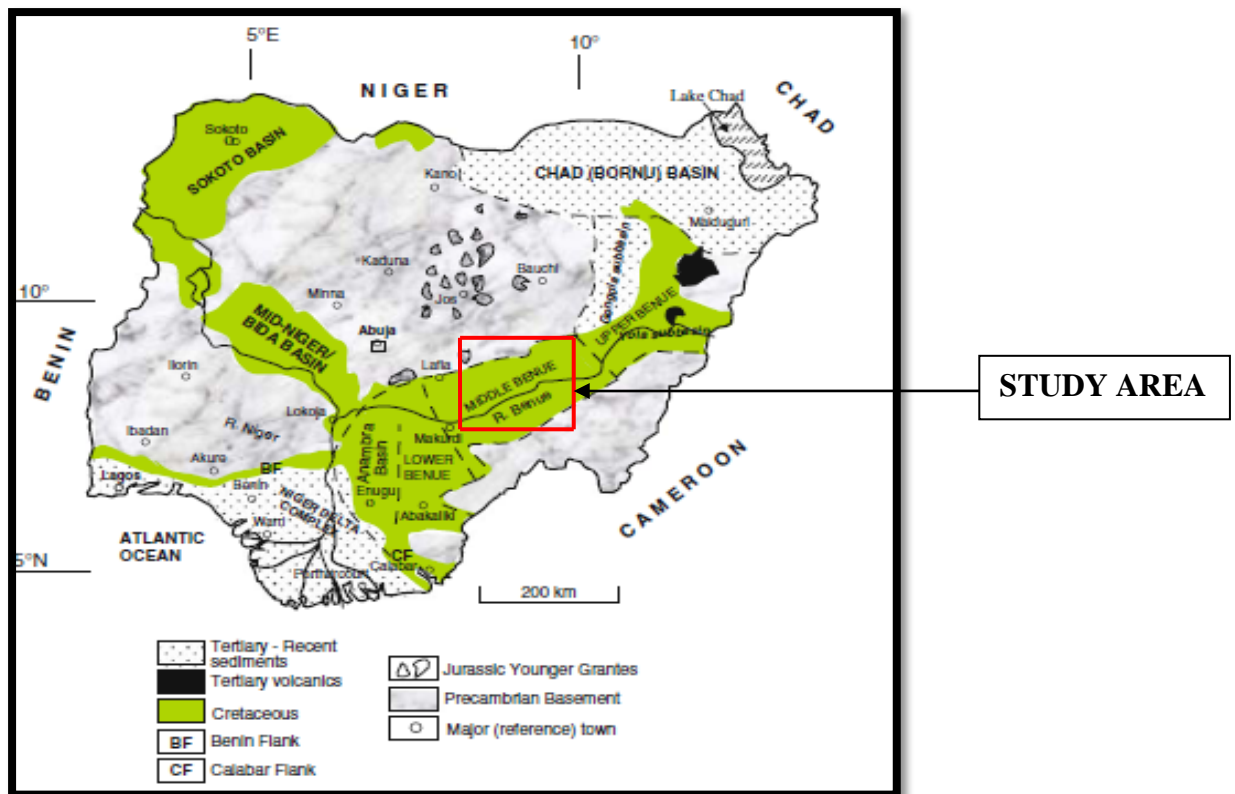
Figure 2.2: Generalized geologic map of Nigeria showing the study area (Obaje, 2009)
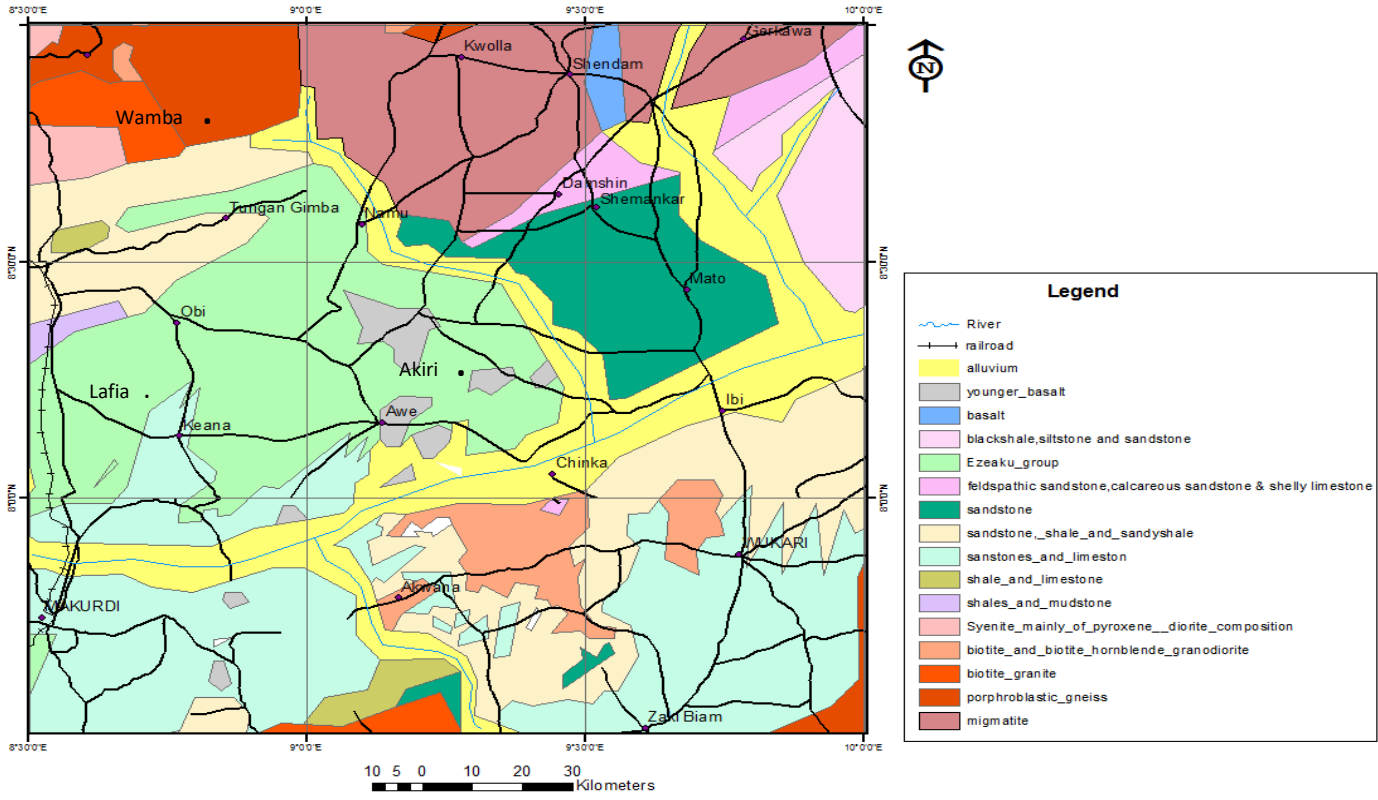
Figure 2.3: Map of the study area showing local geology (NGSA, 2009)

2.5 Magnetism of the Earth

The earth is divided into three parts, i.e. crust, mantle and core. The core of the earth is also divided into two parts; that is the molten outer core and the solid inner core. The core of the earth is the main provider of the heat energy in the earth. Inglis (1955) pointed out that, it is impossible at present to determine the types of convectional motion in the molten core. Reeves (2010) indicated that the movement of the charged electronic particles within the molten core produces a magnetic field around the earth after several theoretical and experimental studies. This magnetic field enveloping the earth give rise to the magnetic features of the various rocks found within or on the surface of the earth. The flow of these electrical charges successfully creates a huge electromagnet (Clark and Emerson, 1991).

The principle underlying the operation of the magnetic method is based on the fact that when a ferrous material is placed within the earth's magnetic field, it develops an induced magnetic field. The induced field is superimposed on the earth's field at that location creating a magnetic anomaly. Detection depends on the amount of magnetic material present and its distance from the sensor. The anomalies are normally presented as profiles or as contour maps.

Ninety percent of the earth's magnetic field (Geomagnetic field) looks like a magnetic field that would be generated from a dipolar magnetic source located at the centre of the earth and aligned at 11.5°, with the Earth's rotational axis (Kearey *et al*., 2002). The remaining 10 % of the magnetic field cannot be explained in terms of simple dipolar sources. The main field (90 %) is the largest component of the magnetic field and is believed to be caused by electrical currents in the earth's fluid outer core. For exploration work, this field acts as the inducing magnetic field. Crustal magnetic field is the portion of the magnetic field associated with the magnetism of crustal rocks. This portion of the field contains both, magnetism caused by induction from the Earth's main magnetic field and from the remnant magnetization of both

surface and crustal rocks. Relatively small portion of the observed magnetic field is generated from magnetic sources external to the earth. This field is believed to be produced by interactions of the earth's ionosphere with the solar wind.

2.5.1 Nature of the Earth Magnetic (Geomagnetic) Field

The earth's magnetic field within the or at the surface of the Earth is produced from the molten outer core (Rivas, 2009). The mantle plays little part in the earth's magnetism, while interaction of the (past and present) geomagnetic field with the rocks of the earth's crust produces the magnetic anomalies. The earth's magnetic field is made up of three parts (Telford *et al*., 1990) namely;

   a. The major field, which differs comparatively gradually and originates within the earth.

   b. The minor field (compared to the major field), which differs rather quickly and of external origin.

   c. The spatial variations of the major field which are usually lesser than the major field, are almost the same in time and place, and are brought by local magnetic anomalies within the Earth's crust. These are the areas of interest in magnetic surveying.

Magnetic field in SI units is defined in terms of the flow of electric current needed in a coil to generate that field (Reeves *et al*., 1997). As a consequence, units of measurement are volt-seconds per square metre or Weber/m^2 or Teslas (T). Since the magnitude of the earth's magnetic field is only about 5×10^{-5} T, a more convenient SI unit of measurement in geophysics is the nanotesla ($nT = 10^{-9}$ T). The geomagnetic field varies from less than 22000 nT in southern Brazil to over 70,000 nT in Antarctica south of New Zealand. Magnetic anomalies as small as about 0.1 nT can be measured in conventional aeromagnetic surveys and may be of geological significance. One nT is numerically equivalent to the gamma which is an old (c.g.s.) unit of magnetic field (Reeves *et al*., 1997). The compass needle aligns itself

in the direction of magnetic field of the Earth when hanged freely at any position on the surface of the earth. This alignment creates an angle between the magnetic and geographic north (Kearey *et al*., 2002).

2.5.2 The International Geomagnetic Reference Field (IGRF)

The magnitude of will fall between 20,000 and 70,000 nT everywhere on earth and it can be expected to have local variations of several hundred nT (sometimes, but less often, several thousand nT) imposed upon it by the effects of the magnetisation of the crustal geology. The 'anomalies' are usually at least two orders of magnitude smaller than the value of the total field. The IGRF provides the means of subtracting on a rational basis the expected variation in the main field to leave anomalies that may be compared from one survey to another, even when surveys are conducted several decades apart and when, as a consequence, the main field may have been subject to considerable secular variation.

The IGRF removal involves the subtraction of about 99% of the measured value; hence, the IGRF needs to be defined with precision if the remainder is to retain accuracy and credibility. The IGRF is published by a working group of the International Association of Geomagnetism and Aeronomy (IAGA) on a five-yearly basis. A mathematical model is advanced which best fits all actual observational data from geomagnetic observatories, satellites and other approved sources for a given epoch (Reeves *et al*., 1997). The model is defined by a set of spherical harmonic coefficients to degree and order 3. Software is available which permits the use of these coefficients to calculate IGRF values over any chosen survey area. It is normal practice in the reduction of aeromagnetic surveys to remove the appropriate IGRF once all other corrections to the data have been made. From the point of view of exploration geophysics, undoubtedly the greatest advantage of the IGRF is the uniformity it offers in magnetic survey practice since the IGRF is freely available and universally accepted (Reeves *et al*., 1997).

2.5.3 Magnetic Susceptibility of Rocks

Magnetic susceptibility is a measure of the ease with which particular sediments are magnetized when subjected to a magnetic field. The ease of magnetization is ultimately related to the concentration and composition (size, shape and mineralogy) of iron oxide in the rocks (Wemegah *et al*., 2009). Magnetisable minerals include the ferromagnetic minerals (strongly magnetisable) and any of the paramagnetic (moderately magnetisable) minerals and other substances (Wemegah *et al*, 2009). The magnetic susceptibility is the ratio between the magnetization effect and the applied magnetic field (Clark, 1997).

Reynolds (1997) indicates that most sedimentary rocks contain negligible quantities of magnetic minerals, and are therefore non-magnetic. Most basic igneous rocks, on the other hand, have high magnetic susceptibilities, while acid igneous rocks and metamorphic rocks can have susceptibilities ranging from negligible to extremely high (Table 2.1). Magnetic susceptibility is a trace parameter of rocks, because the percentage of magnetic minerals is usually one percent or less, even in basic igneous rocks. Slight differences in iron oxide content of a mineral can cause large magnetic susceptibility variations. Remke *et al*., 2004, pointed out that the amount of iron oxides in rocks is influenced by the parent rock, age of rock and weathering processes.

Table 2.1: Magnetic susceptibility of some common rock types (Telford *et al.*, 1990)

ROCKS	SUSCEPTIBILITY (emu(m³/kg))	
Igneous Rocks	**Range**	**Average**
Granite	0 - 400	200
Basalt	20 - 14,500	6,000
Gabbro	80 - 7,200	6,000
Peridorite	7,600 - 15,600	13,000
Metamorphic Rocks	**Range**	**Average**
Quartzite	-	350
Schist	25 - 240	120
Slate	0 - 300	50
gneiss	10 - 2000	-
Sedimentary Rocks	**Range**	**Average**
Sandstone	All very low (< 1)	All very low (< 1)
Shale	"	"
Limestone	"	"
Gypsum	"	"
Coal	"	"
Oil	"	"

2.5.4 Density of Rocks

Density is one of the most important properties of all matter. Simply defined, density is the amount of matter ("mass") in an amount of space ("volume").

$$D = m/v \hspace{8cm} 2.1$$

Where,

D is the density in grams per cubic centimetres (g/cm^3)

m is the mass in grams (g) and

v is volume in cubic centimetres (cm^3).

The importance of density lies in the fact that when there are two objects with different densities and phases, the more density will sink. The fact that you are here at the bottom of the ocean of air is one trivial example. Also, when two fluids (liquids or gases) have different densities, the less dense will rise. "Warm air rises, cool air sinks." This is the physical basis for much of our weather.

Differences in density inside Earth's crust and upper mantle involving molten rocks are behind volcanic eruptions and the slow, massive movement of crustal plates that create oceans and continents. Large-scale, long-term circulation of ocean water that affects climate are also among the many other examples of density-driven circulation patterns that produce our world (Telford *et al.*, 1990).

Table 2.2: Densities of Typical Rock Types (Telford *et al*., 1990)

Rock Type	Range (g/cm^3)	Average (g/cm^3)
Sediments (Wet)		
Overburden	-	1.92
Soil	1.20-2.40	1.92
Clay	1.63-2.60	2.21
Gravel	1.70-2.40	2.00
Sand	1.70-2.30	2.00
Sandstone	1.61-2.76	2.35
Shale	1.77-3.20	2.40
Limestone	1.93-2.90	2.55
Dolomite	2.28-2.90	2.70
Sedimentary rocks	**(average)**	**2.50**
Igneous rocks		
Rhyolite	2.35-2.70	2.52
Andesite	2.40-2.80	2.61
Granite	2.50-2.81	2.64
Porphyry	2.60-2.89	2.74
Migmatite	2.62-2.89	2.74
Quarzdiorite	2.62-2.96	2.79
Diorite	2.72-2.99	2.85
Lavas	2.72-2.99	2.90
Diabase	2.50-3.20	2.91
Basalt	2.70-3.30	2.99
Gabbro	2.70-3.50	3.03
Peridotite	2.78-3.37	3.15
Acid igneous	**2.30-3.11**	**2.61**
Basic igneous	**2.09-3.17**	**2.79**
Metamorphic rocks		
Quartzite	2.50-2.70	2.60
Schists	2.39-2.90	2.64
Greywacke	2.60-2.70	2.65
Marble	2.60-2.70	2.75
Serpentine	2.40-3.10	2.78
Slate	2.70-2.90	2.79
Gneiss	2.59-3.00	2.80
Amphibolite	2.90-3;04	2.96
Eclogite	3.20-3.54	3.37
Metamorphic	**2.40-3.10**	**2.74**

2.5.5 Theory of Magnetism in Rocks and Minerals

Many rocks that contain iron-bearing minerals act as tiny magnets. Many rock-forming minerals are non-magnetic. Only a few magnetic minerals, that include magnetite (Fe_3O_4), ilmenite ($FeTiO_3$) and pyrhotite (FeS), significantly affect the magnetization field of the particular area. Magnetic rocks contain these minerals, usually in small quantities (Clark, 1997). Substantial magnetization can occur only above certain depths since subsurface temperatures increase with depth. In areas with relatively high geothermal gradients, the maximum depth of magnetization is shallower than it is in areas with lower geothermal gradients. Most sedimentary rocks contain negligible quantities of magnetic minerals, and are therefore non-magnetic. Most basic igneous rocks, on the other hand, have high magnetic susceptibilities, while acidic igneous and metamorphic rocks can have susceptibilities ranging from negligible to extremely high (Reynolds, 1997).

Below the Curie temperature is when the magnetic features of rocks can exist. Curie point is defined as the temperature (580^0C and above) at which magnetic minerals lose their magnetic properties or susceptibility as a result of high temperature (Stampolidis and Tsokas, 2002; Nwankwo *et al*., 2011). This temperature varies for different rock types. Present day geothermal studies have indicated that Curie point can be reached at depths 30 to 40km beneath the earth. Based on these assumptions, it is estimated that all crustal rocks are very potent to carry magnetic features. Reeves (1989) suggested that the upper mantle has no magnetic properties hence the earth's crust may be effective depth where magnetic sources can be found.

Magnetic materials can be grouped on the basis of their behaviour when placed in an external field (Telford *et al*., 1990). Many minerals have equal number of electrons and orbiting in opposite direction so that, in the absence of some external magnetic field, their effects cancel out. There are different types of magnetic materials classified according to the extent to

which they can be magnetized when exposed to the external field (depending on the values of their magnetic susceptibility). According to Telford *et al.*, (1990), these materials can be classified as follows;

    a. Diamagnetic materials

    b. Paramagnetic materials

    c. Ferromagnetic materials and

    d. Ferrimagnetic materials

a. Diamagnetic materials

If a magnetic field is applied, the electron orbits are slightly disturbed by electromagnetic induction. This slightly weakens the field inside the material giving a small magnetic effect called diamagnetism. Diamagnetic materials are those that have very low and negative magnetic susceptibilities (Reynolds, 1997). This means that the intensity of induced magnetization in the material is in opposite direction to the inducing or external magnetic field. Diamagnetism is independent of temperature. Diamagnetic materials include quartz, feldspar, calcite, graphite, gypsum, marble and salt (Telford *et al.*, 1990).

b. Paramagnetic materials

Paramagnetic materials have unbalanced electrons so that the individual atoms or molecules act like very tiny magnets. In the absence of an external magnetic field, these molecular magnets are arranged at random, giving no resultant magnetic effect to the material as a whole but if a magnetic field is applied the molecular magnet becomes partially aligned with it thus increasing its strength. This small effect is called paramagnetism. Paramagnetic materials have low and positive magnetic susceptibility. The total magnetic intensity will be bigger than the original magnetic field. Examples of such materials include pyroxene, olivine, pyrite and biotite (Reynolds, 1997).

c. **Ferromagnetic materials**

With ferromagnetic materials, there is almost a perfect arrangement of their domains. They have all their magnetic poles aligned hence there is a magnetization of high effect being produced. Ferromagnetic materials have high and positive magnetic susceptibilities that are hundreds of times higher than that of paramagnetic and diamagnetic materials. Ferromagnetism also decreases with temperature and disappears completely at Curie temperature (Reynolds, 1997). Examples of ferromagnetic materials include iron, cobalt and nickel.

d. **Ferrimagnetic materials**

Ferrimagnetic materials show very strong magnetization effect and its domains align themselves in the direction of applied external field (Reynolds, 1997). Examples of ferrimagnetic materials include magnetite and ilmenite (Telford *et al*., 1990; Reynolds, 1997).

2.6 Aeromagnetic Survey

The concept underlying magnetic prospecting is the existence of a magnetic dipole or monopoles within the rocks constituting the earth (Umeanoh, 2015). Magnetic force expression, F between two magnetic monopoles of strength p_1 and p_2 is given according to Umeanoh, (2015) as:

$$F = p_1 p_2 / \mu r \quad \text{(Coulomb's equation)} \qquad\qquad 2.2$$

Where,

$p_1 \; and \; p_2$ are dipoles

r is in metres and it is the distance between p_1 and p_2

μ is the free space permeability

The above Coulomb's equation is the basic underlying principle of magnetic prospecting. Magnetic monopole p_1 or p_2 exert force per unit pole strength and it can be expressed according to Umeanoh, (2015) as:

$$H = p/r^2$$ 2.3

Where,

p is the magnetic monopole

r is the distance between the force in question and the magnetic monopole

H is the strength of the magnetic field

Generally, the existence of a monopole has never been accounted for (Bello *et al*., 2017). Basically, magnetic monopoles or dipole are made up of positive and negative poles separated by a distance. The force produced and thus existing between monopoles can be estimated by vectorally adding the forces generated by each of the monopoles or dipole (Bello *et al*., 2017). The force generated by a simple bar magnet can be compared to the force generated by a dipole.

Magnetic materials positioned within a magnetic field will acquire magnetic force and will experience magnetic induction. Due to the inducing field, one can measure the strength of the magnetic field known as the intensity of magnetization, Ji, induced on the material and this is expressed according to Umeanoh, (2015) as:

$$J_i = KT$$ 2.4

Where,

J_i is the magnetization

K is susceptibility of the magnetic material

T is the inducing field

On a larger scale, aeromagnetic surveys are used for mapping geological structures. In areas where sedimentary sequence is very thick, it is sometimes possible to delineate major

structural features because the succession includes magnetic horizons which may be ferruginous sandstones or shales, tuffs, or possibly lava flows. In many regions, however, the igneous and metamorphic 'basement' which underlies the sedimentary sequence is the predominant factor controlling the pattern of the anomaly field, for it is usually far more magnetic than the sediments. Where the basement rocks are brought nearer to the surface in structural highs, the magnetic anomalies are large and characterized by strong relief (Dobrin and Savit, 1988).

Once an aeromagnetic data has been collected, the data is then processed to remove the earth's natural magnetic field and any diurnal field changes (variations that occur in day and night) in order to reveal the variations in magnetization due to the underlying geology (Dobrin and Savit, 1988). Thus, individual magnetic anomalies which are magnetic signatures and are different from the background consist of a high and low compared to the average field. In the southern hemisphere, the high is located to the north and the low to the south of the magnetic body, while the reverse is the case in the northern hemisphere. So the position and size of the anomaly depend on the position of the magnetic body (Keating, 1995). Change in latitude will also affect the positioning of anomalies over magnetic body. This situation allows the geophysicist to interpret the position of the magnetic body which has caused the anomalous reading. Often however, the reading is complicated because of the position of the body in relation to other rocks, its size and what happens to the body at depth. The corrected data are usually presented as magnetic contour maps. The magnetic anomalies are usually numerous, erratic, less persistent and of large magnitude. From the magnetic contour maps, geophysicists can locate magnetic bodies, interpret the nature of geologic boundaries at depth, delineate geologic structures such as faults, fractures, dykes, sills, etc. (Gunn, 1997).

An interpreter who is experienced in magnetics can usually identify geological structures by mere looking at a magnetic map just as one can use a topographic map to visualize surface features. When contour lines in a map are close together, they represent a sharp change in values or steep gradient, while widely spaced contour lines represent slow change or shallow gradient. In general, qualitative interpretation of a magnetic data is primarily a map or image based on recognition of patterns, trends, structural grains, discontinuity and offsetting faults and disrupting cross-cutting features (Dobrin and Savit, 1988). Qualitative interpretation is basically concerned with the visual inspection of maps and profiles (or cross-sections). Visual inspection involves the identification of zones with different magnetic characteristics. The quantitative interpretation on the other hand, involves taking profiles on the residual anomaly map and plotting graphs in order to estimate the depth to magnetic sources (or sedimentary thickness) for the area in question.

An aeromagnetic survey is a common type of geophysical survey carried out using a magnetometer aboard or towed behind an aircraft. The principle is similar to a magnetic survey carried out with a hand-held magnetometer, but allows much larger areas of the Earth's surface to be covered quickly for regional reconnaissance. The aircraft typically flies in a grid-like pattern with height and line spacing determining the resolution of the data (Bello *et al*., 2017). As the aircraft flies, the magnetometer records tiny variations in the intensity of the ambient magnetic field due to the temporal effects of the constantly varying solar wind and spatial variations in the Earth's magnetic field, the latter being due both to the regional magnetic field, and the local effect of magnetic minerals in the Earth's crust. By subtracting the solar and regional effects, the resulting aeromagnetic map shows the spatial distribution and relative abundance of magnetic minerals (most commonly the iron oxide mineral magnetite) in the upper levels of the crust (Clark, 1997). Because different rock types differ in their content of magnetic minerals, the magnetic map allows a visualization of the

geological features of the upper crust in the subsurface, particularly the spatial geometry of bodies of rock and the presence of structures (faults and folds). This is particularly useful where bedrock is obscured by surface sand, soil or water. Aeromagnetic surveys are widely used to aid in the production of geological maps; they are also commonly used during mineral exploration and in delineating areas of geothermal energy potentials.

Compared to other geophysical methods, the aeromagnetic data are always readily available therefore it is important to exploit the potential of this data. Aeromagnetic data has been and will continue to be, handy in the geophysical and geological investigation of the earth's interior. Umeanoh (2015) asserted that aeromagnetic data can be used in mapping magnetic basement in sedimentary rocks and delineating igneous bodies within sedimentary sections as well as locating lineaments and structures which could be possible host to varying earth resources like groundwater, hydrocarbon and minerals. Aeromagnetic method has been used mainly for the estimation of depth to basement and thickness of sediments within sedimentary basins. The method was also used in mapping igneous and metamorphic rocks and structures related to them because these rocks have high magnetization compared to other rocks (Reynolds *et al*., 1990). Despite being used in delineating architectural framework of the earth's subsurface geology, aeromagnetic method can be applied successfully in defining geothermal gradient of an area via spectral analysis (Okubo and Matsunaga, 1994; Ofor and Udensi, 2014). It was pointed out that the assessment of variations of the Curie isotherm of an area can provide information about the regional temperature distribution at depth and the concentration of subsurface geothermal energy (Tselentis, 1991).

Ofoegbu (1984) carried out an interpretation of aeromagnetic anomalies over the Lower and Middle Benue Trough using non-linear optimization techniques. He interpreted the anomalies in terms of basic intrusive bodies which occur either within the Cretaceous sediments and/or the metamorphic basement. Detailed interpretation of aeromagnetic anomalies over the

trough revealed that the magnetic anomalies over the Benue Trough can be accounted for in terms of the combined effects of a basement of variable topographic relief and magnetic character and some deeply buried intrusive bodies of basic to intermediate composition (Ofoegbu, 1984; Ofoegbu, 1985; Ofoegbu, 1988). Recently, Salako (2014), worked on Upper Benue Trough using Source Parameter Imagine estimated the depth of sedimentary/basement interface between 0.96 km and 5.862 km. Alkali and Kasidi (2016), worked on depth to magnetic sources using spectral analysis of aeromagnetic data over IBBI and environs, in the Middle Benue Trough. The results suggest the existence of two source depths. The deeper magnetic sources vary between 1.2 km and 4.8 km, and the shallower magnetic sources vary between 0.5 km and 1.0 km.

This present study concerns the evaluation of the total aeromagnetic anomalies for estimation of curie-temperature depth and heat flow to investigate the geothermal energy potential of parts of the Middle Benue Trough Nigeria, which has in the past received limited attention. The reasons may be due to lack of immediate geologic and economic values, although it is fast becoming an important research area for geoscientists. Geophysical studies in the area are limited, without records of crustal temperature studies. Curie-temperature depth combined with heat flow assessment would complement greatly the geophysical information of the area to bridge the gap of lacking crustal temperature information.

2.6.1 Spectral Analysis (Fourier Transform Method)

Spectral analysis is one of the tools of investigating the thermal framework via aeromagnetic studies. In the last few decades, spectral analysis based on statistical models has been used in various geological applications like the estimation of average depth to the top of magnetic basement and the estimation of crustal thickness. This spectral method pioneered by Spector and Grant, 1970, has been used extensively in the interpretation of magnetic anomalies. It is based on the expression of the power spectrum for the total field magnetic anomaly produced

by a uniformly magnetized rectangular prism (Bhattacharyya and Leu, 1975; Hahn *et, al*., 1976). Spector and Grant, 1970 assumed that a number of independent ensembles of rectangular prismatic blocks are responsible for generating anomalies in a magnetic map.

Fourier transforms are predominantly helpful in magnetics (Telford *et al*., 1990) for

    a. Resolution of specific anomalies by downward and upward continuation,

    b. Changing the effective field inclination (reduction to the pole) or conversion of residual magnetic data to vertical component data,

    c. Calculation of derivatives (vertical and horizontal derivatives),

    d. General filtering-separating anomalies caused by sources of different size and depth and

    e. Modelling of magnetic anomalies.

A much faster algorithm developed by Cooley and Tukey (1965) called the Fast Fourier Transform (FFT) is a competent mathematical tool used to calculate the Discrete Fourier Transform (DFT) and its inverse. FFT algorithms can hence be regularly made into data processing programs so as to analyse spectral lines of waveforms of geophysical data.

Fourier transformations operate based on the operation of application program like Microsoft Excel for organizing, analysing and storing data in form of a table (Kearey *et al.*, 2002).

Spectral analysis seeks to describe the frequency content of a signal, random process or system, based on a finite set of data (Nwankwo *et al*., 2008). The spectral method is based on the shape of the power spectrum for buried bodies with a density contrast (Ravat *et al*., 2007). Workers using spectral applications in the processing and interpretation of potential field geophysical data have done, and are still doing extensive and detailed studies. This claim is evident by number of well-known publications in reputable journals and books dated as far back as 40 years ago (Spector and Grant, 1970; Bath, 1974; Mishra and Naidu, 1974; Pal *et*

al., 1978; Maus and Dimri, 1995; Onwuemesi, 1997; Nwankwo *et al.*, 2008; Kasidi and Ndatuwong, 2008; Abdulsalam *et al.,* 2011; Anakwuba *et al.*, 2011; Anudu *et al.*, 2014 etc.). Fourier analysis of aeromagnetic fields has been discussed by Horton *et al.*, (1964) and Hahn (1965). However, the advent of the Fast Fourier Transform algorithm by Cooley and Turkey (1965) added a new dimension in it. Using this algorithms, Spector and Grant (1970) and Negi *et al.*, (1983) have analyzed aeromagnetic data. Spector and Grant (1970) have given a relationship to obtain the depth of subsurface magnetic layers from the slope of the radial spectrum. Odegard and Berg (1975) showed for simple bodies, and Bhattacharyya and Leu (1975) showed for complex shaped bodies that the depth to the centre of mass of the body is easily found from the power spectrum of the gravity field. If the spectrum is plotted on semi-log paper, the slope of the spectrum is equal to the depth to the centre of mass. In this method, any given spatial data are first decomposed into their component harmonics or sine and cosine wave-forms whose frequency and amplitude feature then enable the evaluation of spatial data in the frequency or wave number domain. These amplitudes represent a spectrum for which the depth to sources can be estimated. The average amplitude spectrum of all waves falling within a given frequency range is then computed by summing the Fourier amplitude and dividing by the sum of the frequencies. These average amplitudes are then plotted against the frequency on a semi-log scale. According to Negi *et al.*, 1983 and Tanaka *et al.*, 1999, the depths to magnetic sources are related to the slopes of the line segment. In estimating the depth to centroid of the magnetic source and depth to the top of magnetic source, both the longest wavelength and second longest wavelength parts of the spectral segments are considered (Negi *et al.*, 1983; Okubo *et al.*, 1985 and Tanaka *et al.*, 1999, Bansal *et al.*, 2011, Bansal *et al.*, 2013). The longest wavelength part produces the depth to centroid; while the second longest wavelength produces the depth to top of magnetic source (Bansal *et al.*, 2013) [Figures 2.4(a) and (b)].
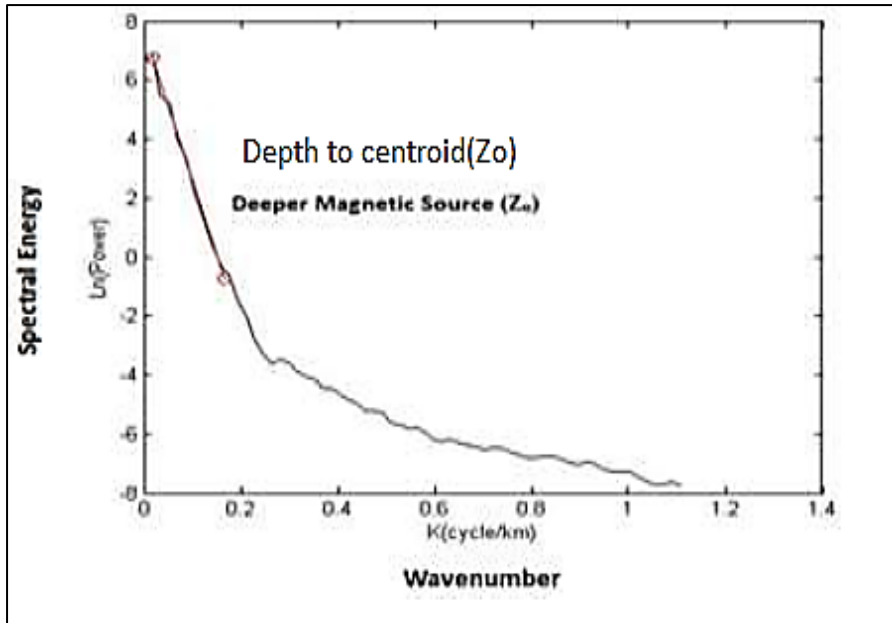
Figure 2.4(a): Typical plot of spectral energy against wave-number showing deeper magnetic source depths (Bansal *et al*., 2013)
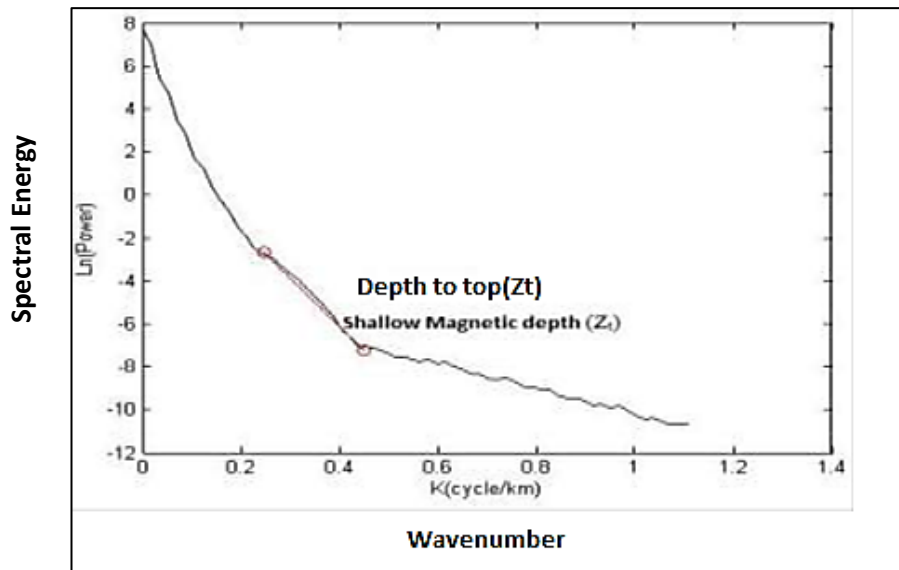

Figure 2.4(b): Typical plot of spectral energy against wave-number showing shallow magnetic source depths (Bansal *et al*., 2013)

There are distinctive advantages in working with potential field anomalies in frequency domain. The spectral domain expressions of these anomalies are generally simple as compared to the expression of the anomalies in space domain. This makes possible the devisal of simpler techniques of interpretation. The noise (observational, instrumental and

those due to near surface in-homogeneities or irregularities of the structure) associated with potential field data generally has high characteristics and by restricting the interpretation to low frequencies, considerable improvement in interpretation is possible (Pal *et al.*, 1978; Olasehinde, 1991).

Furthermore, the regional's, which are generally superimposed over anomalies of interest, being expressed as polynomials of low order, give rise to no non-zero frequencies of the spectrum (Baranov, 1975). Therefore, by employing only non-zero frequencies of the spectrum in the analysis, one can remove the effect of regional's from the interpretation. One important property of spectral analysis is that features with given direction in spectral domain are transformed into a feature with only one direction in the space domain. Moreover, linear features in the power spectrum are perpendicular to the linear space-domain features, which were described (Thorarinsson *et al.*, 1998).

The application of spectral analysis to the interpretation of potential field data is one method that can be used to determine the basement depth, and is now sufficiently well established (Spector and Grant, 1970). Several authors have applied spectral inversion techniques in the determination of sedimentary thickness in various basins of the world (Ofoegbu and Onuoha, 1991; Salem *et al.*, 2000; and Udensi and Osazuwa, 2004. Authors such as Nur *et al.*, 1994; Onwuemesi (1997); Akanbi and Udensi (2006); Nwankwo *et al.*, (2008); Selemo and Akaolisa (2010); Anakwuba *et al.*, (2011) and Ikumbur *et al.*, 2013, applied spectral methods to determine depth to basement and the interpretation of structural lineaments. Selemo and Akaolisa (2010), Anakwuba *et al.*, (2011) and Ikumbur, *et al.*, (2013) went ahead to model the anomalous structures found in their study areas. Modelling of the structures can reveal the sub-basins in a basin, as well as the trend of lineaments.

The magnetic anomaly signature characteristics are results of one or more physical parameters such as the configuration of the anomalous zone, magnetic susceptibility contracts

as well as the anomalous body. The broad magnetic intensity anomaly maps are often due to changes in the rock composition within the basement. If the magnetic units in the basement occur at the basement surface, then depth determinations will map the basin floor morphology (Gunn, 1997). Depth to basement, faults in the basement surface, and the relief of the basement surface have direct relevance to the depositional and structural history of an area and often they are overlain by sediments whose depositional isopachs and/or structure reflect the underlying basement structure (Gunn, 1997). Thus, by studying the map basement, information can be provided on the morphology of the sedimentary basin and its structure. Depth to basement is important in our exploration efforts, particularly for the determination of areas where there may be mature hydrocarbons, solid minerals and geothermal potentials.

2.6.2 Depth to Magnetic Basement and Curie point Depth

The Curie point temperature varies from region to region, depending on the geology of the region and mineralogical content of the rocks (Nwankwo and Shehu, 2015; Saibi *et al.*, 2015). Therefore it is expected that shallow Curie point depths occur in regions that have geothermal potential, young volcanism and thinned crust (Tselentis, 1991; Dolmaz *et al.*, 2005). In order to determine the Curie point depths, i.e. the bottom of the magnetized rocks, and to map these depths, a frequently used method is the analysis of magnetic data (Hsieh *et al.*, 2014; Nwosu and Onuba, 2013). Nur, (1999) estimated the Curie Point Depth of the Upper Benue Trough to be between 23.80 and 28.70 km. They also obtained a depth of 0.83 km as the depth to magnetic sources and concluded that this depth represented the intrusive bodies within the trough.

Nine aeromagnetic maps were analyzed to determine some characteristics of a prominent aeromagnetic anomaly within the Gongola Basin in the Upper Benue Trough, north-eastern Nigeria, by Abubakar *et al.*, (2010). They assumed three magnetic layers in the area and computed average depth values of 1.25 km, 4.03 km, and 5.39 km for the layers, respectively.

The depths to the causative body were determined as 2.40 and 8.09 km and the causative bodies were interpreted as basic and ultrabasic rocks. Kurowska and Schoeneich (2010) compiled a map of geothermal gradient for parts of the Chad Basin (extending towards our study area) from thermal data collected during pumping tests in water wells and several deep oil wells and presented a geothermal gradient map showing a general increase from 1.1 ^{0}C/m to 58 ^{0}C/m. Eletta and Udensi (2012) investigated the Curie Point Depth (CPD) investigation lay between 7^0N and 9^030^lN and between 9^030^lE and 12^0E. Their study area cuts our study area in half toward the southern region and lies within the sedimentary formation of the Middle Benue Trough and partly in the basement complex region of north-central Nigeria. Their estimated Curie Point Depths (CPDs) varied between 2 to 8.4 km. Kasidi and Nur (2012) computed CPDs from aeromagnetic data over Sarti in north-eastern Nigeria located at 7^0N to 8^0N and 10^0E to 12^0E (1^0 below our study area). They obtained CPDs between 26 to 28 km. Onuba *et al.*, (2012) interpreted aeromagnetic data over parts of the Upper Benue Trough and Southern Chad Basin within latitudes of 10^030^lN to 11^030^lN and longitudes of 12^0E to 13^0E (above our study area). They obtained depths to magnetic sources ranging from 0.5 to 2.5 km and concluded that the estimated depths were representative of the sedimentary thicknesses and intrusive bodies within the area. Alagbe and Sunmonu (2014) conducted evaluations on aeromagnetic data from the Upper Benue Trough within latitudes of 7^0N to 8^0N and longitudes of 11^0E to 12^0E (below our study area by a 1^0N interval). Their estimated depth to the magnetic sources ranged between 0.01 and 3.45 km. They attributed the shallow depths to near-surface intrusive rocks in their study area.

Proper estimation of the bottom of magnetic sources in a study area could provide information about the thermal structure of the crust in the region (Bansal *et al.,* 2013). In many studies (Tanaka, *et al.*, 1999; Bansal *et al*., 2011; Abraham *et al*., 2014), the depth to bottom of magnetic sources is used as an estimate of the Curie point depth and therefore as a

proxy for temperature at depth. The Curie point depth is the depth at which rock lose their ferromagnetic magnetization as a result of an increase of the temperature in the crust above the Curie temperature (Okubo *et al.,* 1989; Nwankwo and Shehu, 2015 and Saibi *et al*., 2015). The depth to bottom of magnetic sources and Curie temperature depth can be used to complement geothermal data in regions where deep boreholes are unavailable (Bansal *et al,* 2011; Abraham *et al*., 2014).

In the present study, the objective is to estimate the average sedimentary thickness (average depth to top of magnetic sources), geothermal gradient, Curie point depth (CPD) as well as the heat flow within the study area. This aids in viewing the thermal structure of the crust. The Curie point depth can be defined as the deepest level in the earth crust containing materials which creates discernible signatures in a magnetic anomaly map (Elleta and Udensi, 2012). In other words, the further the depth, the more the material changes from a ferromagnetic state to a paramagnetic one. However, one of the important parameters that determine the relative depth of the Curie isotherm with respect to sea level is the local thermal gradient, that is, heat flow (Hisarlis, 1995). This Curie isotherm generally, has a temperature of between 550^0C and 580^0C (Elleta and Udensi, 2012). This point is assumed to be the depth for the geothermal source (magmatic chamber) where most geothermal reservoirs tapped their heat from in a geothermal environment.

Measurements have shown that a region with significant geothermal energy is characterized by an anomalous high temperature gradient and heat flow (Tselentis, 1991). It is therefore expected that geothermally active areas would be associated with shallow Curie point depth (Nuri *et al*., 2005). It is also a known fact that the temperature inside the earth directly controls most of the geodynamic processes that are visible on the surface (Nwankwo *et al*., 2011). In this regard, Heat flow measurements in several parts of African continent have revealed that the mechanical structure of the African lithosphere is variable (Nur *et al.*, 1999).

2.6.3 Geothermal Gradient and Heat flow Measurements

Geophysical methods play a great role in exploration of geothermal energy. The geophysical surveys are targeted at measuring the physical parameters of the geothermal systems either indirectly from the surface of the earth or from shallow depth (Nwankwo, 2015; Kwaya *et al*., 2016, Nwankwo and Abayomi, 2017). A geothermal system consists of the following: a heat source, a reservoir, a fluid which carries and transfers heat, and a recharge area (Zira, 2013).

The heat source is due to active tectonic plate margins which represent major zones of magmatic matter that is cooling and radioactivity (Uysal, 2009). The reservoir of the geothermal system is the volume of rocks from which heat can be extracted. This reservoir contains hot fluids, vapour and gases. The reservoir is surrounded by colder rocks through which water flows from the outside into the reservoir. The area around the reservoir which water (fluids) flow into the reservoir is called the recharge area. The hot fluid in the reservoir move under the influence of buoyancy forces towards a discharge area. In defining the geothermal system, the power produced by the system is very crucial. The typical geothermal system used for electric power generation must yield approximately 10kg of steam to produce one unit (kWh) of electricity. The production of large quantities of electricity, at rates of hundreds of megawatts, requires the production of great volumes of fluids. The reservoir should be able to maintain great volumes of fluid at high temperature or can be recharged with fluids that are heated by having contact with the rocks. The thermal reservoir is expected to be more than 1km in depth.

The geological setting in which geothermal reservoir is found can vary widely from the rocks of limestone to shale, volcanic rock and granite. The most probable common single rock type in which geothermal reservoir is found is volcanic rocks. The developed geothermal reservoir around the world occur in convectional systems in which hot water rises from deep of the

earth and is trapped in reservoirs whose cap rock has been formed by silification and precipitation of other mineral elements (Zira, 2013).

Basically, geothermal energy involves the taping of thermodynamic quantities that are equivalent to the capacity of a physical system to produce work or heat; from beneath the earth crust. Geothermal heat exists deep inside the earth's interior and usually appears close to the earth's surface through the means of conduction and convention (Nyabeze and Gwavava, 2016). The heat that emanates from the earth crust is as a result of the decay of radioactive isotopes of uranium, thorium, potassium and earth crust core which has a temperature of 1000-4500^{0}C (Kurowska and Schoeneich, 2010). When this heat comes in contact with water it produces pressurized steam which is harnessed by proper application of adequate expertise, for the steam to turn a turbine for electricity to be produced. The magma coming in contact with underground water may not make the water pressurized but make it warm enough for spring spas.

Obande *et al*., 2014, attempted to investigate the geothermal potential of the Wikki Warm Spring area using aeromagnetic data. They applied the spectral method to determine the depths to the top and centroid of magnetic sources in the study area. The power spectrum of magnetic anomalies was used to estimate the basal depth of the magnetic sources. Their results showed an average estimated Curie Point Depth of 8 km and geothermal gradient of 68^{0}C/km with heat flow values averaging 170mW/m^2. The other aspect of geothermal exploration in Nigeria is the investigation of thermal springs and seepages, which occur mainly within sediments of the Middle and Upper Benue Trough. The water of the warmest springs in this area: Akiri and Ruwan Zafi have the temperature of about 54^{0}C and it suggests the occurrence of some geothermal anomalies (Ikechukwu *et al*., 2015; Abraham and Nkitnam, 2017).

So far, there is probably only one (direct) geothermal energy utilization site in Nigeria. It is a swimming pool where water from Ikogosi warm spring (37^0C) is used. It is located in south-western part of the country, in Ekiti state (Garba *et al*., 2012). Most rock forming minerals are non-magnetic but a few that contain sufficient amount of magnetic grains in them can impact magnetism to their host rock thus, producing detectable magnetic anomalies. Therefore, anomalies generated from rocks that contain magnetic grains in them may yield valuable information about the natural remanent magnetization (NRM) of the different rock units in an area and this information could be tied together to distinguish between two or more petrologically similar rock groups if they have different magnetic properties or histories.

The non-utilization/under-utilization of renewable energy resources such as geothermal resources is one of the causes of the insufficient supply of electricity generation and uneven electrical power distribution (Olusola, 2014). According to Nigerian electricity regulatory commission, currently Nigeria's electrical production ranges between 350-4000 Megawatts which is far less than the current demand of 10,000 Megawatts in the whole country (Olusola, 2014; NERC, 2014). Electricity generated is from thermal and hydro power which constitutes of 66.7% and 33.3% of total power production respectively in the country (NERC, 2014). Nigeria has a population of about 180 million as at 2014 and only 40% has access to electricity; that is to show that the energy equity in the country is drastically poor (World Energy Council, 2014).

Nigeria produces 120 million tons of oil per year and 4.39 M tons of gas as reported by the world energy council website (World Energy Council, 2014). In as much as Nigeria produces much oil and gas it would be very true today that the greenhouse gasses produced in the country would be dangerously high. The idea of using renewable energy in the country should be greatly encouraged, since geothermal energy production uses very similar

equipment and technology to that used by the oil and gas industries. Therefore, it would be a very big advantage for Nigeria as a rich oil region to develop its geothermal resources. However, due to the general problem within Nigerian energy sector made the authority to search for some other solutions, including the alternative sources of energy (Sedara and Joshua, 2013). Moves to install geothermal plants have not been widely known in Nigeria, but documented investigations of subsurface temperature of rock mass has been carried out in hundreds of wells, due to exploration for oil and gas within sedimentary basins (Obaje, 2009). Knowledge of subsurface temperature and geothermal gradients are necessary for the analysis of reservoir fluid properties as well as plate tectonics interpretation. Temperature is one of the primary factors controlling hydrocarbon generation, sediment diagenesis and migration of hydrocarbon and other pore fluids.

2.7 Radiometric Survey

Radiometric surveys detect and map radioactive emanations gamma rays from rocks and soils. All detectable gamma radiation from earth materials come from the naturally occurring radionuclide's that is uranium (U^{238}), thorium (Th^{232}) and potassium (K^{40}) (Coker *et al*., 2014). The basic purpose of radiometric surveys is to determine either the absolute or relative amounts of uranium, thorium and potassium in the surface rocks and soils which are of importance in geologic mapping and mineral exploration (Urquhart, 1988 and Faure, 1977). The application of radioactivity in geosciences is based on knowledge of the physical properties of radiation sources, and the ability to detect these sources through the analysis of remotely sensed data. A radiometric survey is the most economical method of understanding a geophysical reconnaissance of any relatively unexplored or inaccessible region. It provides data on a broad scale of structural trends and the occurrence of volcanic rocks within a sedimentary basin. Recent advancements in high-resolution aeroradiometric data acquisition techniques are used to identify the earth's surface phenomenon, with the emphasis on mineral

exploration, where those minerals show considerable radiometric anomalies (Coker *et al.*, 2014).

2.7.1 **Basic Radioactivity**

Radioactivity is the process where an unstable atom becomes stable through the process of decay, or breakdown of its nucleus. During decay, energy is released in the form of three types of radiation; alpha, beta and gamma (Gunn *et al.*, 1997).

i.   Alpha radiation is helium nuclei, which are absorbed by a few centimetres in air;

ii.   Beta radiation is electrons, which can travel up to a metre in air; and

iii.   Gamma rays are parcels of electromagnetic radiation (similar to visible light).

Gamma rays can travel for up to 300 m through air, but are stopped by water and other molecules (e.g. soil and rock). The energy of each gamma ray is characteristic of the radioactive element it came from. They have much shorter wavelengths than most other electromagnetic rays. Gamma rays can penetrate up to 30 m of rock and several hundred metres of air, and are the only choice available for the remote sensing of terrestrial radioactivity (Gunn *et al.*, 1997).

Radiometric surveys detect and map natural radiometric emanations, called gamma rays, from rocks and soils. The gamma ray spectrometer is used to measure the gamma ray emissions. At least 20 naturally occurred elements are known to be radioactive (Telford *et al.*, 1990). All detectable gamma radiation from earth materials come from the natural decay products of only three elements, i.e. Uranium, Thorium and Potassium. While many naturally occurring elements have radioactive isotopes, only potassium, uranium and thorium decay series, have radioisotopes that produce gamma rays of sufficient energy and intensity to be measured by gamma ray spectrometry. This is because they are relatively abundant in the natural environment. Average crustal abundances of these elements quoted in the literature are in the range 2-2.5% of K, 2-3 ppm of U and 8-12 ppm of Th (Minty, 1997). The basic

purpose of radiometric surveys is to determine either the absolute or relative amounts of U, Th, and K in the surface rocks and soils which are of importance in geologic mapping and mineral exploration (Urquhart, 1988 and Faure, 1977).

The application of airborne radiometric surveying is useful in geologic mapping because of its ability to detect radioactivity emanating from the natural decay of elements such as uranium, thorium and potassium from the earth material. There is good correlation between patterns in the radiometric data and unweathered rocks. This information compliments magnetic, electromagnetic and geochemical data normally acquired during mineral exploration programs (Gunn *et al*., 1997). This is one of the most cost-effective and rapid techniques for geochemical mapping of the radioactive elements: potassium, uranium and thorium. Radiometric survey can also be used for geothermal exploration. The product of this decay results in the emission of alpha, beta and gamma radiations which can be detected on the surface using radioactive element detectors. The goal of radiometric survey is to recognize and understand radiometric signatures associated with the host rocks important to mineralization and heat in the subsurface (Beamish and Busby, 2016).

Magnetic and radiometric data have been conjunctively used in the study of lithologies and structures in Yola area, Nigeria by (Bassey and Ishaku, 2012), in Ashanti gold belt of Ghana by (Boadi *et al*., 2013). Radiometric exploration for uranium in N.E. Nigeria has been done by several workers such as (Omanga *et al*., 2001; Bassey and Ishaku, 2012; Boadi *et al*., 2013). Radiometric survey of the Wikki Warm Spring region (Omanga *et al*., 2001, revealed high gamma activity leading to the conclusion of possible radioactivity being the source of heat for the spring. Aeromagnetic and aeroradiometric data were used to correlate the geothermal heat flow and radioactive heat production of the Anambra basin to ascertain if areas with high geothermal heat flow values corresponds with that of the radioactive heat production (Olorunsola and Aigbogun, 2017). The radioactive heat map was interpreted to

know productive areas based on the geographic projection of important towns. The digitized and georeferenced geological map of the study area outlined the rock boundaries. Apart from geothermal exploration, radioactive heat can also be applied to detect uranium exploration (Grasty, 1979), identify sedimentary facies for oil and gas exploration (Myers and Bristow, 1989), and detect radioactive contamination and mineral exploration (Rybach and Schwarz, 1995).

Radioactive decay of rocks is probably the greatest overall source of heat in the earth's crust by a substantial factor, although, there are other sources that may be peculiar to specific areas (Jessop, 1990). In some studies, radioactive heat production was calculated from concentrations of radio-elements measured in the laboratory by Fernandez *et al*., (1998) and directly from gamma-ray log by Bucker and Rybach (1996) in order to get the accurate radioactive heat values. Also, radioactive heat production was assessed from airborne gamma-ray data (Salem *et al*., 2005; Thompson *et al.*, 1996; Richardson and Killeen, 1980).

2.7.2 Geochemistry of the Radioelements (K, U and Th)

a) Potassium

Potassium (K) is a major component of the earth's crust (2.35%). It is an alkali element and shows a simple chemistry. The major hosts of K in rocks are potassic feldspars (principally orthoclase and microcline with -13% K) and micas (biotite and muscovite with typically 8% K). Potassium is absent from mafic minerals. Consequently K is relatively high in felsic rocks (granites, etc.), but low in mafic basalts and very low in dunites and peridotites (Fertl, 1983). The potassium content of sedimentary rocks is highly variable but tends to be higher in shales than in carbonates or sandstones (Dickson and Scott, 1997). The weathering behaviour of the K-bearing minerals determines the radioelement contents of weathered rocks and soils. During weathering, the major K hosts will be destroyed in the order biotite-K-feldspar-muscovite. Potassium released during weathering can be taken up in the formation of K-

bearing minerals such as illite or adsorbed in minor amounts into other clays, e.g. montmorillonite, under suitable conditions. The efficient uptake of K by clays is reflected in the low concentration of K in sea water (380 ppm) (Dickson and Scott, 1997). Potassium is detected in a gamma-ray survey by measurement of the 1.46 MeV gamma-ray emitted by the decay of 40K. This isotope constitutes 0.02% of natural K and is, therefore, a direct measurement of the K content in the ground.

b) Thorium

Thorium is a minor component of the earth's crust (~12 ppm), occurring only in valence state Th4+. Thorium may be present in allanite, monazite, xenotime and zircon at levels >1000 ppm or as trace amounts in other rock-forming minerals (Dickson and Scott, 1997). Major Th-bearing minerals (monazite and zircon) are stable during weathering and may accumulate in heavy mineral sand deposits. Thorium freed by the breakdown of minerals during weathering may be retained in Fe or Ti oxides-hydroxides and with clays. As with U, Th may also be transported and adsorbed on colloidal clays and iron oxides. Like U, Th does not emit gamma-rays during its decay, but is also the parent of a decay series which ends in stable [208]Pb (Dickson and Scott, 1997).

c) Uranium

Uranium is a minor component of the earth's crust (~3 ppm). Its chemistry is dominated by two valence states U^{4+} and $U^{6+.}$ The more reduced form, $U^{4+,}$ is generally contained in insoluble minerals. Uranium may be present in rocks as the oxide and silicate minerals, uraninite and uranothorite; in major U-bearing minerals such as monazite, xenotime and zircon; as trace amounts in other rock-forming minerals; or along grain boundaries, possibly as U oxides or silicates. Of the major U-bearing minerals, only zircon and monazite are stable during weathering. Uranium is the parent of a decay series which ends in stable [206]Pb. Uranium itself does not emit gamma-rays during its decay and the most energetic gamma-

rays emitted by its daughter isotopes come from ^{214}Bi which occurs late in the decay series (Dickson and Scott, 1997).

The three main types of radiation that arise from radioactive decay are alpha, beta and gamma rays. The emission of an alpha or beta particle usually leaves the new nucleus in an excited state and the surplus energy is radiated as gamma rays (Minty, 1997). These are quanta or photons of energy which are neither very penetrating because they possess neither charge nor mass. The major assignment of a structural geologist in the field is to delineate as correctly as possible the rock units existing in the field (Amadi *et al.*, 2012). One of the ways to achieve greater accuracy in facies delineation is by the use of radiation (alpha, beta and gamma) emanating from the decay of radioactive element contained in the rock unit. The most useful of these radiations in radiometric survey are gamma radiations.

2.8 Summary of Literature Review

Nigeria has very challenging needs for energy, where the generation is far less than the demand. There is inequitable access by the citizens to the meagre and unstable electricity services in the country. With the main power generating source being gas-fired thermal power stations and despite her increasing population of over 170 million, Nigeria's energy generation capacity dwindle to as low as between 2,800 and 5,700 MW (Akinsoji, 2016). Alternative energy sources (preferably renewable sources) would provide some relief to the current energy challenge (Akinsoji, 2016). Uninterrupted energy supply is a vital issue for all countries today and future economic growth depends crucially on the long–term availability of energy from sources that are affordable, accessible and environmentally friendly (Akinsoji, 2016). A lack of access to energy can contribute to economic decline. Availability of energy sources would give rise to good productivity, income growth, good education and health (Bhattacharyya and Leu, 1975). In the African continent, Nigeria has one of the lowest consumption rates of electricity per capita (Abraham and Nkitnam, 2017).

Geothermal energy is important in the long–term vision of providing secure, abundant, cost effective and clean sources of energy for Nigeria. Recent evaluation indicates that Nigeria has generation capability of 5,700 MW; 86% of the capability comes from gas–fired thermal power stations. The remaining 14% is from the three large hydroelectric power stations in the country (Akinsoji, 2016). At present, there are no installed geothermal plants in Nigeria.

Below the Curie temperature is when the magnetic features of rocks can exist. Curie point is defined as the temperature (580^0C and above) at which magnetic minerals lose their magnetic properties or susceptibility as a result of high temperature (Stampolidis and Tsokas, 2002; Nwankwo *et al*., 2011). This temperature varies for different rock types. Present day geothermal studies have indicated that Curie point can be reached at depths 30 to 40km beneath the earth. Based on these assumptions, it is estimated that all crustal rocks are very potent to carry magnetic features. Reeves (1989) suggested that the upper mantle has no magnetic properties hence the earth's crust may be effective depth where magnetic sources can be found. Apart from being used in delineating architectural framework of the earth's subsurface geology, aeromagnetic method can be applied successfully in defining geothermal gradient and geothermal heat flow of an area via spectral analysis (Okubo and Matsunaga, 1994; Ofor and Udensi, 2014).

The study area is located in the middle part of the Benue Trough of Nigeria. It is bounded by latitudes 7^030^l N to 9^000^l N and longitudes 8^030^l E to 10^000^l E (Figure 2.2 (a) and (b)). This present study concerns the evaluation of the total aeromagnetic anomalies for estimation of curie-temperature depth and heat flow to investigate the geothermal energy potential of parts of the Middle Benue Trough Nigeria, which has in the past received limited attention. Geophysical studies in the study area are limited, with little records of crustal temperature studies. Curie-temperature depth combined with heat flow assessment would complement greatly the geophysical information of the area to bridge the gap of lacking crustal

temperature information. According to Negi *et al*., 1983 and Tanaka *et al*., 1999, the depths to magnetic sources are related to the slopes of the line segment. In estimating the depth to centroid of the magnetic source and depth to the top of magnetic source, both the longest wavelength and second longest wavelength parts of the spectral segments are considered (Negi *et al*., 1983; Okubo *et al*., 1985 and Tanaka *et al*., 1999). The longest wavelength part produces the depth to centroid, while the second longest wavelength produces the depth to top of magnetic source.

Obande *et al*., 2014, attempted to investigate the geothermal potential of the Wikki Warm Spring area; which is near the study area, using aeromagnetic data. They applied the spectral method to determine the depths to the top and centroid of magnetic sources in the study area. The power spectrum of magnetic anomalies was used to estimate the basal depth of the magnetic sources. Their results showed an average estimated Curie Point Depth of 8 km and geothermal gradient of 68^0C/km with heat flow values averaging 170mW/m^2. The other aspect of geothermal exploration in Nigeria is the investigation of thermal springs and seepages, which occur mainly within sediments of the Middle and Upper Benue Trough. The water of the warmest springs in this area: Akiri and Ruwan Zafi have the temperature of about 54°C and it suggests the occurrence of some geothermal anomalies (Ikechukwu *et al*., 2015; Abraham and Nkitnam, 2017).

All detectable gamma radiation from earth materials come from the decay of naturally occurring radionuclides; that is uranium (U^{238}), thorium (Th^{232}) and potassium (K^{40}) [Coker *et al*., 2014]. The product of this decay results in the emission of alpha, beta and gamma radiations which can be detected on the surface using radioactive element detectors. The goal of radiometric survey is to recognize and understand radiometric signatures associated with the host rocks important to mineralization and heat in the subsurface (Beamish and Busby, 2016). Beamish and Busby, 2016 stated that, both magnetic and radiometric surveys can be

used for geothermal exploration. Aeromagnetic and aeroradiometric data were used to correlate the geothermal heat flow and radioactive heat production of the Anambra basin to ascertain if areas with high geothermal heat flow values corresponds with that of the radioactive heat production (Olorunsola and Aigbogun, 2017). Radioactive decay of rocks is the greatest overall source of heat in the earth's crust, although there are other sources that may be peculiar to specific areas (Jessop, 1990). Ajibade and Fitches, 1988 revealed that warm springs which serve as indicators for geothermal energy potential are Akiri (within the study area) Wikki and Ruwan Zafi warm springs (near the study area).

CHAPTER THREE

MATERIALS AND METHODS

3.1 Data Acquisition and Processing

Both the aeromagnetic and aeroradiometric data sets were obtained from the Nigerian Geological Survey Agency (NGSA) in digitized form. The data sets were from the new high-resolution airborne survey coverage in Nigeria carried out by Fugro Airborne Surveys between 2006 and 2009 for the Nigerian Geological Survey Agency. The aeromagnetic and aeroradiometric surveys were flown along a series of NW-SE flight lines, spaced 500m, with 2000m tie-line spacing in a NE-SW direction and 80m nominal flight height. The data were recorded at 0.1 second interval. Since the survey was flown closer to ground (80m flight height) with narrow line spacing and very small recording interval, the resolution of anomalies is more superior to that of conventional high-altitude surveys. It consists of nine square map sheets: [210 (Wamba), 211 (Kwolla), 212 (Shendam), 231 (Lafia), 232 (Akiri), 233 (Ibi), 251 (Makurdi), 252 (Akwana) and 253 (Wukari)]. Each square block represents a map on the scale of 1:100,000 and is (55x55) km^2 covering an area of 3,025 km^2, hence the study area is 27, 225 km^2.

All magnetic data corrections were carried out by Fugro Airborne Surveys. The geomagnetic gradient was removed from the aeromagnetic data using the January 2005 International Geomagnetic Reference Field (IGRF) model referenced to the World Geodetic System, 1984 ellipsoid. The aeromagnetic data were geo-referenced to the Universal Transverse Mercator (UTM) coordinate system for comparative study with geologic map of the study area. Acquisition, processing and compilation of the high resolution aeromagnetic and aeroradiometric data were jointly financed by the Federal Government of Nigeria and the World Bank as part of the Sustainability Management for Mineral Resources Project (SMMRP) in Nigeria.

The first step in the present study is to assemble the nine aeromagnetic maps covering the survey area to form a composite map (Figure 3.1). The next step is to contour the map to produce the total magnetic intensity (TMI) anomaly map. The contouring was done using contouring software (Surfer Version 32).

Figure 3.1: The composite aeromagnetic map

Similarly, the nine radiometric data sheets were later contoured to produce one map for each of the three radiometric elements, potassium (K), thorium (Th) and Uranium (U). From the heat calculations, a single radiometric heat map was later produced.

3.2 Separation of Aeromagnetic Data

The contoured total magnetic intensity (TMI) map contains both the regional and residual anomaly. The regional gradient was removed from the map by fitting a linear surface to the aeromagnetic data using a multiple regression technique.

The surface linear equation on the data can be given according to Likkason (1993) as:

$$p(x, y) = ax + by + c \tag{3.1}$$

Where, a, b and c are constants; x and y are distances in x and y axes;

$p(x, y)$ = the magnetic value at x and y co-ordinates.

The Least squares method of statistical analysis was used to obtain the constants (a, b and c).

The trend surface equation was then subtracted from the aeromagnetic (observed) data and the resultant residual aeromagnetic anomaly data was obtained and contoured.

3.3 Data Enhancement Techniques

Usually, the original total magnetic intensity grid is visually difficult to observe and interpret the various structures. A variety of enhancement techniques when applied to geophysical data tends to improve the data quality on the basis of mathematical principles. Mathematical enhancement filters which include downward and upward continuation, reduction to the pole, analytical signal, vertical derivative, etc. are extremely helpful in developing near surface geological features except that their restrictions are based on the value of the data and extra reasons like the angle the earth's magnetic field makes with the horizontal (angle of inclination) and angle between the vertical component and the true north (magnetic declination).

3.3.1 Continuation Techniques

Potential fields known at a set of points can be expressed at neighbouring higher or lower spatial locations in a source free region using the continuation integral that results from one of the Green's theorems (Blakely, 1995). The principal uses of this concept are to adjust altitude of observations to a datum as an aid to the interpretation of a survey, reduce short-wavelength data noise by continuing the field upward, and increasing the horizontal resolution of anomalies and their sources by continuing the field downward.

Continuation methods project the observed potential (gravity and magnetic) anomaly field to higher elevations (upward continuation) or lower elevations (downward continuation) and therefore, effectively serve as low-pass and high-pass filters respectively (Khalil, 2012), which have been applied in numerous applications (Li and Devriese, 2009; Li *et al*., 2013).

The main advantage of the continuation methods is that the character of the geopotential field anomaly is retained as long as the continuation does not extend into the sources (Khalil, 2012). This method is strongly dependent on the sampling interval of the original data and is able to downward-continue only to very shallow depths equal to 2-10 times of the sampling spaces.

Applications also vary widely; from environmental and exploration applications involving short-wave length anomaly fields over small height differences (a few meters to kilometres) to global distribution of anomalies measured by satellites in which anomalies are downward continued from satellite altitudes (300-700km) to earth's surface.

The effect of upward/downward continuation process on the fields can be understood by examining the continuation operator in the wavenumber domain. According to Dean, (1958), the operator has the form a $e^{+-/k/z}$ or $e^{+-2\pi\lambda z}$

Where /k/ is the wavenumber (/k/ = $2\pi\lambda$),

λ is the full wavelength and

Z is the continuation level

The negative sign in the exponent indicates upward continuation (away from the sources of the field) and the positive sign implies the downward continuation of the sources of the field.

(a) Downward Continuation

In downward continuation, the long-wavelength (deeper magnetic sources) anomalies in magnetic data are suppressed; while the shorter wavelengths (shallow magnetic features) are improved or enhanced. Downward continuation is a mathematical procedure that computes magnetic field at a lower level. This process emphasizes shorter wavelengths, but can be unstable and produces artefacts.

Downward continuation enhances the responses of source at a depth by effectively bringing the plane of measurement closer to the source. Downward continuation

highlights the components of higher wave-number, increases the anomaly resolution of the individual sources and provides a more accurate determination of both horizontal and vertical extents of near-surface magnetic sources (Boschetti, 2005). But, its usefulness depends on the elimination of noise, as the computation of downward continuation is unstable and easily distorts the true feature of potential field data (Fedi and Florio, 2001, 2002, 2013).

(b) Upward Continuation

In upward continuation, the shallow feature (i.e. short-wavelength) anomalies are suppressed and the long-wavelength (deeper sources) anomalies are enhanced. Upward continuation is a method used to separate regional magnetic anomaly resulting from deep sources from the observed magnetic anomaly data. Upward continuation of the data attenuates high wavenumber anomalies associated with shallow magnetic sources allowing easy interpretation of deep magnetic sources. Upward continuation is a stable computation, at higher heights, which is the contribution of the most extended sources (Pal et al., 1978).

This is a mathematical technique that project data taken at an elevation to a higher elevation. Upward continuation was employed in potential field interpretation in order to determine the form of regional variation over the study area. Upward continuation is a straight forward operation because the projection is into a force free region. Upward continuation was applied to suppress the effects of small scale features near the surface and also to reduce topographic effects.

3.4 Application of Discrete Fourier Transform (DFT) method

The Fourier Transform theory is named after Joseph Fourier who propagated the theory. The Fourier Transform theory states that the amplitude Y_i, at a point X_i is determined by the sum of the amplitudes of the component sine and cosine waves at a distance X_i from the origin of

the series. The Fourier Transform of geophysical data is a mathematical operation that converts time series data to frequency dependent data. It is aimed at converting a spatial (real space) data into a frequency data. It decomposes a function into simpler pieces and is applied to regularly spaced data such as aeromagnetic data. The main signal (or raw data), are composed of three parts:

(i)   a linear trend - drift in the average value of the signal

(ii)   a signal - periodic or cyclic components

(iii)   Noise - the random components.

Trend removal is necessary in the method of Fourier analysis and may be accomplished by converting the time series to the deviations from a fitted straight line. This was done during the separation of the digitized data (see equation 3.1). Fourier analysis extracts the dominant periodic components. After removing the trend, the remaining part of the time series consists of a signal (the periodic components) and noise (the random components). Therefore, a periodic function such as a sinusoidal wave can be represented by a Fourier series.

For simple sequences such as;

$$f(x) = a_1 \cos(x) + a_2 \cos(2x) \dots \dots + a_n \cos(nx) + b_1 \sin(x) + b_2 \sin(2x) \dots \dots +$$

$$bnsin\,(nx) \qquad\qquad 3.2$$

The Fourier series is:

$$f(x) = a_0 + \sum_{n=1}^{\infty} \left(a_n \cos\frac{2n\pi x}{L} + b_n \sin\frac{2n\pi x}{L} \right) \qquad\qquad 3.3$$

In geophysical data, according to Davis (2014);

$$f(x) = Y_i, \text{ then } Y_i = a_0 + \sum_{n=1}^{N} \left(a_n \cos\frac{2n\pi x}{L} + b_n \sin\frac{2n\pi x}{L} \right) \qquad\qquad 3.4$$

Where:

$Y_i(x)$ = the amplitude at a point x_i

x_i = position distance along x axis

L = length of the cross-section of the anomaly (or wavelength of the sampling distance)
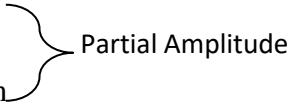
n = harmonic number of the partial wave (or the frequency of the partial wave)

(Note: n should not exceed the Nyquist frequency; Nyquist frequency ≈ L/2. If

Nyquist frequency is exceeded, there will be a spectral folding i.e. repetition of

transformed data)

N = number of data points

a_n = real part of the amplitude spectrum

b_n = imaginary part of the amplitude spectrum — Partial Amplitude

(Where a_n and b_n are coefficients of the first harmonic or partial amplitudes)

i = 0, 1, 2, 3, … n

The Partial amplitudes (a_n and b_n) are calculated using the following equations according to Davis (2014):

$$a_n = 2/N \sum_{n=1}^{N} Y_i \cos \frac{2n\pi x}{L} \hspace{4cm} 3.5$$

$$b_n = 2/N \sum_{n=1}^{N} Y_i \sin \frac{2n\pi x}{L} \hspace{4cm} 3.6$$

Hence, the main amplitude spectrum (A_n) is given according to Davis (2014) as:

$$A_n = \sqrt{a_n^2 + b_n^2} \hspace{5cm} 3.7$$

3.5 Estimation of Depth to Magnetic Basement

In order to estimate depths to basement (sedimentary thicknesses) across the study area using spectral methods, several profiles were taken cutting across anomalous features for the interpretation of the geophysical anomalies in the area under study. The anomalies identified on these profiles were then subjected to the spectral analysis. The Discrete Fourier Transform

is the mathematical tool for spectral analysis and is applied to regularly spaced data such as the aeromagnetic data.

Equations 3.5 to 3.7 were applied for the calculation of the partial amplitudes (a_n and b_n) and the main amplitude spectrum (A_n).

Graphs of the natural logarithms of the main amplitude (A_n) against frequency (n) were plotted and the linear segments from the low frequency portion of the spectral were drawn from the graphs. The gradient of the linear segments were computed and the depths to the basement were determined using the equation according to Negi *et al.* (1983), given as;

$$Z_t = -ML/2\pi \qquad\qquad 3.8$$

Where,

Z_t = depth to the basement (depth to top)

M = gradient of the linear segment

L = length of the cross-section of the anomaly.

The essence of quantitative interpretation is to obtain information about the depth to magnetic sources, its shape and size, subsurface temperature and probably details about the susceptibility of the magnetic sources. The most important parameter in the quantitative interpretation is the depth of the anomalous body. Other parameters like temperature (or heat) and susceptibility are secondary. The shape of the anomaly contains information on depth to source of the anomaly. Due to the obvious importance of the sedimentary thickness to the petroleum geophysicist, the depth to source normally called the depth to the magnetic basement, is of vital importance. Depth information may also be important when potential mineral deposits are covered by thick layer of consolidated or unconsolidated overburden.

In the present study, the parameters needed are the depth-to-top of magnetic source, depth to centroid, depth to base (or depth to bottom) of magnetic source which is known as Curie point depth. Curie point depth is the depth at which magnetic minerals lose their magnetism

due to the effect of temperature (temperature range of 530^0C to 580^0C is taken as the Curie point temperature). In order to estimate depths to basement across the study area using the spectral (Fourier) method, many profiles were later taken on the residual aeromagnetic anomaly map of the study area.

3.6 Curie Point Depth Estimation

The methods for estimating the depth extent of magnetic source are classified into two categories; those that examine the shape of isolated anomalies (Bhattacharyya and Leu, 1975) and those that examine the patterns of the anomalies (Spector and Grant, 1970). However, both methods provide the relationship between the spectrum of the magnetic anomalies and the depth to magnetic sources by transforming the spatial data into frequency domain. In this research work, the method used is the later. To obtain the depth to Curie point, spectral analysis of 2-dimensional Fourier transform of the aeromagnetic data has to be performed.

To carry out spectral analysis, several profiles were taken on the residual aeromagnetic anomaly map of the study area. The method was chosen because of its advantage of filtering all the noise away from the data. Seven (7) selected magnetic profiles were used for detailed interpretation. The analysis was carried out using computer software Microsoft Excel 2010.

To perform the analysis, the first step is to estimate the depth to centroid (Z_o) of the magnetic source from the slope of the longest wavelength (slope of the low frequency component) part of the energy spectrum. The second step is the estimation of the depth to the top (Z_t) of the magnetic source from the slope of the second longest wavelength (slope of the high frequency component) part of spectral segment (Okubo, Graff, Hansen, Ogawa and Tsu, 1985). Then, the depth to base (Z_b) of magnetic sources in the study area is assumed to be Curie point depth (CPD) (Bhattacharyya and Leu, 1975; and Okubo *et al*., 1985). The depth to base (Z$_b$) of the magnetic source is calculated from the equation below according to Okubo *et al*., (1985),

$$Z_b = 2Z_o - Z_t \qquad\qquad 3.9$$

Where,

Z_o is the centroid depth (depth to centre of magnetic source),

Z_t is the depth to top of magnetic source (sedimentary thickness) and

Z_b is the basal depth (depth to the bottom of magnetic source)

3.7 Estimation of Heat flow and geothermal gradient

To calculate the heat flow and geothermal gradient values we use the Fourier's law according to Tanaka *et al., (*1999) with the following formula;

$$Q = \lambda dT/dZ \qquad\qquad 3.10$$

Where,

Q is the geothermal heat flow and λ is the thermal conductivity (given as 2.5 W/m^{0}C).

In this equation, it is assumed that the direction of the temperature variation is vertical and the temperature gradient *dT/dZ* is constant as there is no heat gain or heat loss above the crust and below the Curie point depth. According to Tanaka *et al*., (1999), the Curie temperature (θ_c) was obtained from the Curie point depth (Z_b) and the thermal gradient $^{dT}/_{dZ}$ using the following equation;

$$\theta_c = \{dT/dZ\}Z_b \q\qquad\qquad 3.11$$

Provided that there are no heat sources or heat sinks between the earth's surface and the Curie-point depth, the surface temperature is 0^0C and $^{dT}/_{dZ}$ is constant. The Curie temperature (the temperature at which rocks loose their spontaneous magnetization) depends on magnetic mineralogy. Although the curie temperature of magnetite (*Fe$_2$0$_4$*), in view of that, the Curie temperature is approximately 580^0C, and an increase in Titanium (*Ti)* content of Titanomagnetite (*Fe$_{2-x}$, Ti$_x$0$_3$*) causes reduction in Curie temperature (Nwankwo *et al*., 2011).

In addition to the above, from equation (3.10) and (3.11), a relationship was determined between the Curie point depth (Z_b) and the heat flow (Q) as follows;

$$Q = \{Z_b/\theta_c\}\lambda \qquad\qquad 3.12\ (a)$$

In this equation, the Curie point depth is inversely proportional to the heat flow, Tanaka *et al*, 1999; Stampolidis *et al*., 2005). In this research, the Curie point temperature of 580^0C and thermal conductivity of 2.5 W/m^{0}C as an average for igneous rocks was used as standard (Nwankwo *et al*., 2011) in the study area.

Equation (3.11) was utilized to compute the geothermal gradient of the region as the ratio of Curie temperature to Curie point depth.

Hence, according to Tanaka *et al.,* (1999), we have:

$$\frac{dT}{dZ} = \frac{\theta_c}{Z_b} \qquad\qquad 3.12\ (b)$$

Where,

dT/dT is geothermal gradient,

Z_b is the basal depth and

θ_c is the standard Curie point temperature of 580^0C

 The relationship between Curie point depth and Heat flow was determined by constructing graphs of Heat flow versus Curie depth and Heat flow versus geothermal gradient.

3.8 Radiometric Data Processing

Radiometric Heat Analysis:

Radioactive heat production from radiometric data is given according to (Salem and Fairhead, 2011) by the expression:

$$A(\mu W/m^3) = \rho(0.0952C_U + 0.0256C_{Th} + 0.0348C_K)$$ 3.13

Where,

A = radiometric heat (in μW/m³)

ρ = density of rock in kg/m² (Telford *et al.*, 1990)

C_U, C_{Th} and C_K are the concentrations of uranium, thorium and potassium (in ppm for C_U and C_{Th}, and % for C_K) respectively.

The concentration of the three radiometric elements is read from the radiometric map covering the nine (9) sheets adopted for magnetic data processing.

The value of the radiometric element's concentration and various rock densities are applied in equation (3.13) to compute the radioactive heat for the study area.

3.9 Method of Interpretation

The methods of interpretation employed in this study were; the qualitative and quantitative interpretation methods. The two methods are discussed below.

3.9.1 Qualitative Interpretation

The qualitative interpretation of the aeromagnetic data was done by visual inspection of the total magnetic intensity map (TMI), the residual anomaly map, the upward continuation map and the magnetic lineament map. The following features were noted during the qualitative interpretation:

    a. The trend of contours.

    b. The positive and negative values of the contours.

    c. The maximum and minimum values of the contours and their aerial extent.

    d. The direction of the magnetic structures.

There are three important features in qualitative interpretation, these are;

    a. The alignment of closed anomalies suggests the presence of magnetic bodies.

    b. The alignment of lateral shift suggests faulting and presence of local fractured zones.

c. Sharp changes in contour gradient defines structural trend.

3.9.2 Quantitative Interpretation

A full quantitative interpretation of the aeromagnetic data was carried out in the study area. The quantitative interpretation was aimed at obtaining information about the depth to magnetic sources (depth to top and bottom), its shape and size, and susceptibility. The reason for obtaining these parameters is to estimate the sedimentary thickness variations, calculate the Curie temperature depths and associated geothermal gradient and heat flow. These methods can reveal the origin of hot springs within or close to the study area and petroleum potentials of the study area as well. To achieve the needed interpretation, the spectral method was adopted.

The application of radiometric surveying is useful in geothermal energy potential investigation because of its ability to detect radioactivity emanating from the natural decay of elements such as uranium, thorium and potassium from the earth material. The product of this decay results in the emission of alpha, beta and gamma radiations which can be detected on the surface using radioactive element detectors. The study of radiometric heat production and geothermal heat flow (estimated from magnetic data) are the main tools for the identification and location of geothermal resources. The radiometric heat in the study area was calculated using equation 3.13, by substituting the values of potassium, k, thorium, Th, and uranium, U concentrations obtained from the radiometric data and densities of various rocks in the study area.. The result of this analysis shows the areas of high and low radioactive heat in the study area which was compared with the result of heat flow obtained from the aeromagnetic analysis. These analyses helped in delineating the areas of high anomalous heat in the area which are the geothermal potential areas.

CHAPTER FOUR

RESULTS AND DISCUSSION

4.1 Qualitative Interpretation
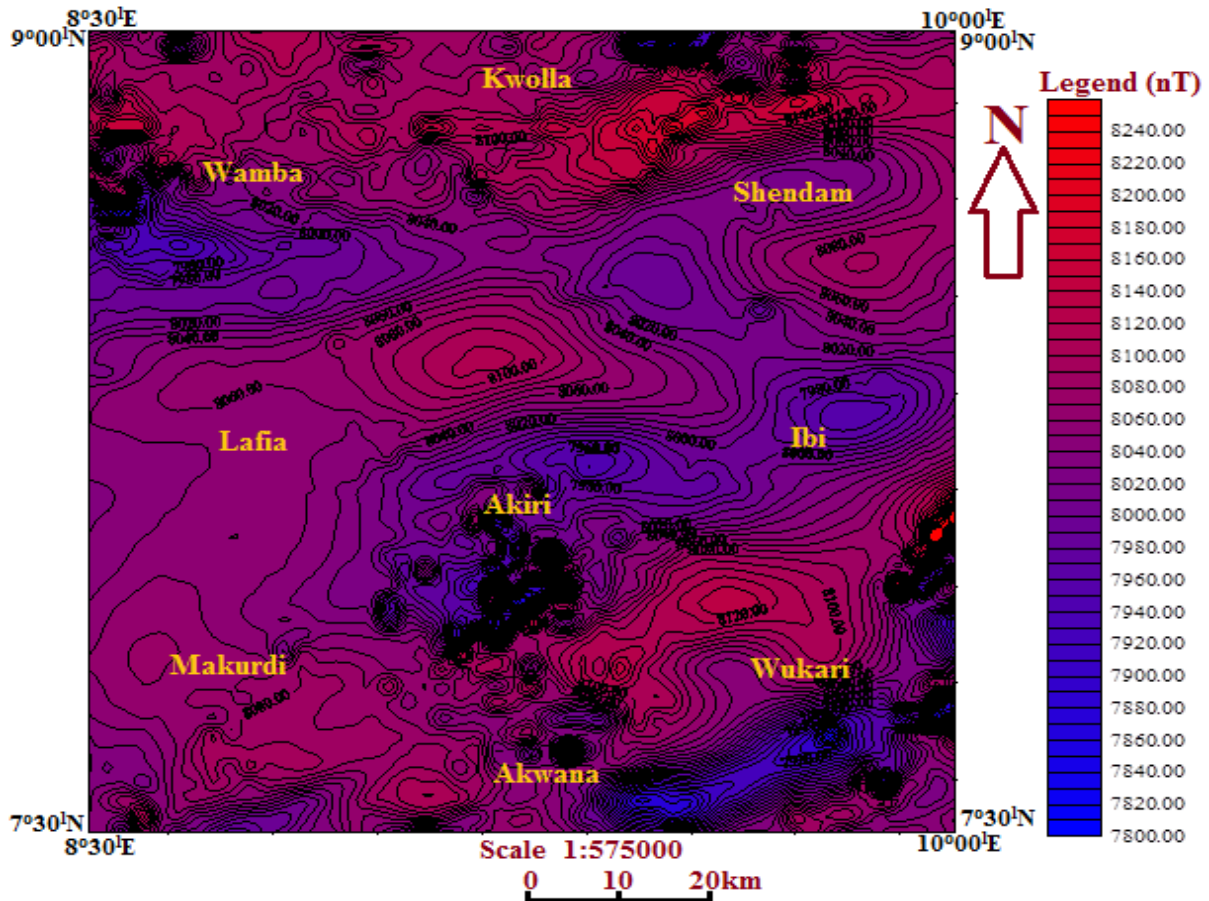
Figure 4.1: Total Magnetic Intensity (TMI) Map of the Study Area

[Contour Interval = 10 nT]

The Total Magnetic Intensity (TMI) map of the study area is shown in Figure 4.1. The total magnetic field from the study area ranges from 7800 to 8240 nanotesla (nT). Higher values (shown in red) are found in the northern, north central, western, south western and southern parts of the study area; while lower magnetic intensity values (shown in blue) are found in the northwest, northeast, central and south-eastern regions.
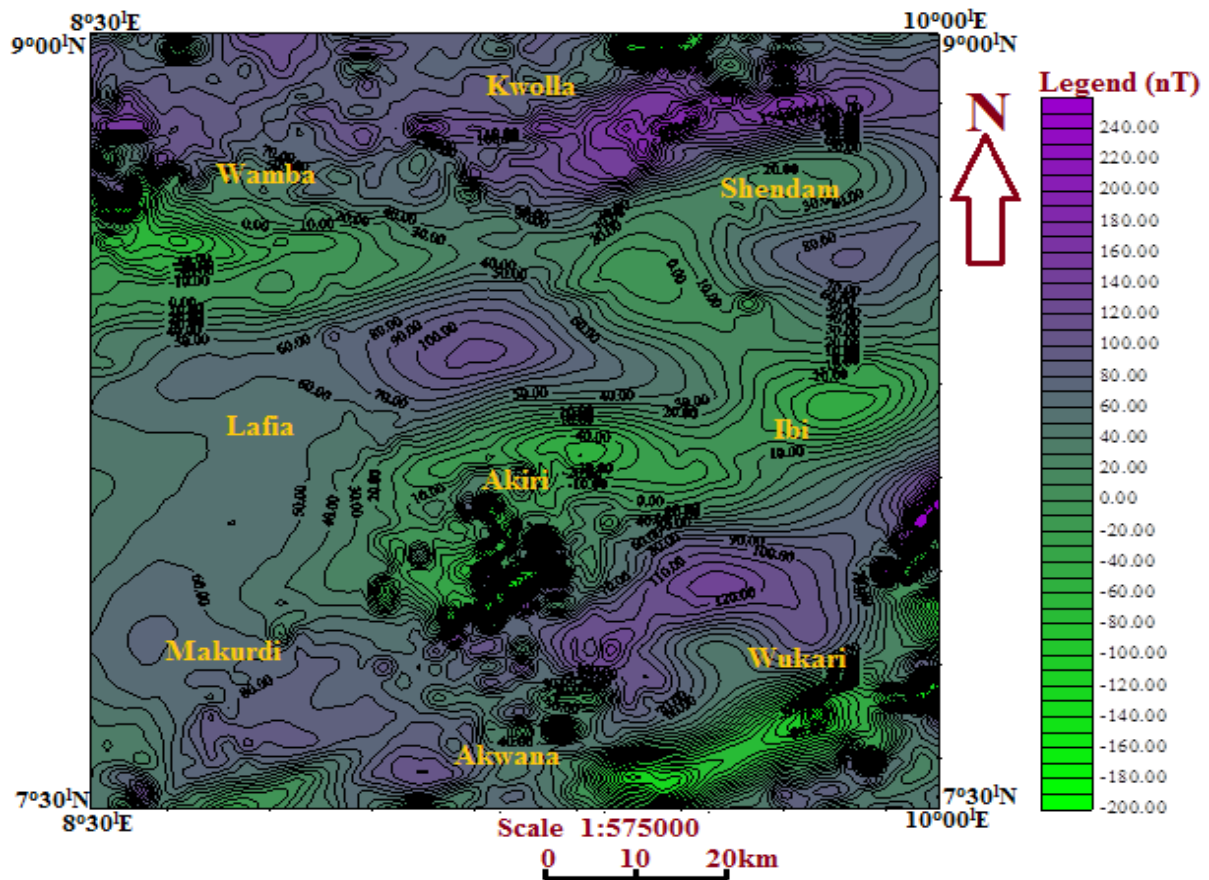
Figure 4.2: Residual Anomaly Map of the Study Area [Contour Interval = 10 nT]

The residual anomaly map of the study area is shown in figure 4.2. The study area is characterized by closely spaced linear sub-parallel contours which suggest that faults or local fractured zones may possibly pass through such areas. The general trending fabric of the TMI anomalies is northeast (NE) to southwest (SW) direction. The residual magnetic field map shows a general trending fabric of NE to SW direction similar to those of the TMI map. The elliptical contour closures seen in the study area suggests the presence of magnetic bodies. These features represent geologic lineaments and their positions are indicated by lines drawn parallel to the elongation and through the centre of the anomalies represented in Figure 4.5.

The residual anomaly map shows that the contour lines are widely spaced in the NW, West and SW parts of the study area which shows that there are thicker sediments in those regions

(Wamba, Lafia, and Makurdi), indicating that the depth to basement is deeper in these areas compared to the areas where there are closely spaced contours which suggests shallow sedimentary thickness. Figure 4.2 also shows positive magnetic anomalies in areas like Wamba, Lafia and Makurdi which suggests deeper depths in such areas, while areas around Shendam, Ibi and Akiri show negative anomalies which indicates shallower depths to magnetic bodies.
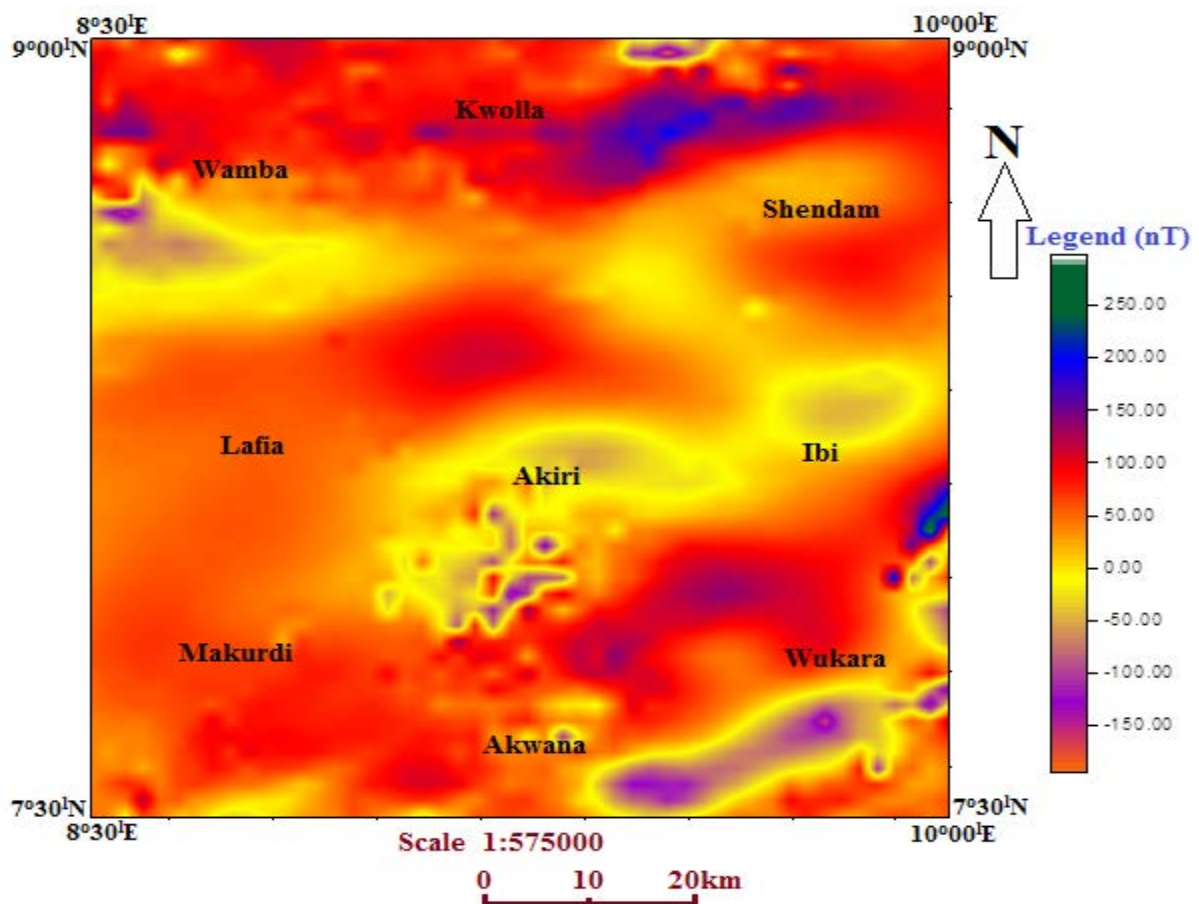
Figure 4.3: Upward Continuation Map of the study area

In upward continuation, the shallow feature (i.e. short-wavelength) anomalies are suppressed and the long-wavelength (deeper sources) anomalies are enhanced. Upward continuation is a method used to separate regional magnetic anomaly resulting from deep sources from the observed magnetic anomaly data. Upward continuation of the data attenuates high wavenumber anomalies associated with shallow magnetic sources allowing easy

interpretation of deep magnetic sources. Upward continuation was applied to suppress the effects of small scale features near the surface and also to reduce topographic effects. The Upward Continuation map of the study area (Figure 4.3) shows areas with highest magnetic intensity in blue colour (near Kwolla), Wamba (north), Lafia, Makurdi and Akwana have higher intensity (red colour), while Akiri, Ibi, Wukari and Wamba (south) have lowest intensities (yellow colour).
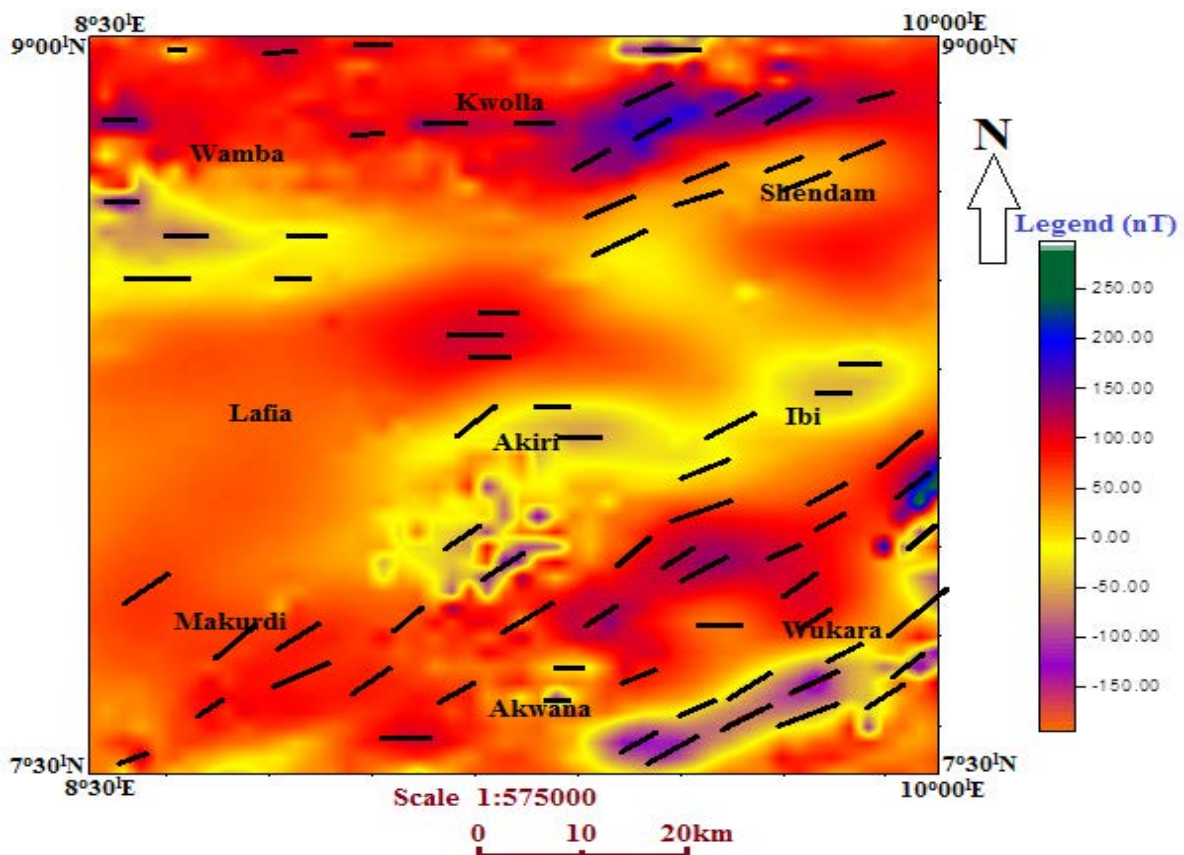
Figure 4.4: Superimposed Magnetic lineament map onto Upward Continuation map within the study area
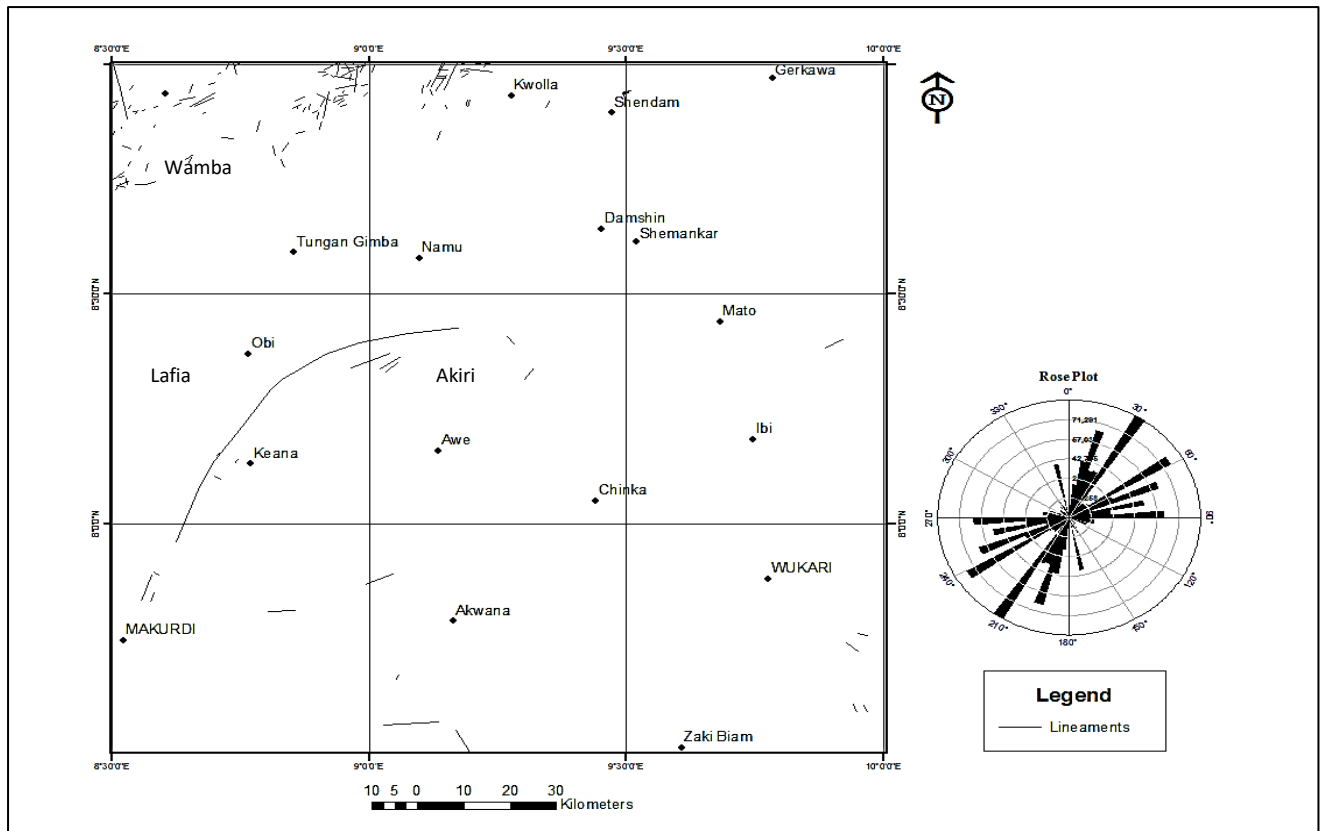
Figure 4.5: Lineament map of the study Area with Rose Diagram

Figures 4.4 and 4.5 show that the main trend of the lineaments is NE-SW, while minor ones trend E-W and NNE-SSW directions. The major anticline identified on the map (Figure 4.5) coincide with the Keana Anticline, trends NE-SW and extends from northeast of Makurdi via north of Keana to the north of Awe (Akiri). Three minor anticlines close to the major one with axis trending NE-SW also occurs. In addition, the geological structures (magnetic lineaments and dykes) are relatively long suggesting that they are regional structures (Anudu, *et al*., 2014). The main structural trends (NE-SW and E-W) agree with the magnetic trend results.

4.2 Quantitative Interpretation

4.2.1 Aeromagnetic Interpretation
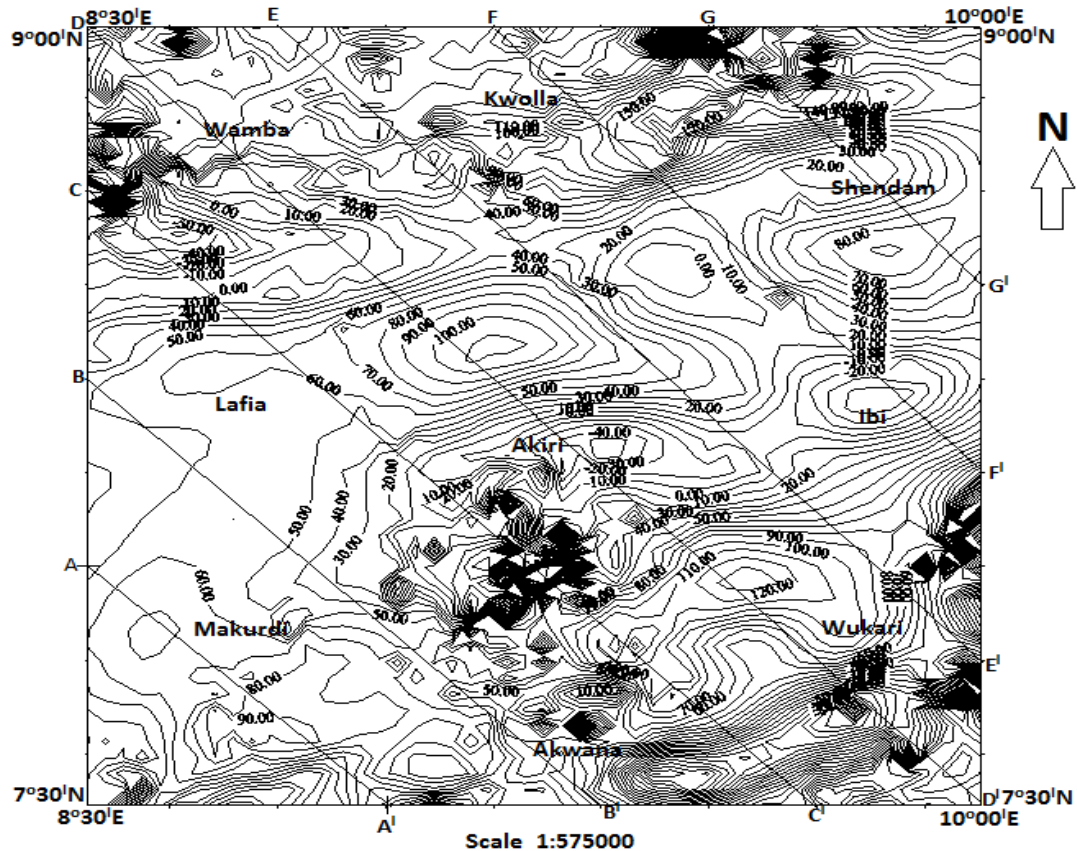
Figure 4.6: Residual Anomaly Map of Study Area Showing the Profile Lines (Contour Interval = 10 nT)

Figure 4.6 shows the residual anomaly map of the study area with profile lines. Seven (7) profile lines (or cross-sections), namely AA^l - GG^l were taken in the northwest-southeast (NW-SE) direction, and used for detailed interpretation. The cross-sections were taken perpendicular to the direction of the contours so as to obtain clear information about the anomalies.
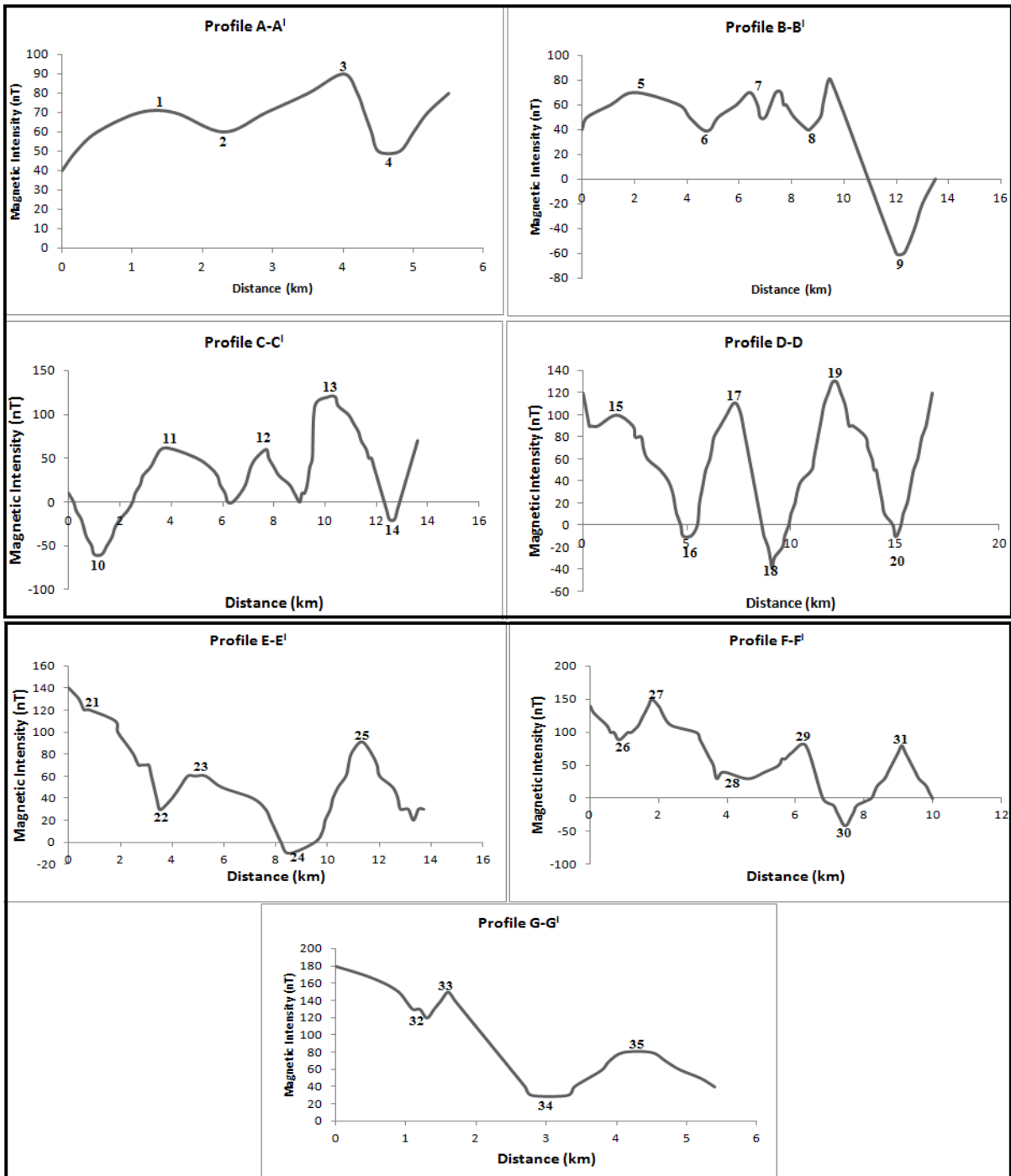
Figure 4.7: Magnetic Anomaly Graphs shown on Profiles A-A^l to G-G^l

Figure 4.7 shows the magnetic anomaly graphs drawn on profiles A-A^l to G-G^l. Using the Microsoft Excel package, the graphs of magnetic intensity against distance on the cross-sections (profiles) were drawn to show the nature of magnetic anomalies found in the study area.

4.2.2 Interpretation of the Profiles and Anomaly Graphs

All the profiles taken run in the NW-SE direction. This direction was chosen so that the profile lines will be perpendicular to the direction of the magnetic contours (Figure 4.6). The profiles taken across the study area were interpreted as below.

4.2.2.1 Profile A-A[I]

The profile passes through Makurdi (sheet 251) which is in the south-western part of the study area. The maximum magnetic intensity value along the profile is 90nT and the minimum value is 40nT (Figures 4.6 and 4.7).

4.2.2.2 Profile B-B[I]

This profile passes through the south-western part of the study area. It cuts across Lafia, Makurdi and Akwana areas (sheets 231, 251 and 252 respectively). The maximum magnetic intensity value along this profile is 80nT and the minimum value is – 60nT (Figures 4.6 and 4.7).

4.2.2.3 Profile C-C[I]

This profile passes through Wamba (in the NW), Lafia (in the West), and Akwana (in the southern part of the study area). The maximum magnetic intensity value along this profile is 125nT, while the minimum value is – 60nT (Figures 4.6 and 4.7).

4.2.2.4 Profile D-D[I]

The profile D-D' cuts across Wamba (NW), Akiri (Central) and Wukari (SE). The maximum magnetic intensity value along this profile is 135nT and the minimum value is -38nT (Figures 4.6 and 4.7).

4.2.2.5 Profile E-E^l

This profile passes in-between Wamba and Kwolla, Akiri and Ibi, and cuts across Wukari in the south-eastern part of the study area. The maximum magnetic intensity value along this profile is 140nT and the minimum value is -10nT (Figures 4.6 and 4.7).

4.2.2.6 Profile F-F^l

This profile passes through Kwolla and Shendam in the NE and Ibi in the East. The maximum magnetic value along the profile is 150nT and the minimum value is -40nT (Figures 4.6 and 4.7).

4.2.2.7 Profile G-G^l

The profile runs in the extreme north-eastern part of the study area. It passes through Shendam area (sheet 212). The maximum magnetic intensity value along this profile is 180nT and the minimum value is 30nT (Figures 4.6 and 4.7).

4.2.3 Spectral Graphs
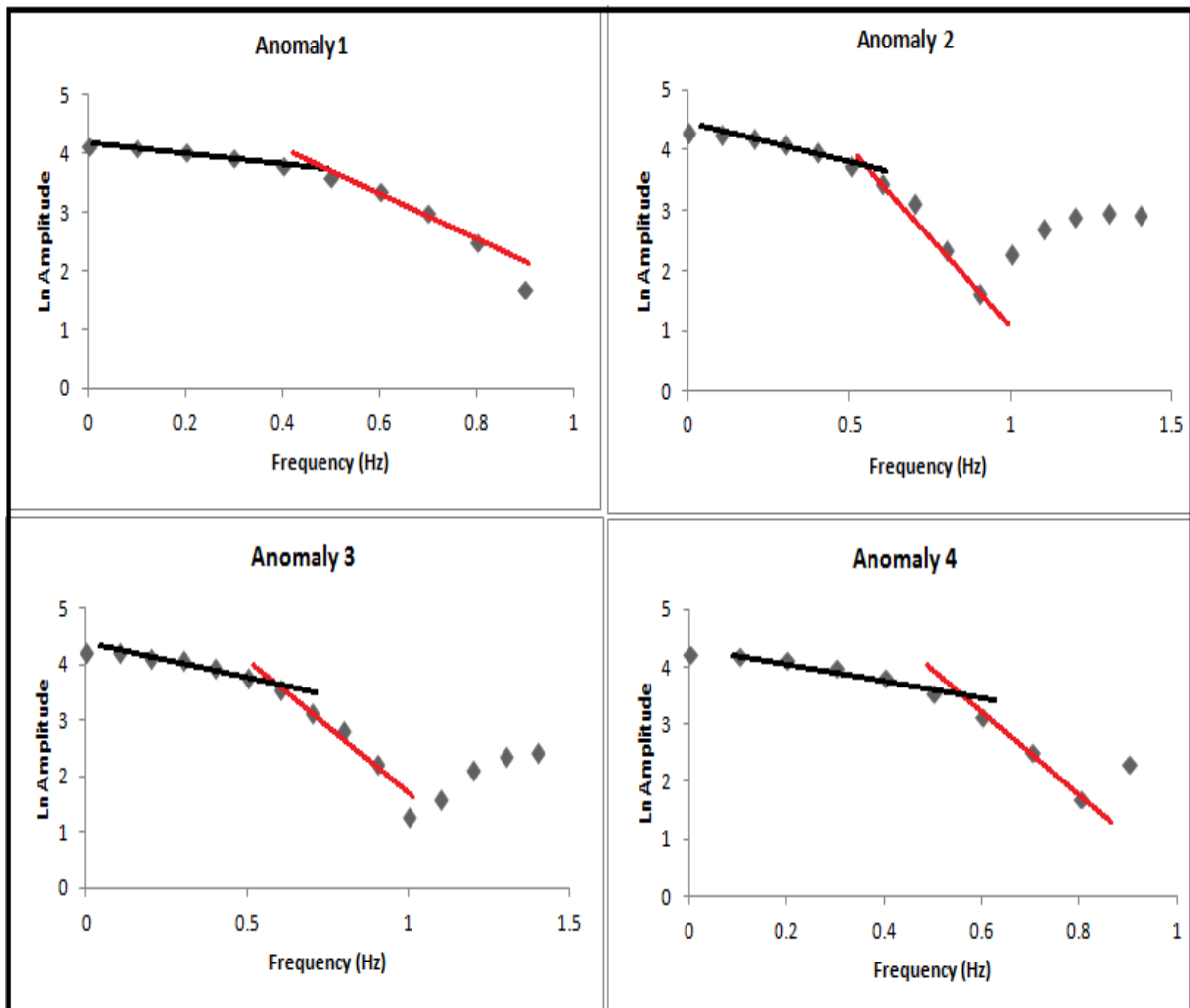
Figure 4.8(a): Spectral graphs of profile A-A^l
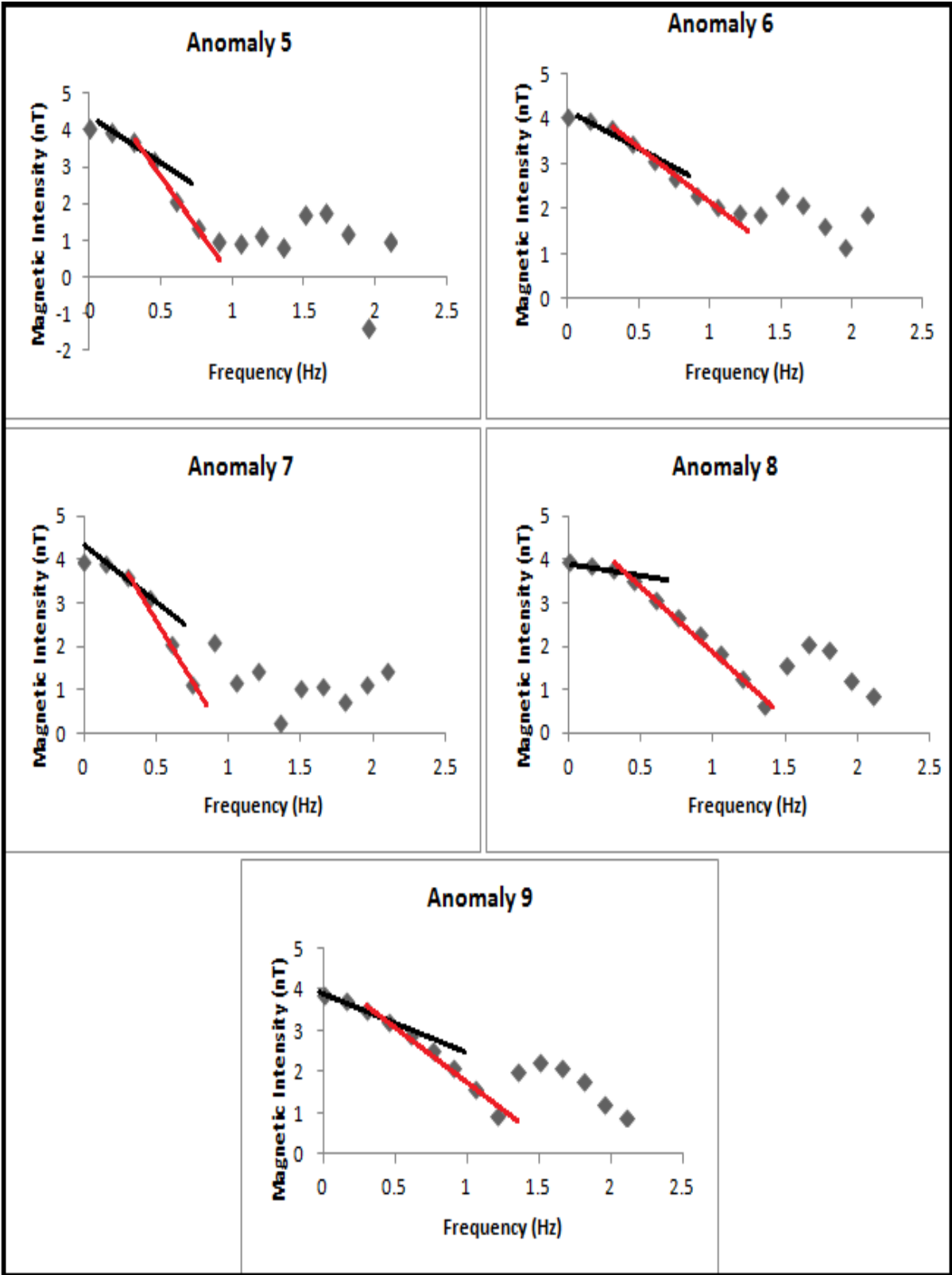
Figure 4.8(b): Spectral graphs of profile B-B^l
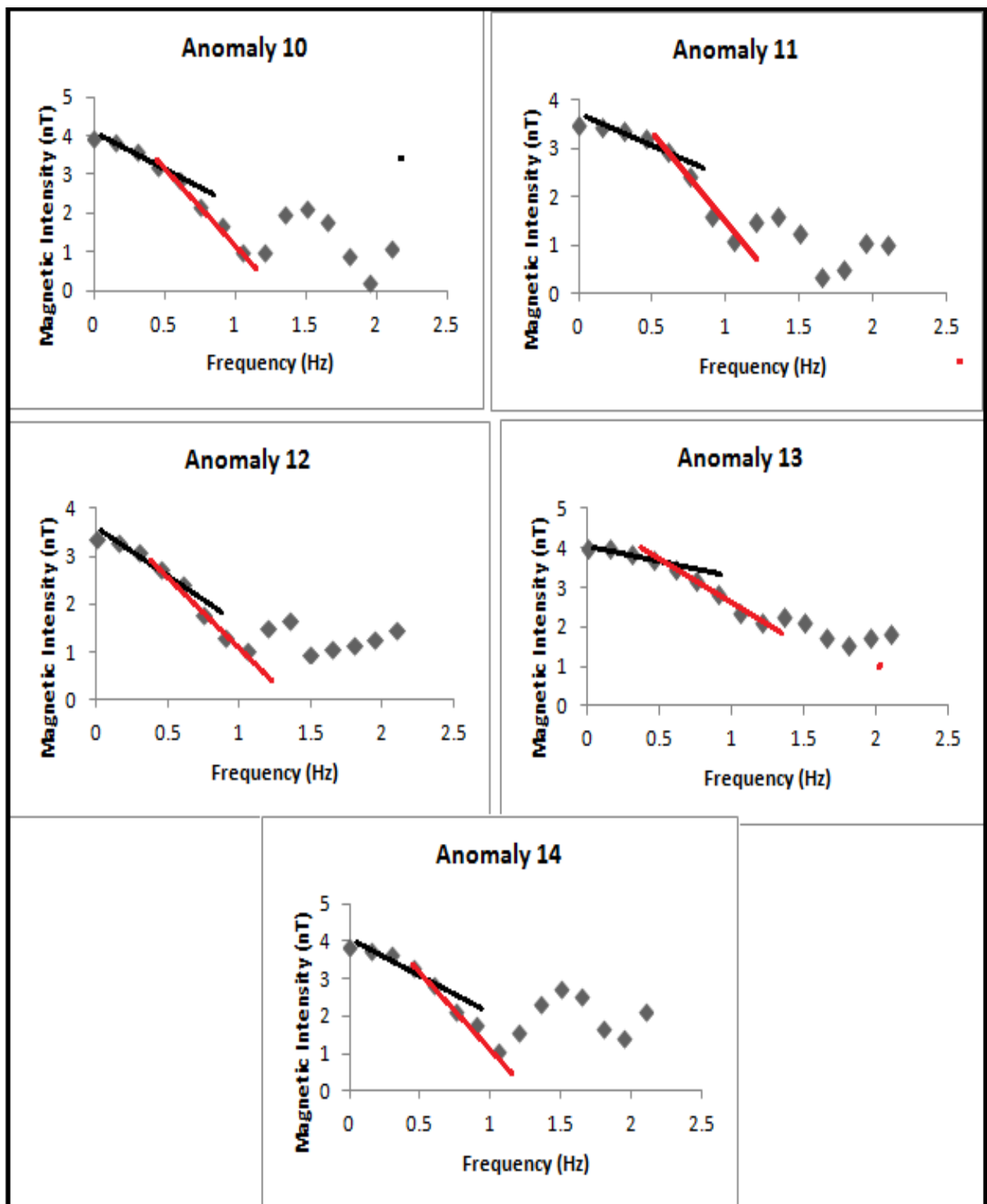
Figure 4.8(c): Spectral graphs of profile C-C^{l}
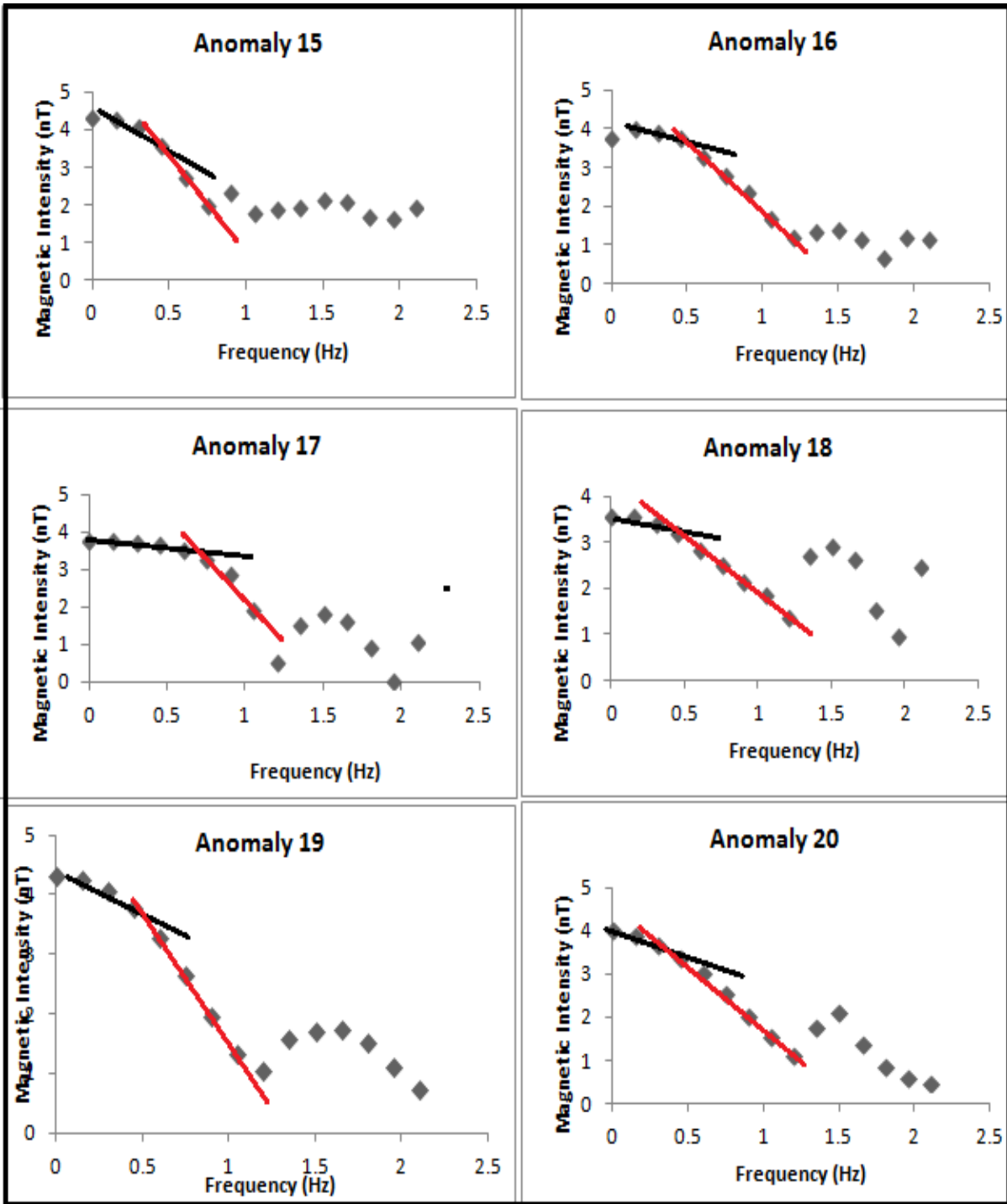
Figure 4.8(d): Spectral graphs of profile D-D^{I}
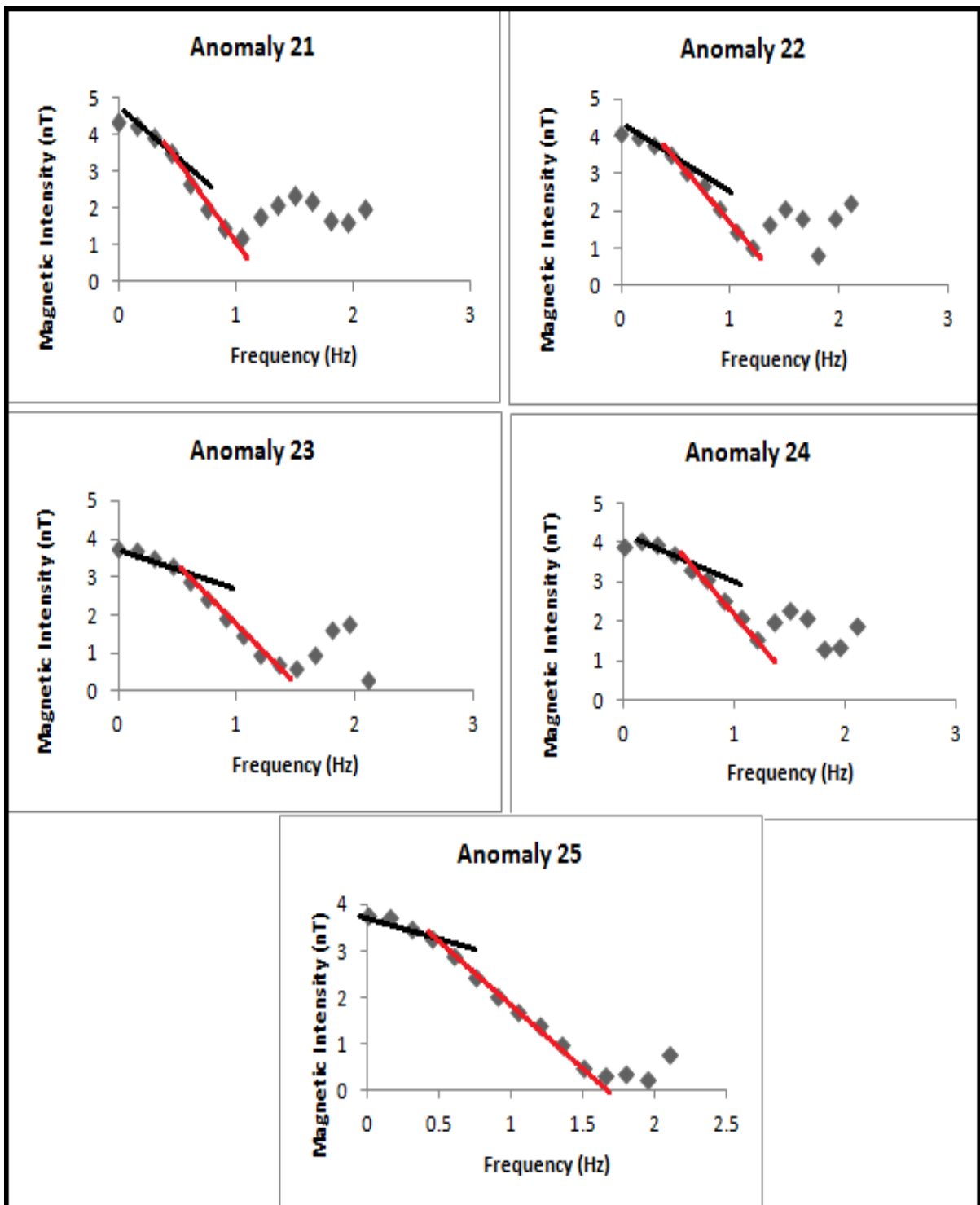
Figure 4.8(e): Spectral graphs of profile E-E^{l}
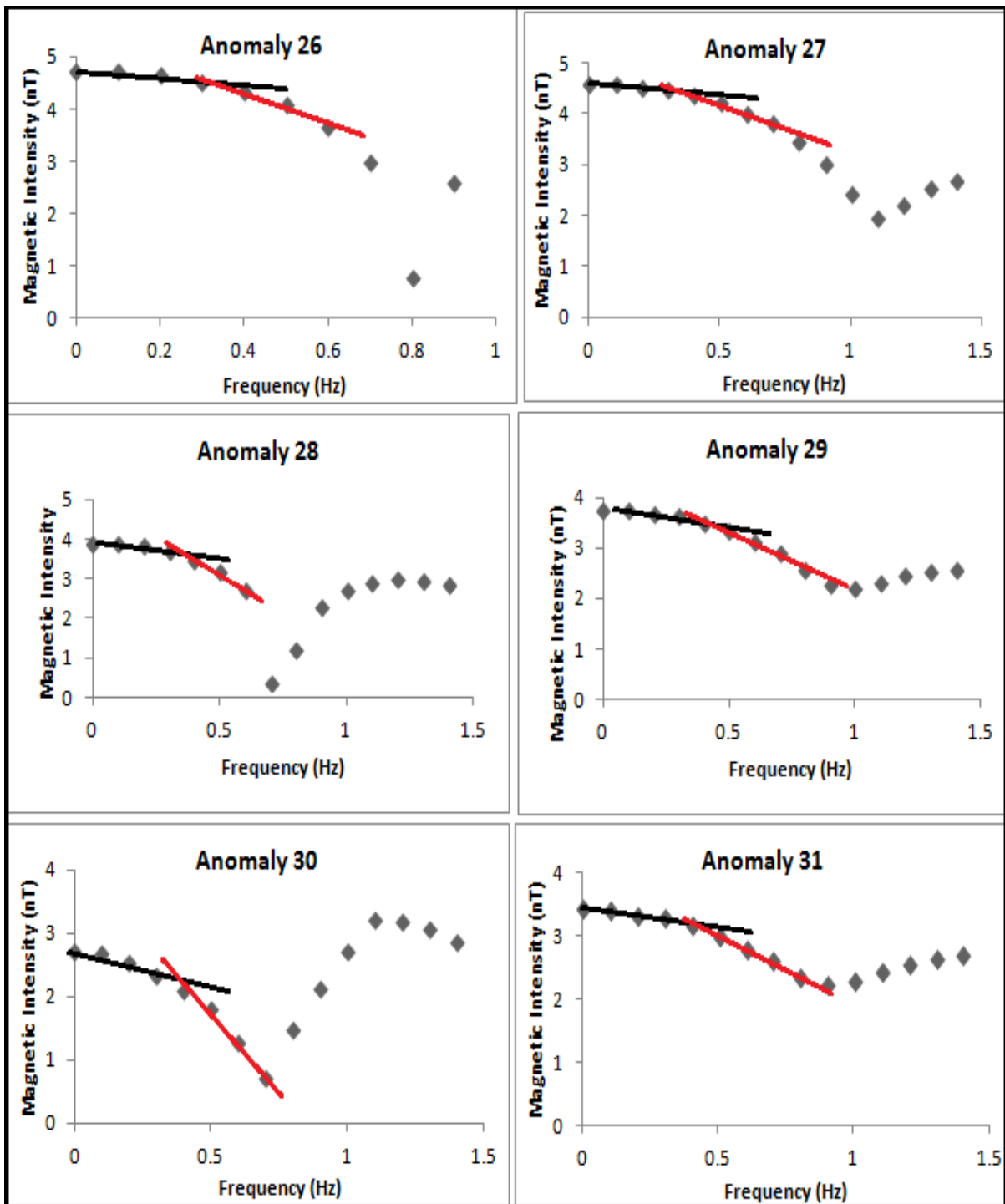
Figure 4.8(f): Spectral graphs of profile F-F^{l}
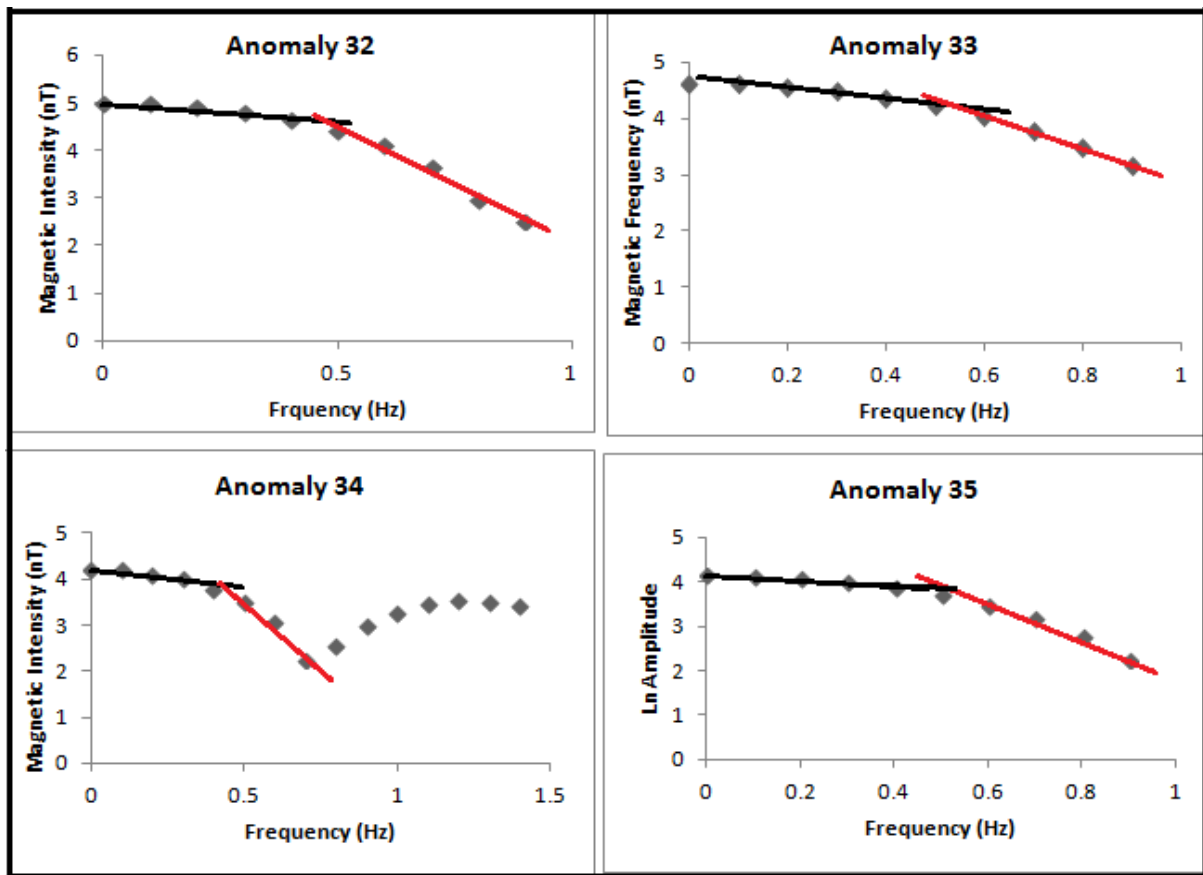
Figure 4.8(g): Spectral graphs of profile G-G^l

Spectral graphs were then obtained from the profiles by plotting the values of magnetic intensity against frequencies. These are graphs of the natural logarithms of the amplitudes against frequencies obtained for various profiles (A–A^l to G-G^l). Linear segments from the low frequency portion of the spectral, representing contributions from the deep-seated causative bodies were drawn from each graph. Each graph has two line segments: the first line segment gives the depth-to-centroid (Z_o), while the second line segment gives the depth-to-top (Z_t) of magnetic sources which shows shallower depths to magnetic sources.

The gradient of the linear segments were calculated and the depth to magnetic sources (Z_o and Z_t) were determined. The graphs obtained are negative because in spectral analysis, the graph decreases as the frequency increases. Hence, the gradients of the line segments must

also be negative. The points outside the line segments represent noise; hence the points were not joined. This is in accordance with the laws of spectral analysis.

TABLE 4.1: Estimated Curie Point Depths and Geothermal Parameters obtained from Spectral Analysis (KEY: Least values are in Italics, while highest values are underlined)

Profile Name	Profile Location	Anomaly	Depth to Top (km)	Centroid Depth (km)	Curie Point Depth (km)	Geothermal gradient (^{0}C/km)	Heat Flow (mW/m^2)	Radiometric Heat (μW/m^3)
A-A^l	Makurdi Axis	1	1.34	12.21	23.08	25.1230	62.8250	1.3466
		2	1.72	13.76	25.80	22.4806	56.2016	1.4151
		3	1.27	13.09	24.91	23.2838	58.2096	1.6432
		4	1.73	12.89	24.05	24.1164	60.2911	1.7474
B-B^l	Lafia-Makurdi-	5	2.41	16.51	30.61	18.9481	47.3701	2.2341
	Akwana Axis	6	1.51	14.49	27.47	21.1139	52.7849	2.3064
		7	**4.46**	16.38	28.30	20.4947	51.2368	2.4415
		8	2.16	13.51	24.86	23.3307	58.3266	2.2957
		9	2.32	15.67	29.02	19.9862	49.9655	**2.5547**
C-C^l	Wamba-Lafia-	10	2.49	16.31	30.13	19.2499	48.1248	2.0605
	Akiri-Akwana	11	2.80	14.12	25.44	22.7987	56.9969	1.8994
		12	2.08	10.92	19.76	29.3522	73.3806	1.9742
		13	1.54	15.87	30.20	19.2053	48.0133	1.2730
		14	3.09	15.85	28.61	20.2726	50.6816	*1.2623*
D-D^l	Wamba-Akiri-	15	3.62	15.76	27.90	20.7885	51.9713	1.3984
	Wukari Axis	16	2.30	16.18	30.06	19.2947	48.2369	1.4312
		17	2.27	11.31	20.35	28.5012	71.2531	1.6747
		18	1.98	**19.60**	**37.22**	*15.5830*	*38.9576*	1.7224
		19	2.57	18.11	33.65	17.2363	43.0906	2.1448
		20	2.14	11.27	20.40	28.4314	71.0784	2.1297
E-E^l	Wamba/Kwolla-	21	2.57	12.62	22.67	25.5845	63.9612	1.8973
	Akiri- Wukari	22	2.28	19.24	36.20	16.0221	40.0553	1.8276
		23	2.14	17.38	32.62	17.7805	44.4513	1.7945
		24	1.91	18.41	34.91	16.6142	41.5354	1.5559
		25	1.73	17.76	33.79	17.1648	42.9121	1.8143
F-F^l	Kwolla-Shendam-Ibi Axis	26	1.94	10.21	18.48	31.3853	78.4632	2.1630
		27	1.72	18.27	34.82	16.6571	41.6427	2.2121
		28	2.11	11.34	20.57	28.1964	70.4910	1.9483
		29	2.31	9.29	16.27	35.6484	89.1211	1.9630
		30	2.18	18.75	35.32	16.4213	41.0532	2.0028
		31	1.88	*7.29*	*12.70*	**45.6693**	**114.1732**	1.9248
G-G^l	Shendam Axis	32	1.08	12.39	23.70	24.4726	61.1814	2.0491
		33	*0.76*	11.18	21.60	26.8519	67.1296	1.5892
		34	2.27	9.36	16.45	35.2584	88.1459	1.3975
		35	2.19	10.19	18.19	31.8857	79.7141	1.3483
Average			**2.14**	**14.21**	**26.29**	**23.5772**	**58.9436**	**1.8412**

4.2.4 Interpretation of the Spectral Graphs and Structural Models

Each spectral graph has two line segments: the first line segment gives the depth-to-centroid (Z_o) which is obtained by fitting a straight line through the low wave number part of the radially averaged power spectrum (RAPS), while the second line segment gives the depth-to-top of magnetic sources.

Two dimensional structural models were constructed to show the calculated depths (depth-to-top or sedimentary thickness, depth-to-bottom or Curie point depth) and estimated depth to Mantle plume (Figure 4.9 (a)-(g). The structural models show the sedimentary thickness, magnetic crust which hosts the Ferromagnetic materials and Paramagnetic materials. The Ferromagnetic materials have high magnetic susceptibility, while the Paramagnetic materials have low magnetic susceptibility. In the Mantle, there are no magnetic materials because they lost their magnetic properties due to high temperature.

4.2.4.1 Profile A-A^I

The estimated depth to top along this profile ranges from 1.27 to 1.73km, while the depth to centroid ranges from 12.21 to 13.76km. The estimated Curie point depths and associated geothermal gradients ranges from 23.08 to 25.80km and 22.48 to 25.12^{0}C/km respectively, while the corresponding heat flow ranges from 56.20 to 62.83mW/m^2. In Profile A-A^I (along Makurdi axis), the Curie Point Depth (CPD) is high due to deeper depth of Mantle Plume, because there is no evidence of uplift. This gives rise to lower values of geothermal heat flow (Figure 4.9(a) & Table 4.1).

4.2.4.2 Profile B-B^I

The depth to top estimated on this profile is within the range of 1.51 to 4.46km and the depth to the centroid ranges from 13.51 to 16.38km. The estimated Curie point depths and associated geothermal gradients ranges from 24.86 to 30.61km and 18.95 to 23.33^{0}C/km respectively, while the corresponding heat flow values range from 47.37 to 58.33mW/m^2. In

Profile B-B^l (along Lafia-Makurdi-Akwana axis), the CPD is also high and the corresponding values of geothermal heat flow are low. No evidence of uplifts (Figure 4.9(b) & Table 4.1).

4.2.4.3 Profile C-C^l

The estimated depth to top of magnetic sources ranges from 1.54 to 3.09km, while the depth to the centroid ranges from 10.92 to 16.31km. The estimated Curie point depths and associated geothermal gradient range from 19.76 to 30.20km and 19.21 to 29.35^{0}C/km respectively, while the corresponding heat flow values range from 48.01 to 73.38mW/m^2. There is evidence of uplift in the middle of profile C- C^l which lies on Wamba-Lafia-Akiri-Akwana Axis. The uplift gives rise to low CPD and causes high geothermal heat flow (Figure 4.9(c) & Table 4.1).

4.2.4.4 Profile D-D^l

The estimated depth to top ranges from 1.98 to 3.62km, while the depth to the centroid ranges from 11.27 to 19.60km. The Curie point depth estimates and associated geothermal gradients range from 22.67 to 36.20km and 15.58 to 28.50^{0}C/km respectively, while the corresponding heat flow values range from 38.96mW/m^2 to 71.25mW/m^2. Along Profile D-D^l (Wamba-Akiri-Wukari Axis), there are uplifts which give rise to low Curie Point Depth and this causes high geothermal heat flow in the area (Figure 4.9(d) & Table 4.1).

4.2.4.5 Profile E-E^l

The estimated depth to top of magnetic sources ranges between 1.73km and 2.57km, while the depth to centroid ranges between 12.62km and 19.24km. The estimated Curie point depths and associated geothermal gradients range from 22.67km to 36.20km and 16.02^{0}C/km to 25.58^{0}C/km respectively. The corresponding heat flow values along the profile range from 40.06mW/m^2 to 63.96mW/m^2. Along Profile E-E^l (along Wamba-Kwolla-Akiri-Wukari axis), there deeper Curie point depth, this causes lower geothermal heat flow on average (Figure 4.9(e) & Table 4.1).

4.2.4.6 Profile F-F^l

The estimated depth to top varies from 1.72 to 2.31km, while the depth to the centroid varies from 7.29 to 18.75km. The estimated Curie point depths and associated geothermal gradients range from 12.70 to 35.32km and 16.42 to 45.67^{0}C/km respectively. The corresponding heat flow values range from 41.05 to 114.17mw/m^2. There is evidence of uplifts along Profile F-F^l (along Kwolla-Shendam-Ibi axis), these cause low CPD and hence high heat flow in the area (Figure 4.9(f)& Table 4.1).

4.2.4.7 Profile G-G^l

The estimated depth to top of magnetic sources ranges from 0.76 to 2.27km and the depth to the centroid ranges from 9.36 to 12.39km. The Curie point depth estimates and associated geothermal gradients range from 16.45 to 23.70km and 24.47 to 35.26^{0}C/km respectively, while the corresponding heat flow values range from 61.18 to 88.15mW/m^2. The Mantle has been uplifted along Profile G-G^l (along Shendam axis). The Curie Point Depth on average is low, while the geothermal heat flow is high (Figure 4.9(g) & Table 4.1).
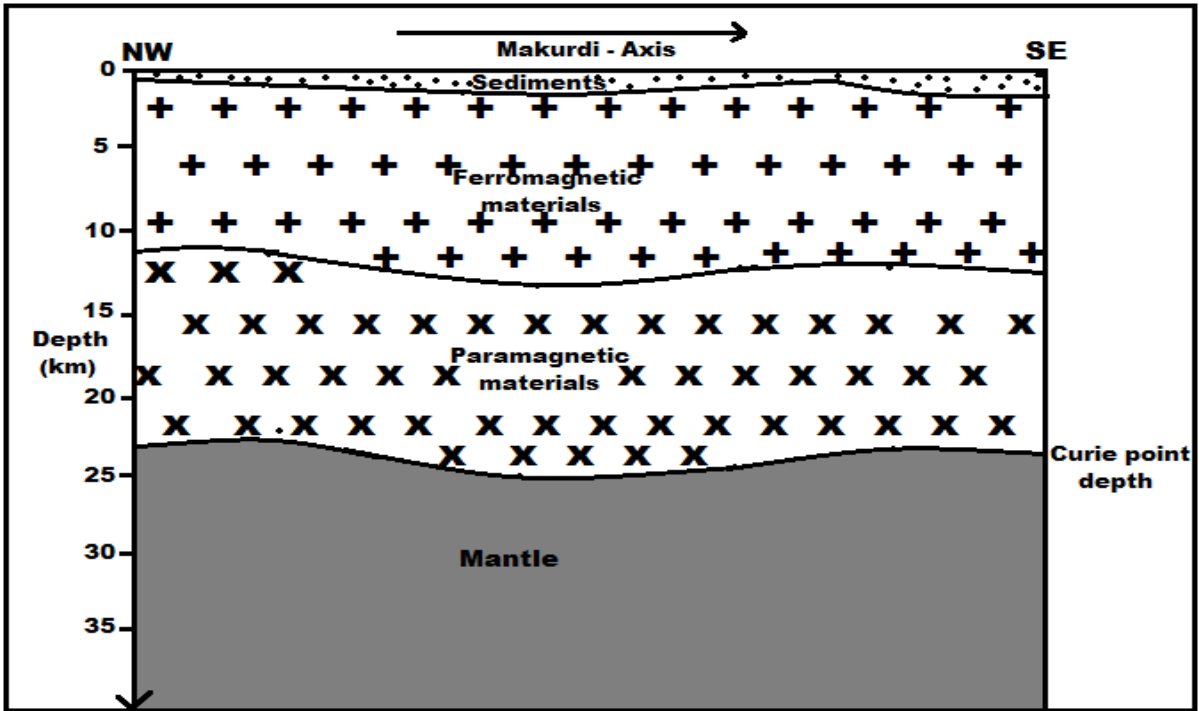
Figure 4.9(a): Structural modelling along Profile A-A^l within the study area
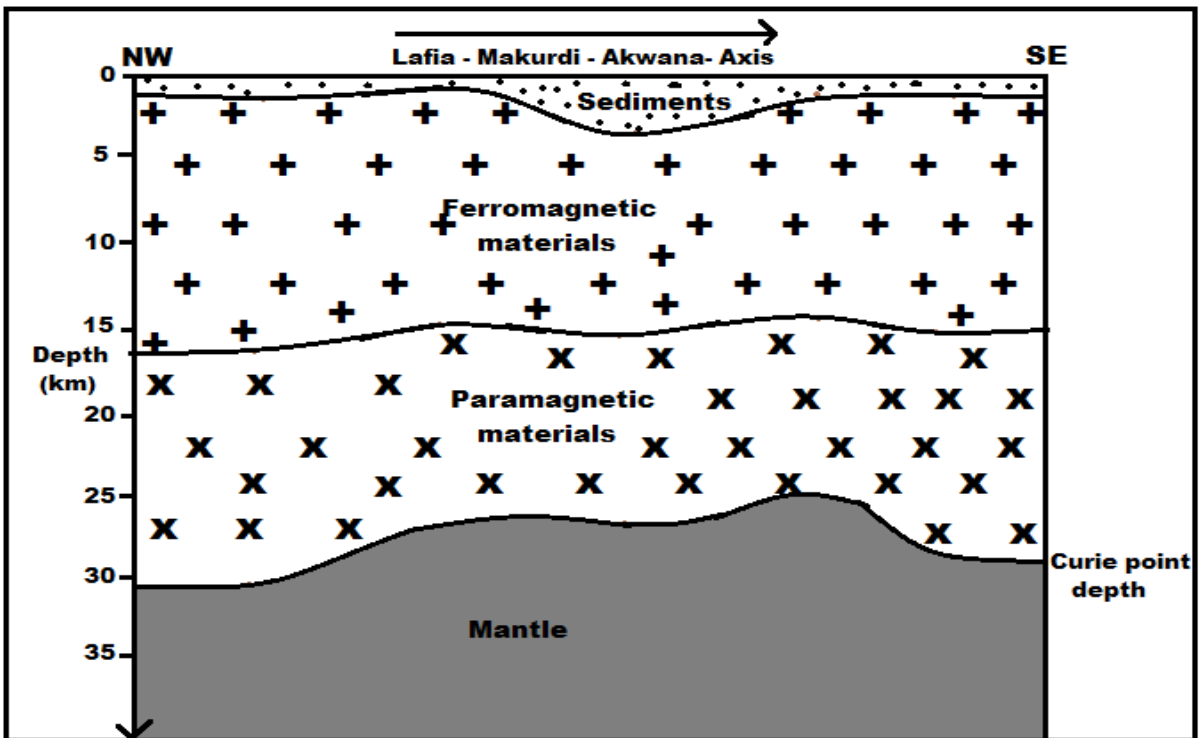
Figure 4.9(b): Structural modelling along Profile B-B^l within the study area
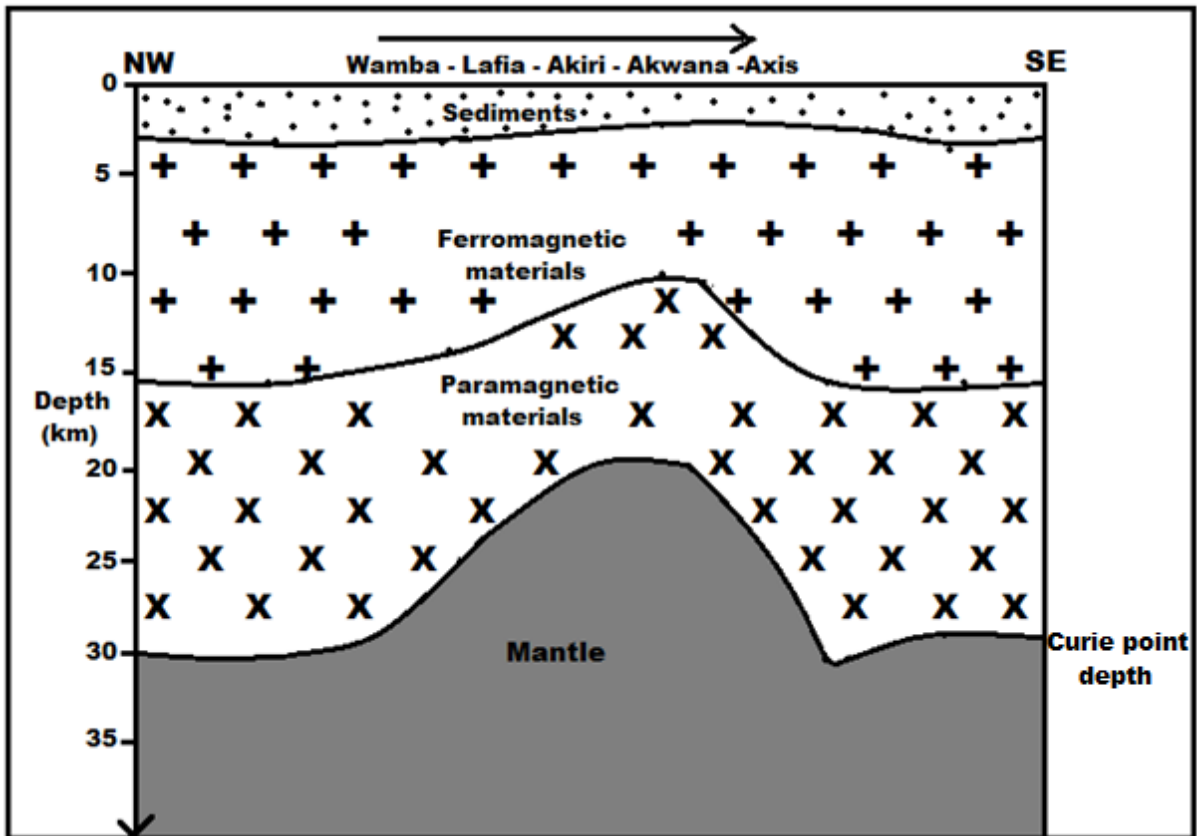
Figure 4.9(c): Structural modelling along Profile C-C*l* within the study area
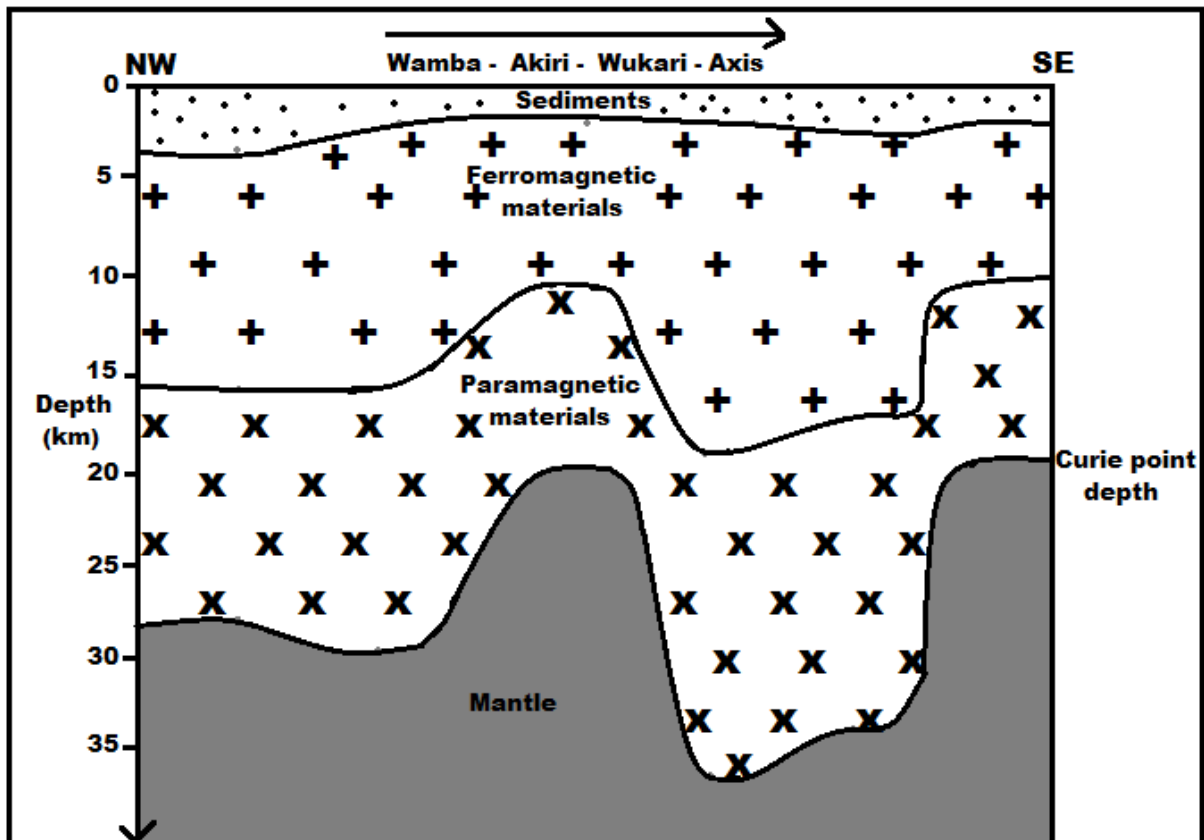
Figure 4.9(d): Structural modelling along Profile D-D*l* within the study area
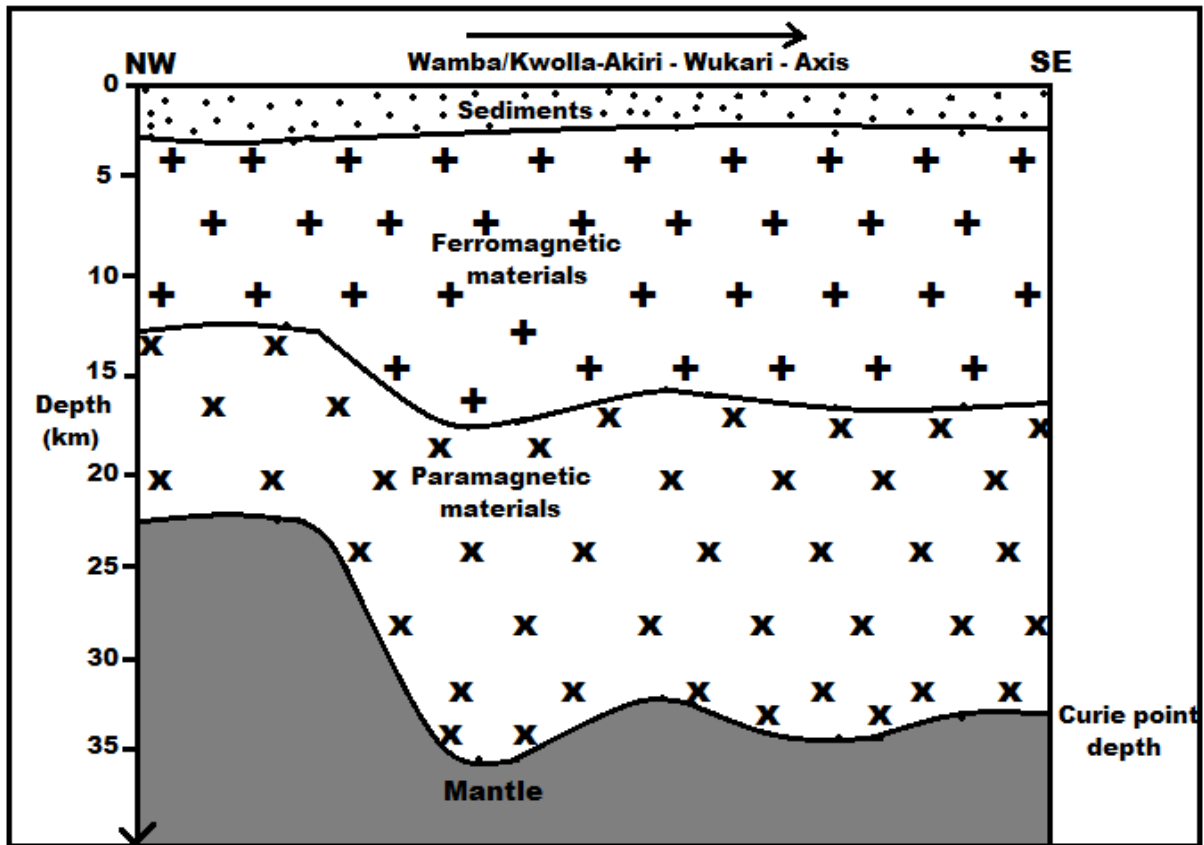
Figure 4.9(e): Structural modelling along Profile E-E^l within the study area
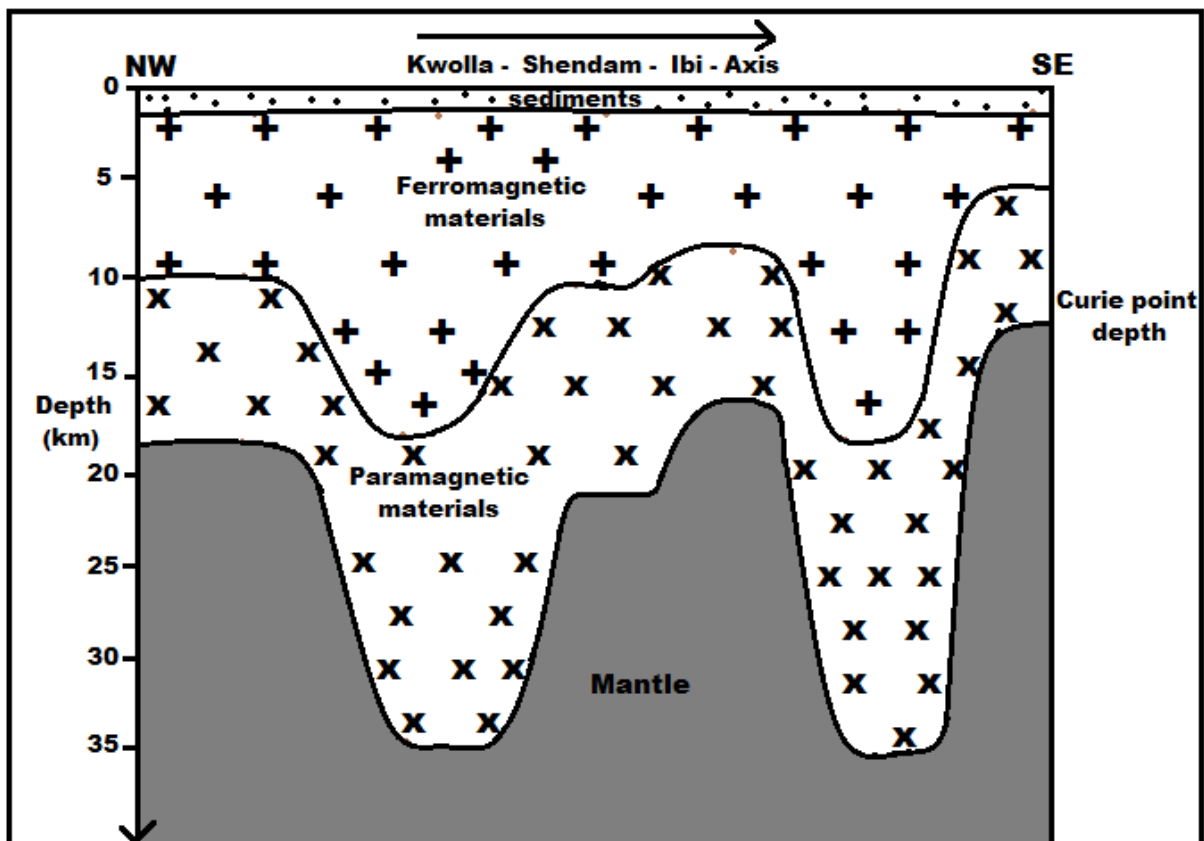
Figure 4.9(f): Structural modelling along Profile F-F^l within the study area
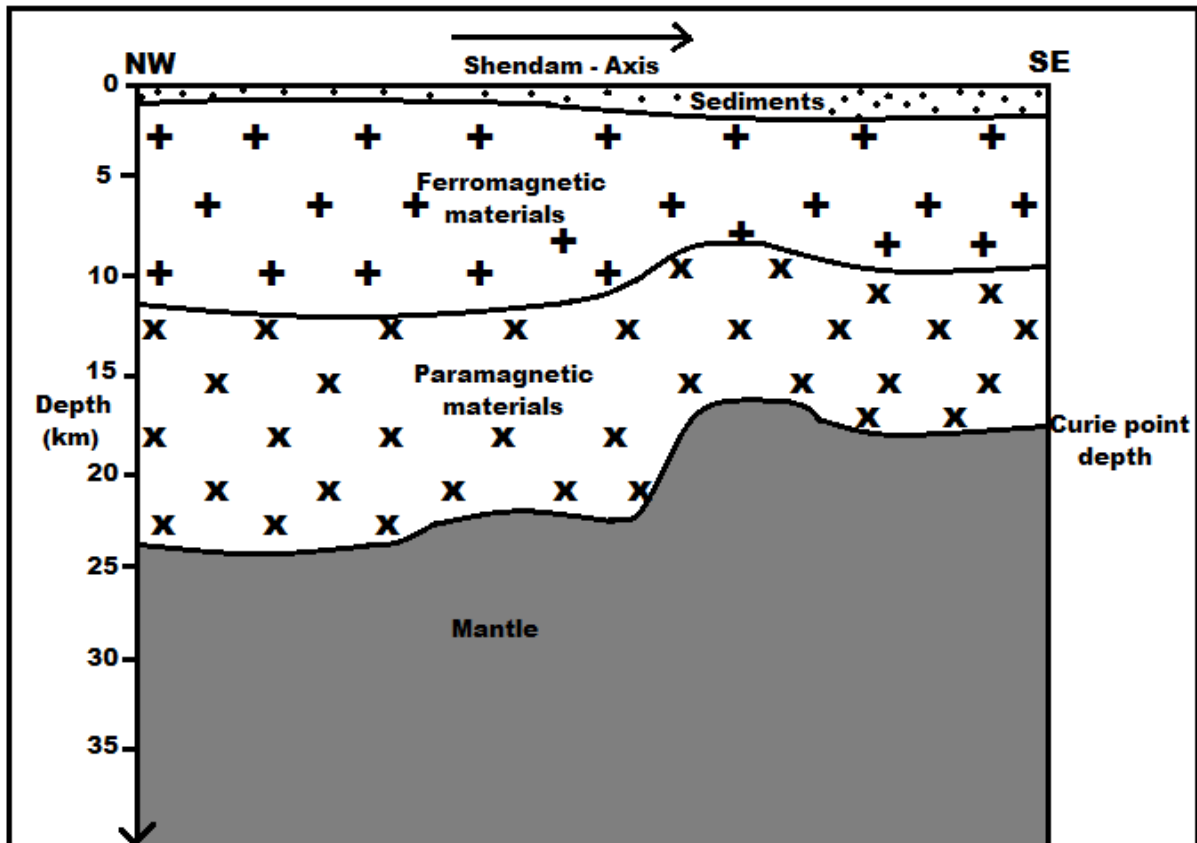
Figure 4.9(g): Structural modelling along Profile G-G^l within the study area

4.2.5 Curie Point Depth and Geothermal Parameters

Table 4.1 shows the estimated Curie point depths and geothermal parameters obtained from spectral analysis. Apart from the Curie point depth (Z_b), the geothermal parameters include: depth-to-top (Z_t) and depth-to-centroid (Z_o) of magnetic source, geothermal gradient (dT/dZ) and geothermal heat flow (Q).

Depth to top of Magnetic Sources (Z_t):

The values of Z_t range from 0.76 km to 4.46 km with an average value of 2.14 km. This shows that the average sedimentary thickness in the study is 2.14 km. The depths to top of magnetic sources represent shallower depths in the study area.

Depth to Centroid of Magnetic Sources (Z_o):

The values of Z_o range from 7.29 km to 19.60 km, with an average value of 14.21 km. The depths to centroid of magnetic sources represent the depths to deeper sources.

Curie point Depth (Z_b):

The Curie point depth or basal depth of magnetic sources range from 12.70 km to 37.22 km, with an average depth of 26.29 km. This is the same as the average depth to bottom of magnetic source in the study area (26.29 km).

Geothermal Gradient (dT/dZ):

The geothermal gradient varies from 15.58^0C/km to 45.67^0C/km, with an average of 23.58^0C/km. The lowest geothermal gradient value corresponds to the lowest heat flow value, while the highest value corresponds to the highest heat flow value.

Geothermal Heat Flow (Q):

The geothermal heat flow values in the study area range from 38.958mW/m^2 to 114.173mW/m^2. The average heat flow in the area is 58.94mW/m^2. The lowest heat flow value corresponds to the highest Curie point depth, while the highest heat flow value corresponds to the lowest Curie point depth. This means that, the Curie point varies inversely with the heat flow, while the geothermal gradient varies directly with the heat flow.

The results obtained from the graphs of amplitude spectral for the anomalies (Figure 4.8 (a)-(g) were used to construct the maps of depth to top (Z_t) and depth to centroid (Z_o) of magnetic sources in the study area (Figures 4.10 and 4.11). The highest value of Z_t is observed in profiles B-B^l (along Lafia-Akwana axis), while the lowest value (0.76 km) is observed in profile G-G^l at Shendam (north-eastern part of the study area).

4.2.6 Presentation of Results in Contour Maps
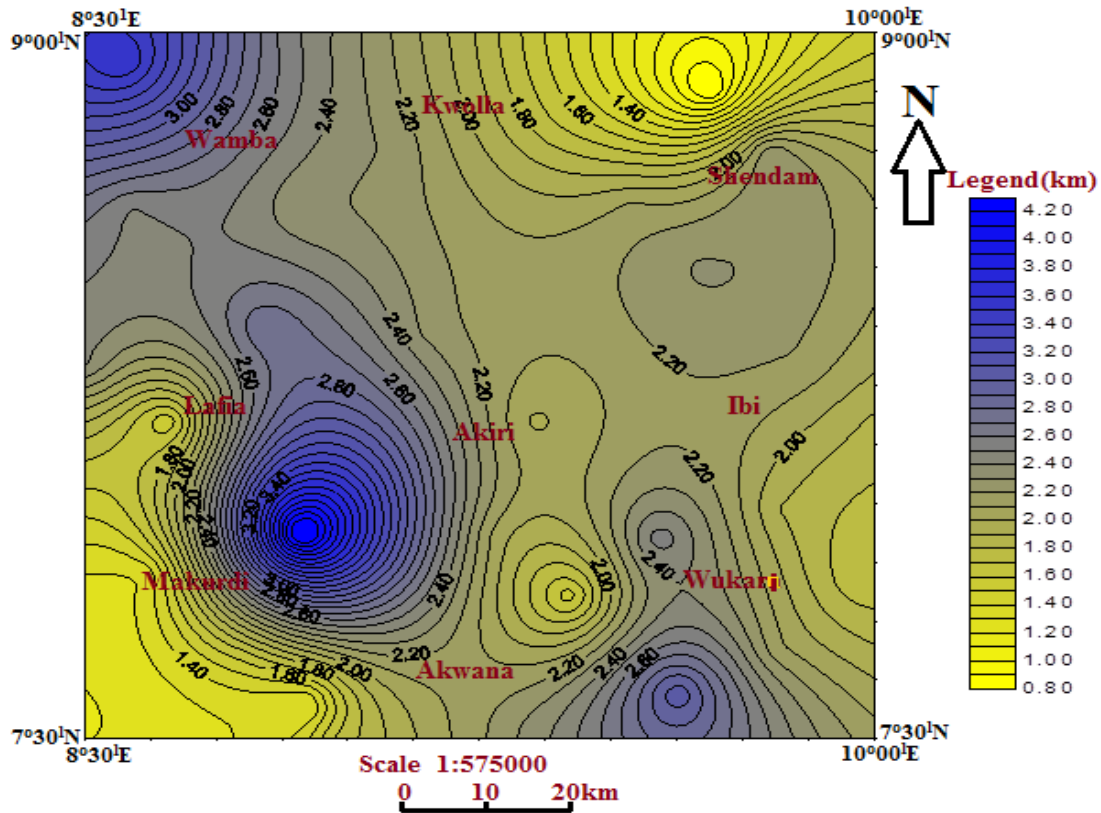
Figure 4.10(a): Map showing the depth to the top of the magnetic body within the study area (Contour interval~ 0.1km)
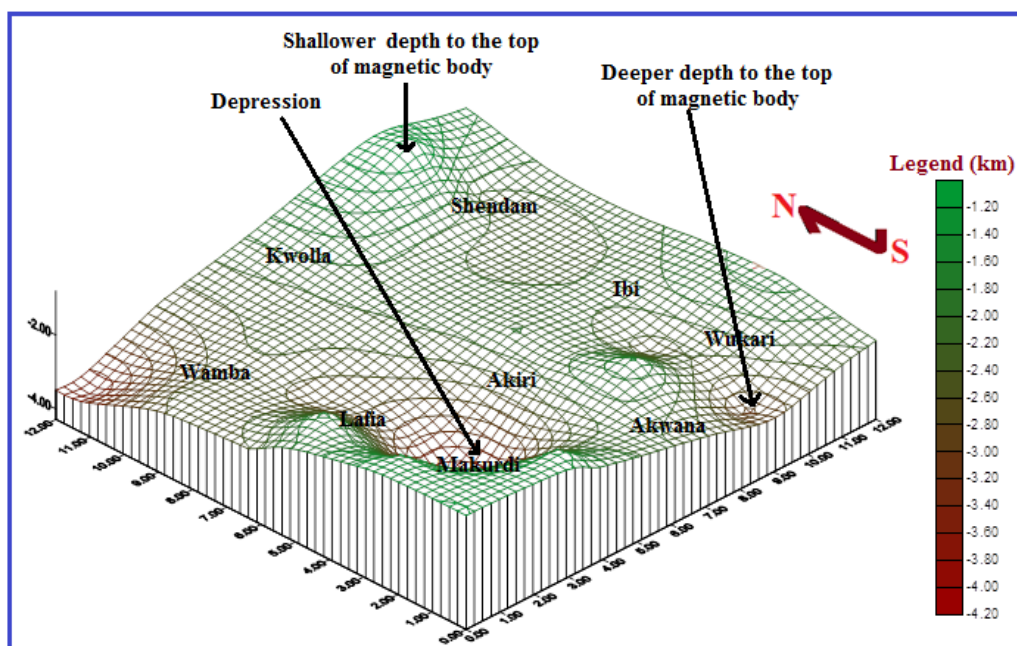

Figure 4.10(b): 3D view of depth to the top within the study area

Figures 4.10 (a) & (b) shows the depth to the top of the magnetic body within the study area in 2D and 3D maps. The Figures show shallow depth to top of magnetic sources (Z_t) around Shendam, Ibi, Akiri and Wukari, northeast to south-eastern part of the study area, while higher values of Z_t were observed at Wamba, Lafia, Akiri and Makurdi (a region trending NW to SW part of the study area).
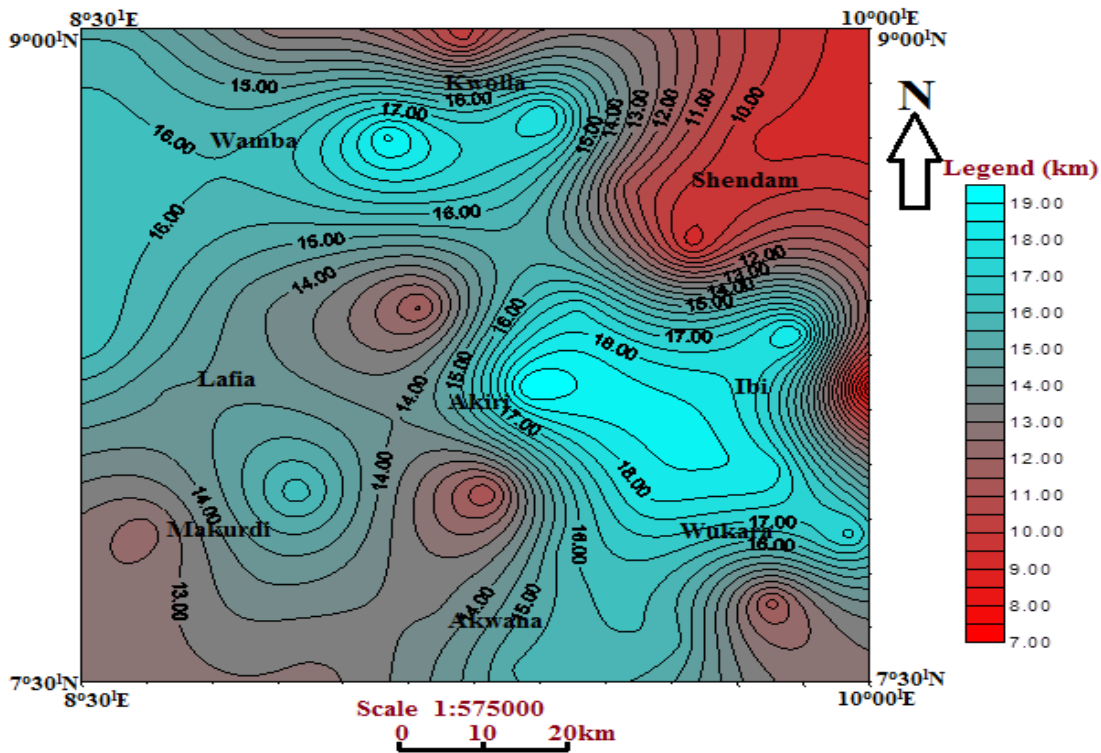
Figure 4.11(a): The depth to the Centroid map of the study area (Contour interval~ 0.5km)
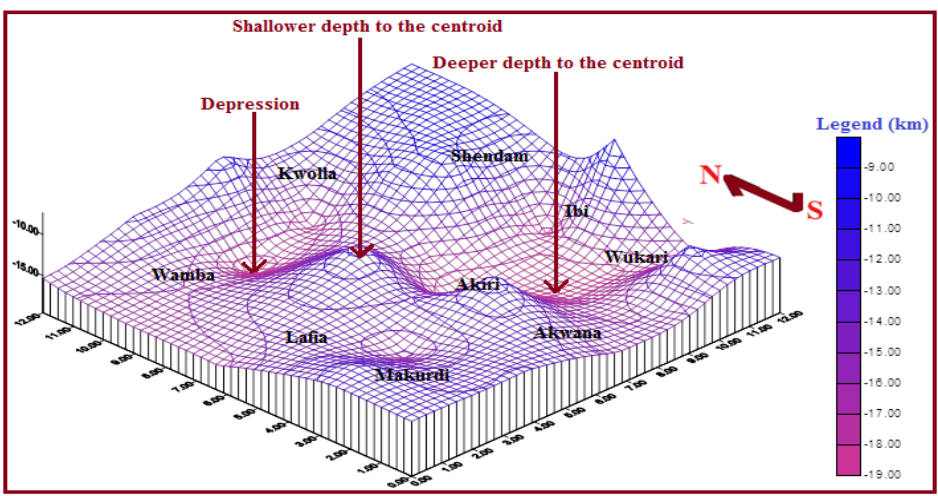
Figure 4.11(b): 3D view of depth to the centroid within the study area

98

Figures 4.11(a) & (b) represent the 2D and 3D depth to the centroid map of the study area. The figures show coloured representation of the depth to centroid of the magnetic sources (Z_o). It indicates high values of Z_o around Kwolla and Wamba in the north, Ibi and Wukari in the east, which extends to Akwana in the southern part; this is shown in blue colour, while low values of Z_o are observed around Shendam (NE), Akiri (central part), Akwana (south), part of Wukari (SE) and part of Makurdi (SW). The lower depths to centroid are indicated in red colour.
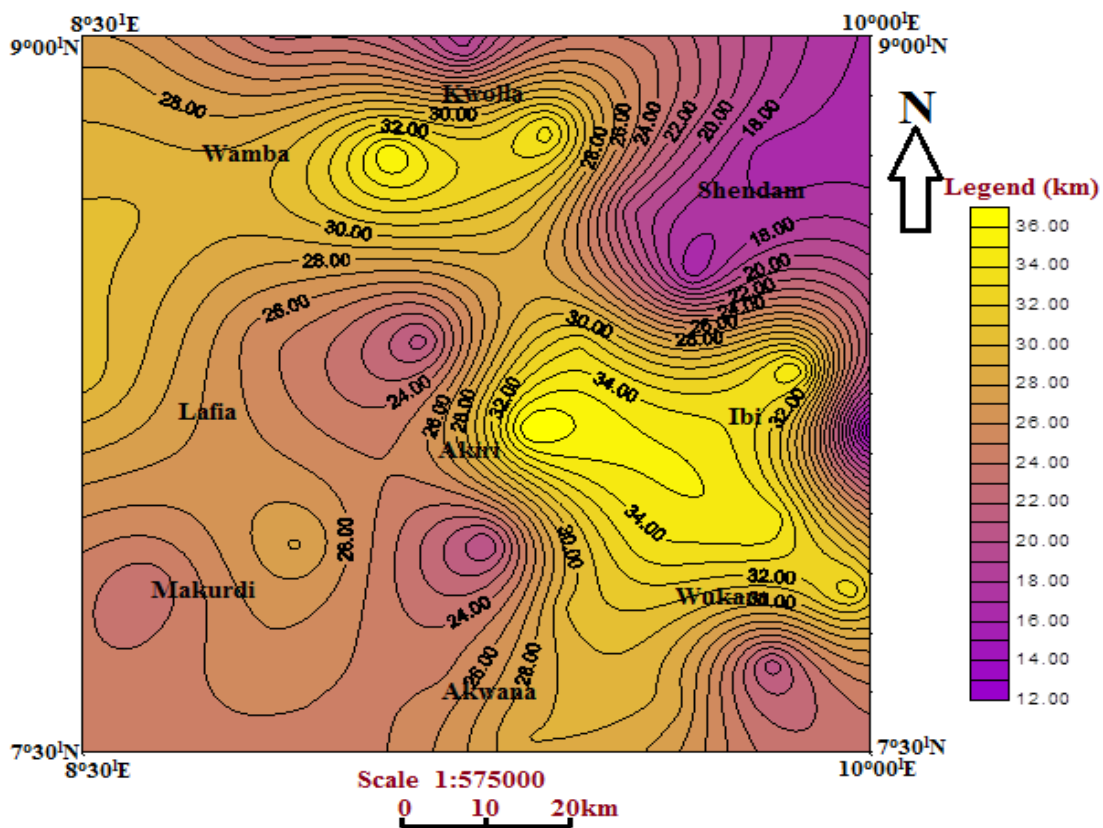
Figure 4.12(a): The Curie Depth map of the study area (Contour interval~ 1.0km)
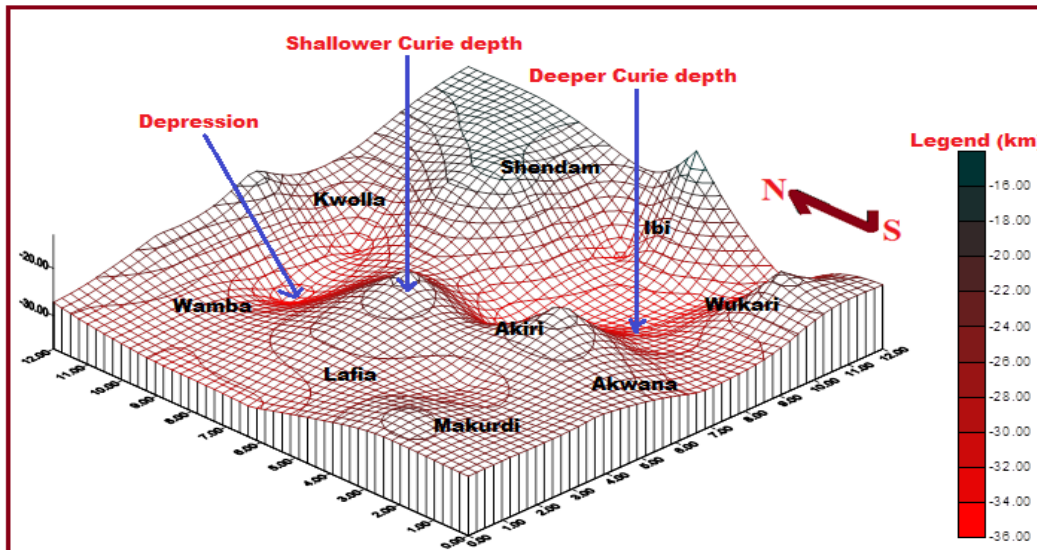
Figure 4.12(b): 3D view of Curie point depth within the study area

Figures 4.12 (a) & (b) show the 2D and 3D Curie depth map of the study area. The Curie depth ranges from 12.70 to 37.22 km (Below Sea Level). The Curie point depths obtained were used to construct Curie point isotherm depth map (Figures 4.12 (a) & (b). The Curie point depths reflect the depths to which the thermal nature of the crust is described. Previous studies by Stampolidis *et al*., (2005) showed that the Curie point depth is linked to the geological context of an area. Figures 4.12 (a) & (b) show that the regions around north-west and north-central (Wamba and Kwolla) and east to south-east (Ibi and Wukari) have higher Curie point isotherm depths ranging from 28.30 km to 37.22 km, while lower depths ranging from 12.70 km to 27.90 km are found around northern part of Wamba and Kwolla, Shendam (NE), Akiri (Central), Lafia and Makurdi (SW) and Wukari south (SE). Yamano, (1995) made an assertion that shallow Curie point depths are consistent with high heat flow values as seen in back arc, and young volcanic regions. In view of this assertion, the area of shallow Curie point depth of 12.70 km to 27.90 km has a geothermal potential which can be utilized.
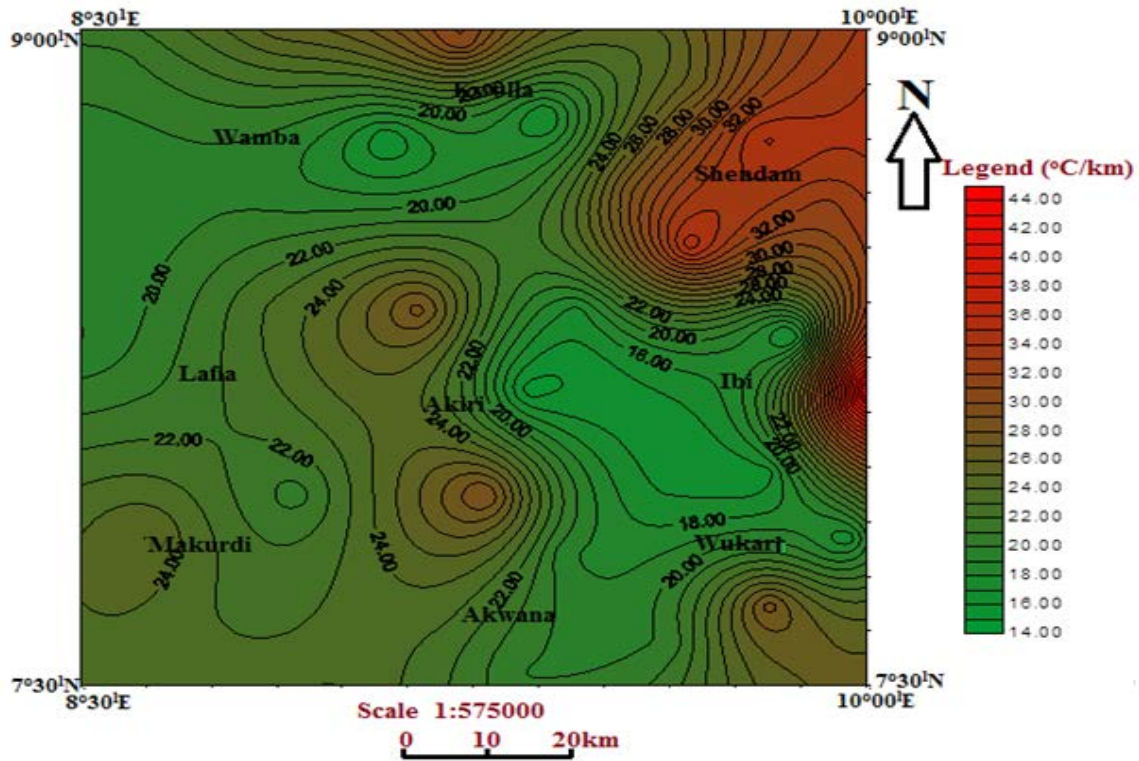
Figure 4.13(a): Map showing Geothermal gradient of the study area (Contour interval~ 1.0°C/km)
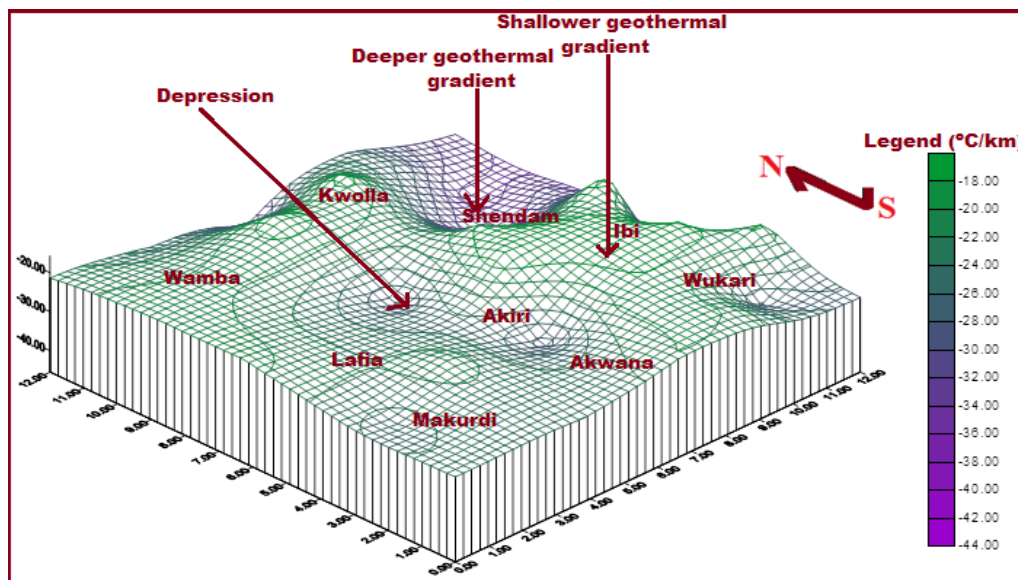

Figure 4.13(b): 3D view of geothermal gradient within the study area

Figures 4.13 (a) & (b) represent 2D and 3D maps of geothermal gradient of the study area.

Utilizing the Curie temperature of 580^0C and the derived Curie point depths (Nwankwo *et al.,*

2011), the geothermal gradient map was plotted. Areas around northern part of Kwolla, Shendam, Ibi, Akiri, Makurdi and southern part of Wukari have high values of geothermal gradient.
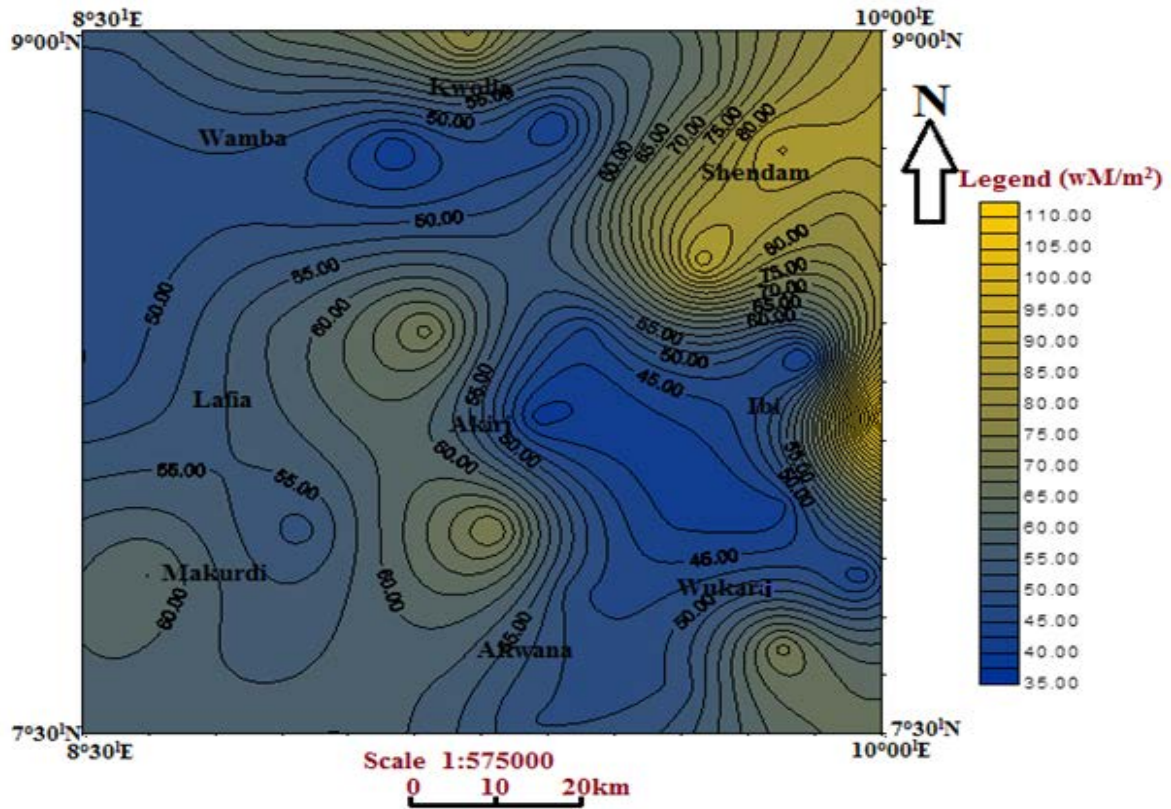

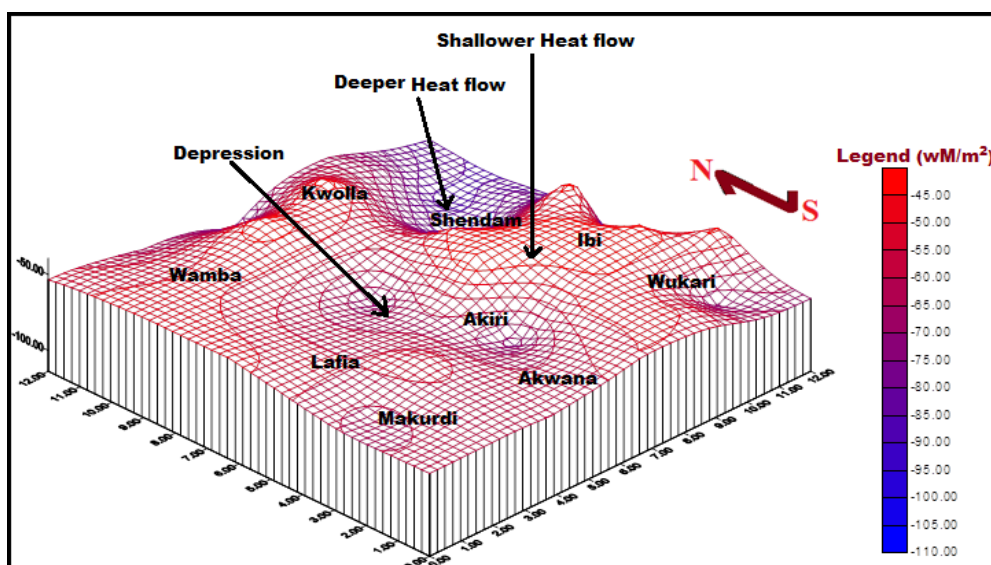Figure 4.14(a): Map showing Heat Flow within the study area (Contour interval 1.0 wM/m^2)

Figure 4.14(b): 3D view of heat flow within the study area

Figures 4.14 (a) & (b) represent 2D and 3D maps of heat flow within the study area. Figures 4.14 (a & b) indicate high values of geothermal heat flow (Q) around northern part of Kwolla, Shendam, Ibi, Akiri, Makurdi and southern part of Wukari, while low values of heat flow occur around, Wamba, southern part of Kwolla, Western part of Ibi, northern Wukari and Akwana areas. Figure 4.13 has a close relationship with the heat flow map (Figure 4.14), the higher the geothermal gradient, the higher the heat flow.

4.2.7 Relationship between Curie point Depth, Geothermal Gradient and Heat Flow within the Study Area

Figure 4.15 shows that the geothermal heat flow in the area increases with a decrease in Curie point depth with a quadratic relationship of the general form $y = ax^2 + bx + c$, hence $Q = 0.1135x^2 - 8.3879Z + 196.48$; while the geothermal heat flow increases with an increase in geothermal gradient (this is a linear relationship of the general form $y = mx + c$; thus, $Q = 2.5Z + 0.0002$) (Figure 4.16).
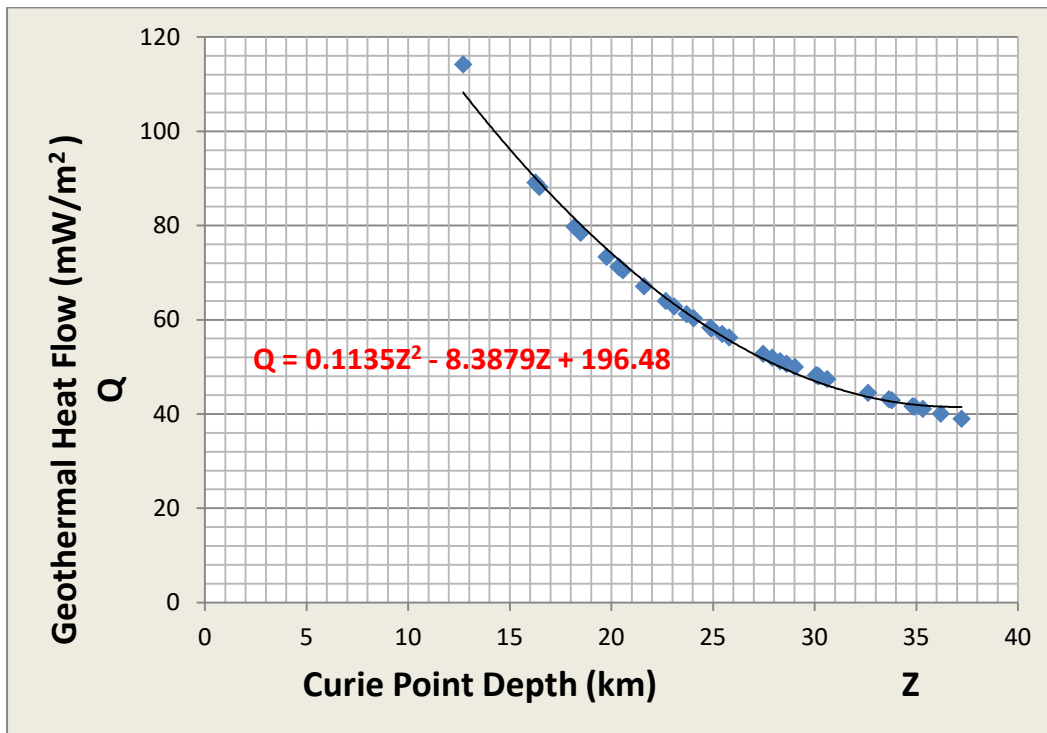

Figure 4.15: Relationship between Curie point Depth and Heat Flow within the study area
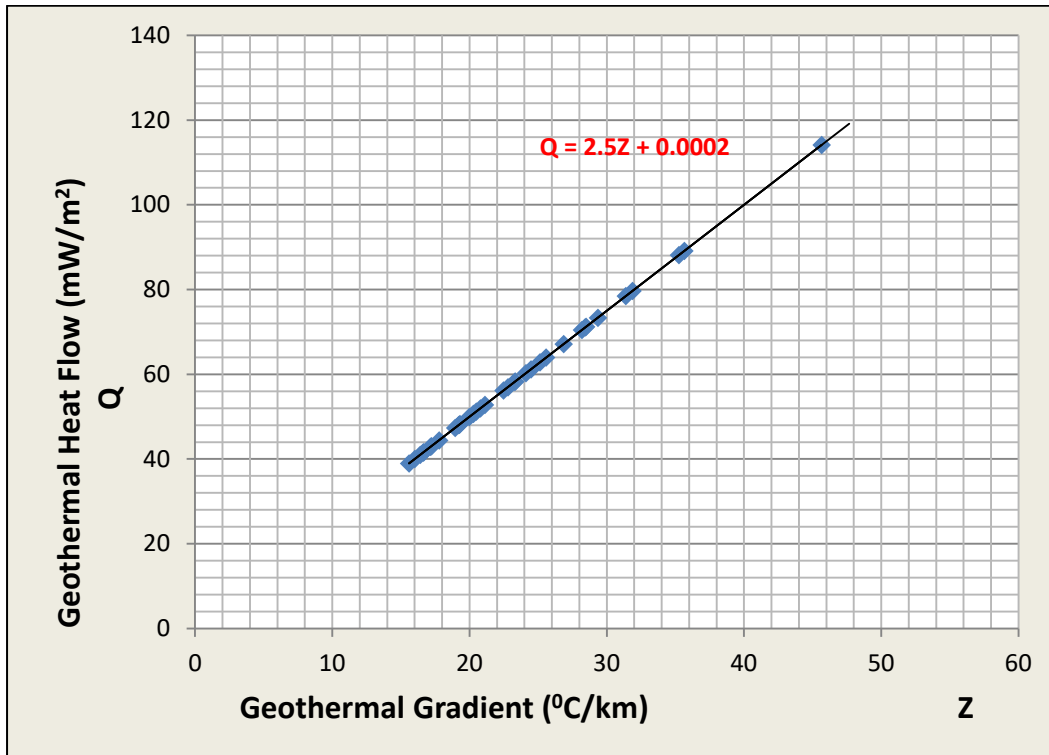
Figure 4.16: Relationship between Geothermal gradient and Heat flow within the study area

As the Curie point depths in the study area decreases, the geothermal heat flow increases (Figure 4.15); and as the geothermal gradient increases, the geothermal heat flow also increases (Figure 4.16). The relationships show that the heat flow increases with decrease in Curie point depths; while the heat flow increases with increasing geothermal gradient. This implies that the Curie point depths vary inversely with the geothermal heat flow values, while the geothermal gradient varies directly with the heat flow. The assessment of the variations of the Curie isotherms of an area can provide valuable information about the regional temperature distribution at depth and concentration of subsurface geothermal energy. One of the important parameters that determine the relative depth of the Curie isotherm with respect to sea level is the local thermal gradient (i.e. Heat flow and thermal conductivity structure) (Blakely, 1988).

4.2.8 Geological and Structural Implication of Curie point Depth and Geothermal Heat Flow in the Study Area

The study area is underlain by crystalline basement rocks in the northern and south-eastern parts of the study area, younger granites in the north around Kwolla and Shendam, and in the northwest around Wamba.

Most parts of the study area are underlain by Cretaceous sedimentary rocks which include sandstone, shale, limestone, mudstone, siltstone, sandy shale and alluvium. Cretaceous sedimentary rocks older than the Santonian were deformed during the Santonian tectonic event (about 86 Ma) to produce several uplifts, faults and numerous folds, generally trending in a NE-SW direction, parallel to the trough margin (Burke *et al.,* 1972; Benkhelil, 1989). The Cretaceous Middle Benue Trough experienced the same volcanic activity in the Palaeocene (about 65.5 Ma). The volcanic intrusive rocks of Palaeocene age are found in the middle part of the study area around Akiri, Lafia and Makurdi.

It is observed that those areas covered by Crystalline basement rocks, younger granites and volcanic intrusive rocks have the lowest value of Curie point depths (12.70 to 27.90 km) and corresponding higher heat flow (about 60 to 115 Mw/m^2) found in the study area; while the areas covered by the Cretaceous sedimentary rocks have high Curie point depths with lower values of geothermal heat flow. It is also found that in areas where there are uplifts and the Curie point depths are shallow (e.g. on profiles C-C^l, D-D^l and F-F^l), the corresponding geothermal heat flow is high.

Measurements have shown that a region with significant geothermal energy is characterized by an anomalously high temperature gradient and high geothermal heat flow. It is therefore to be expected that geothermally active areas will be associated with shallow Curie point depths. Therefore areas around Wamba and Kwolla (North), Shendam (NE), Akiri (Central), Lafia and Makurdi (West) and Wukari south (SE) which have low Curie point depths with

corresponding high heat flow are areas that are geothermally active. These areas have geothermal energy potential which can be utilized.

4.3 Radiometric Interpretation
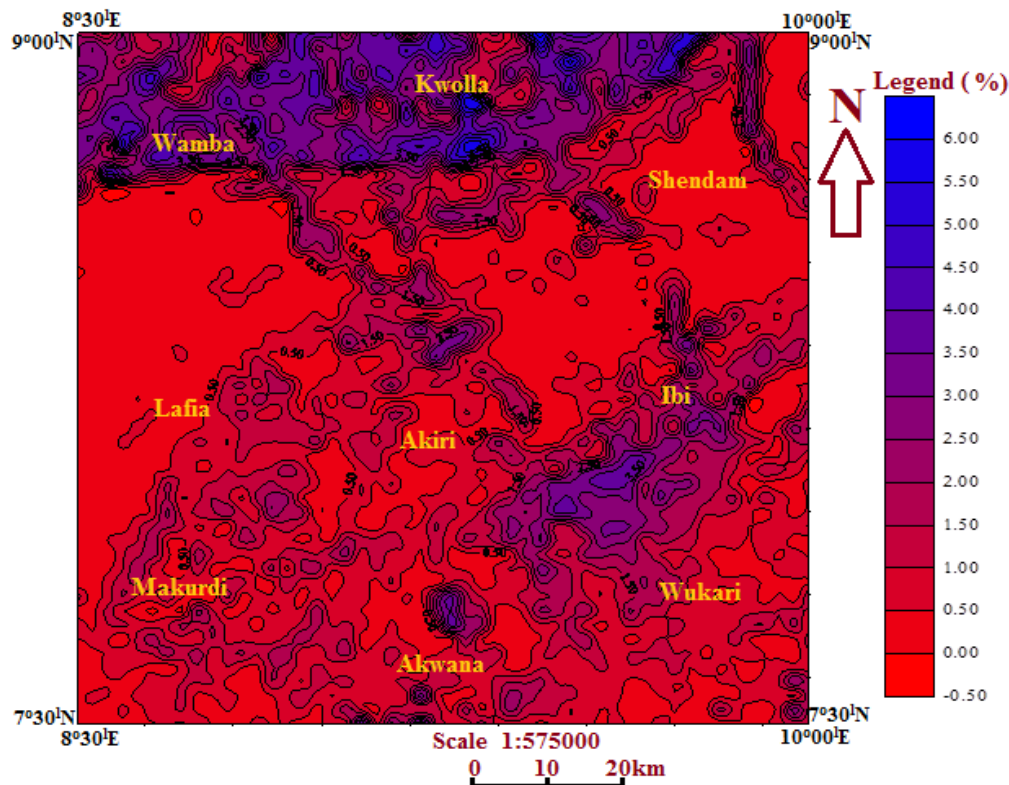
4.3.1 Potassium (K) content map:

Figure 4.17: Potassium Data Map of the Study Area (contour Interval≈0.5%)

Figure 4.17 is the Potassium content map of the study area. The map shows high concentration potassium (K) around Wamba, Kwolla and part of Shendam (in the northern part of the study area), between Ibi and Wukari, and Akwana. Low concentration of Potassium is prevalent around Lafia, Makurdi, part of Shendam, Akiri and part of Wukari. Shales, Sandstones and Granite (especially Feldspar) are rocks associated with high potassium activity.
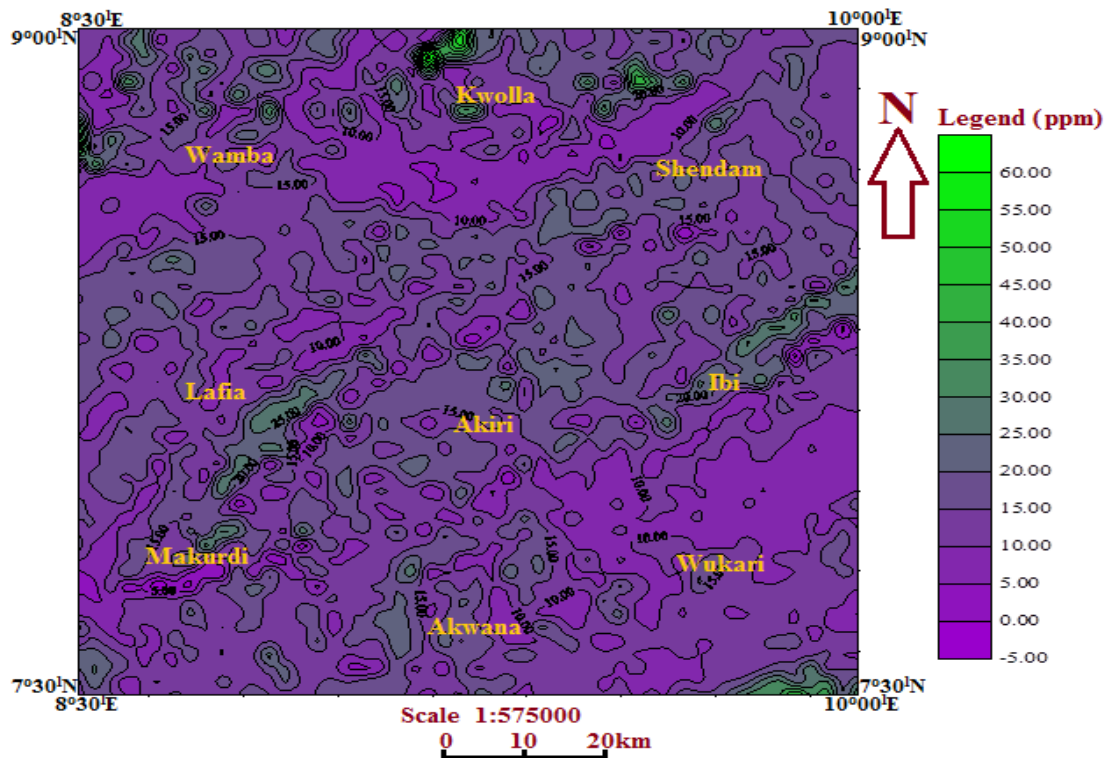
4.3.2 Thorium (Th) content map:

Figure 4.18: Thorium Data map for the Study Area (contour Interval≈5.0ppm)

Figure 4.18 is the Thorium content map of the study area. The map shows high concentration of Thorium around Wamba, Kwolla, Shendam, Lafia, Akiri, Ibi and Wukari south. Low concentrations of Thorium are predominant around Makurdi, Akwana, Akiri and Wukari. Mineralization associated with thorium includes basement granitic rocks, migmatite, shales and clay.

4.3.3 Uranium (U) content map:
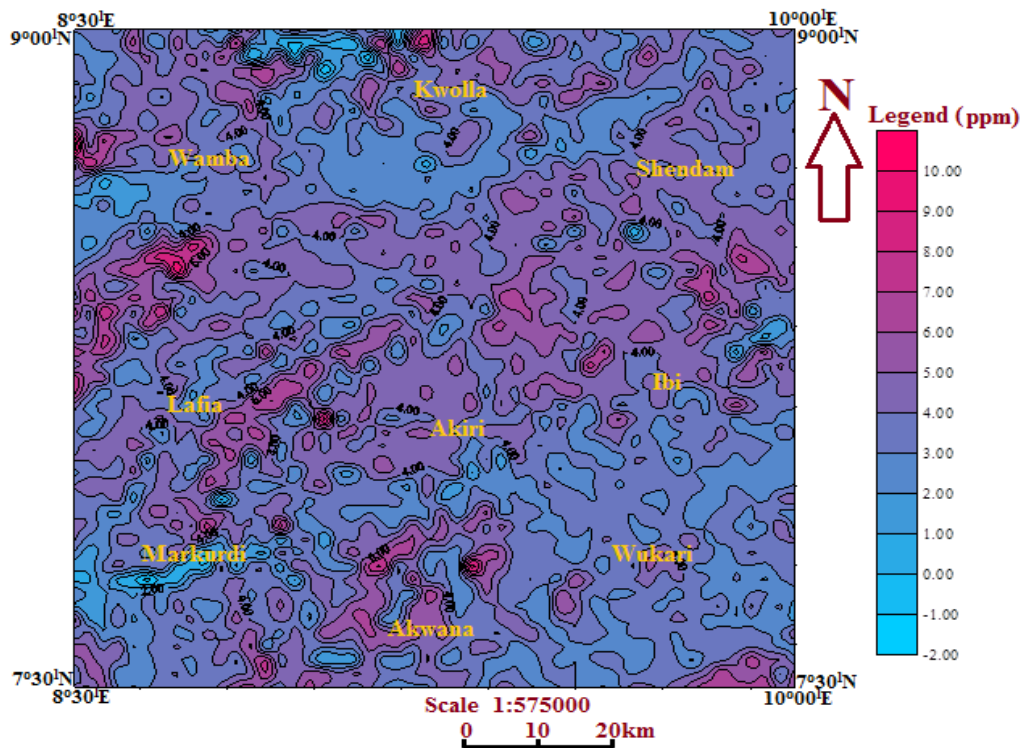
Figure 4.19: Uranium Data map for the Study Area (contour Interval≈1.0ppm)

Figure 4.19 is the Uranium content map of the study area. The map shows high concentration of Uranium around Lafia, Akiri, Ibi, Akwana, south of Wukari and Makurdi north. Low concentration of U is found around Kwolla, Shendam, Wamba, Wukari and Makurdi south. Shales, clay and basement complex rocks (such as granite and migmatite) are associated with uranium mineralization.

4.3.4 Radiometric Heat Map
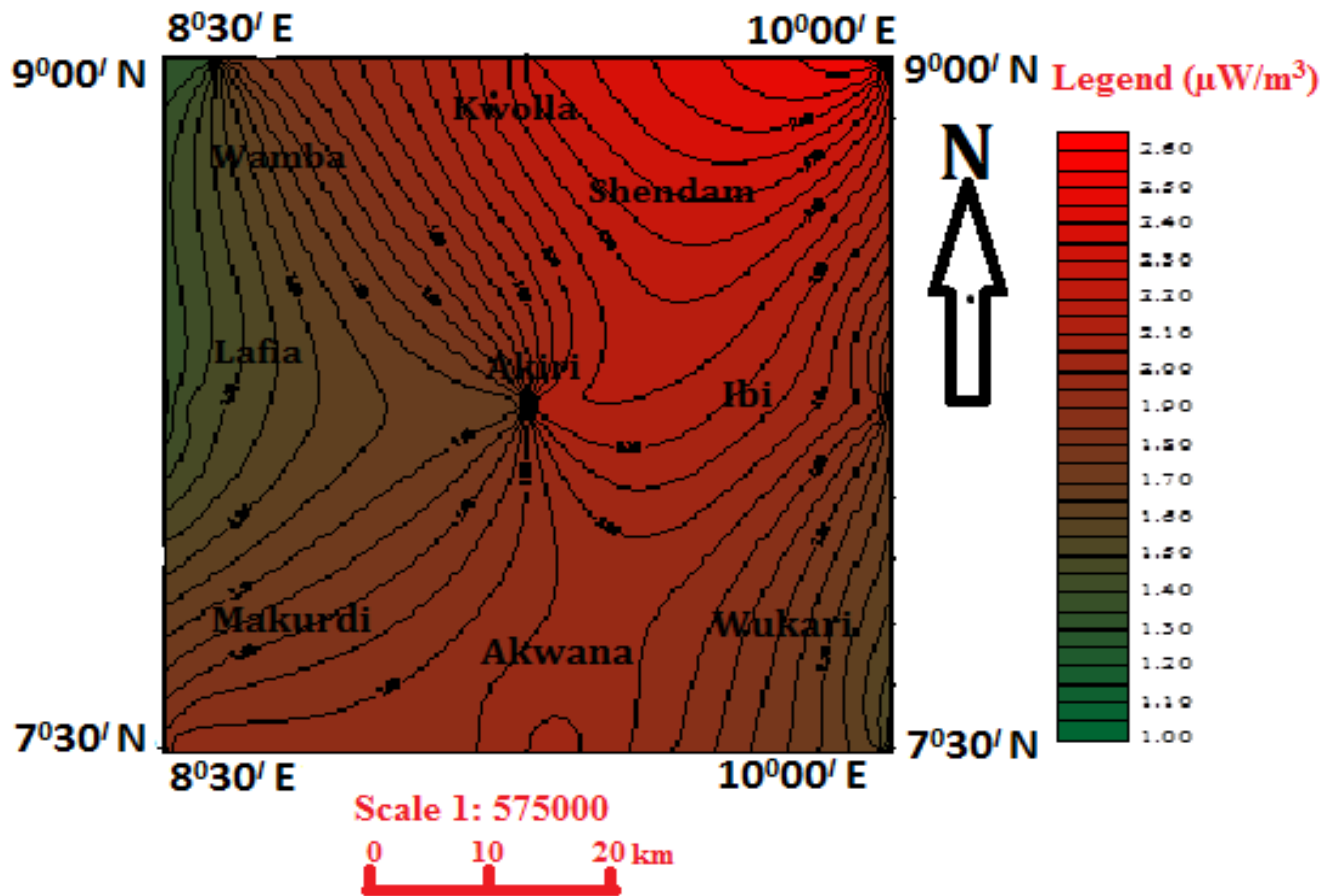

Figure 4.20 Radiometric Heat Map of the Study Area (Contour Interval $\approx$ 0.05 μW/m^3)

High concentration of radiometric heat has the highest occurrence around Kwolla, Shendam, Akiri, Ibi, Makurdi and Akwana. These areas are the hot spots which are potential geothermal areas. Low concentrations are found around Wamba, Lafia and Wukari (Figure 4.20).

4.3.5 Correlation between Geothermal Heat Flow, Radiometric Heat and Geology of the Study Area
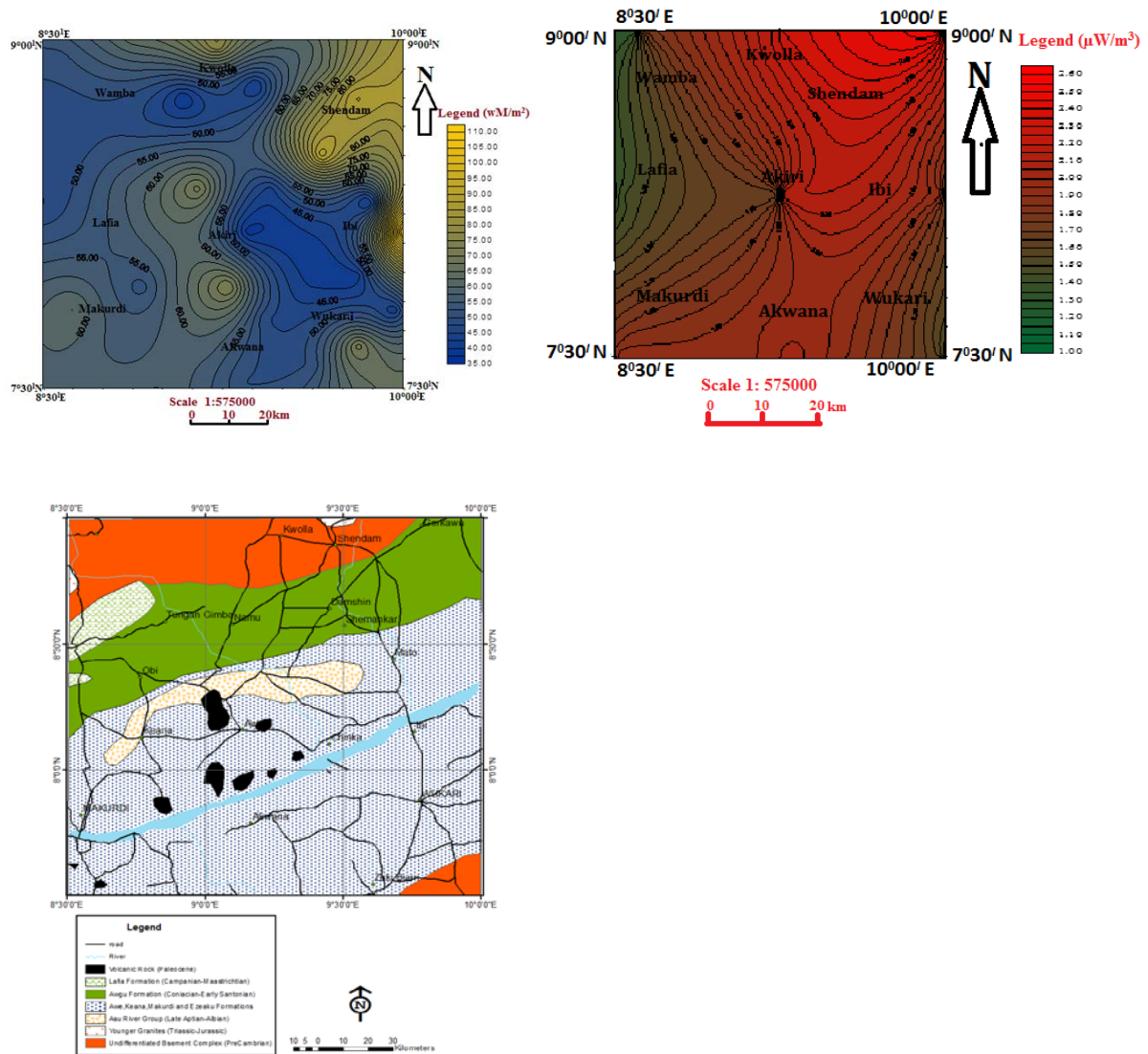
Figure 4.21: Correlation of (a) Geothermal Heat Flow Map, (b) Radiometric Heat Map and (c) Geologic map of the Study Area

Figure 4.21 shows that areas with high geothermal heat are the same areas with high radiometric heat in the study area (Kwolla, Shendam, Akiri, Ibi, Makurdi and Akwana). Compared with the geology of the area, those areas with high geothermal heat flow and high radiometric heat concentration are those covered by basement complex, volcanic intrusives; and sandstones and shales.

4.3.6 Correlation of Geothermal Energy Potential deduced from Aeromagnetic Data and Aeroradiometric Data of the Study Area
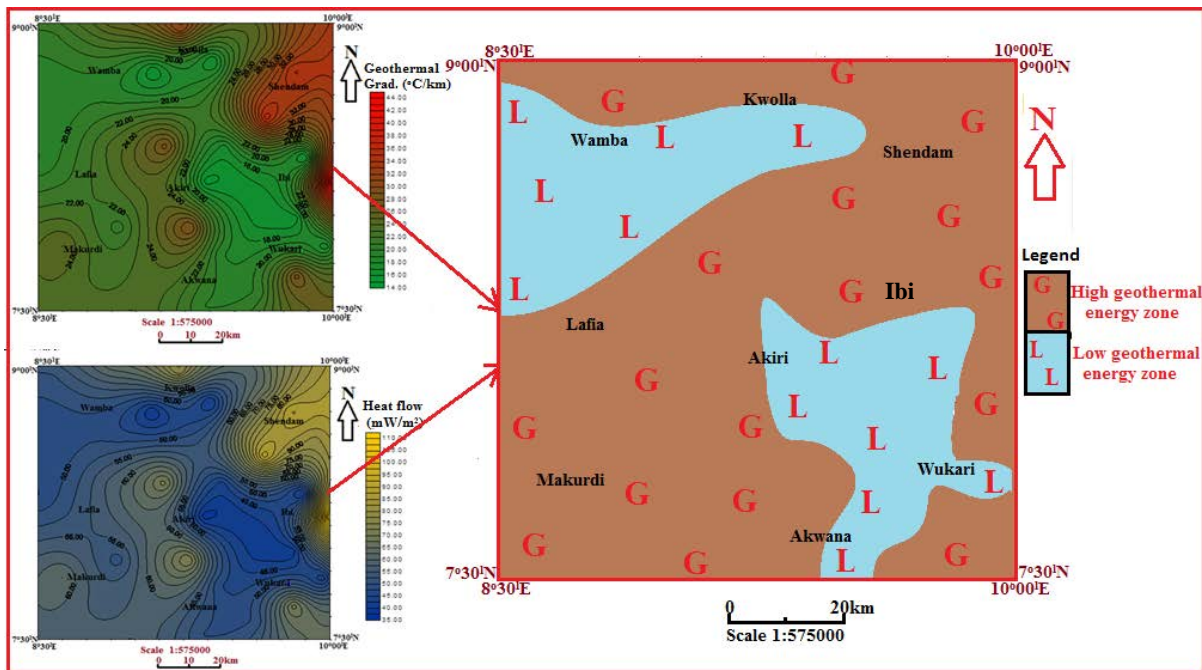
Figure 4.22(a): A Geothermal Energy Potential map Deduced from Magnetic Interpretation across the Study Area
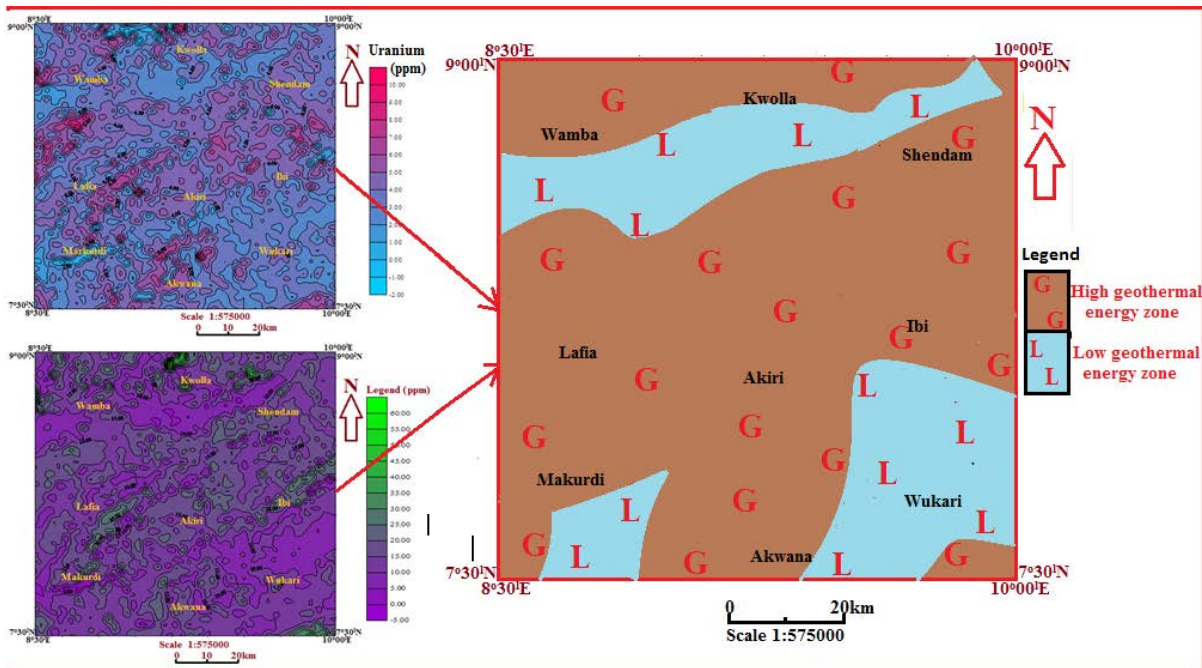
Figure 4.22(b): A Geothermal Energy Potential map deduced from Radiometric Interpretation across the Study Area
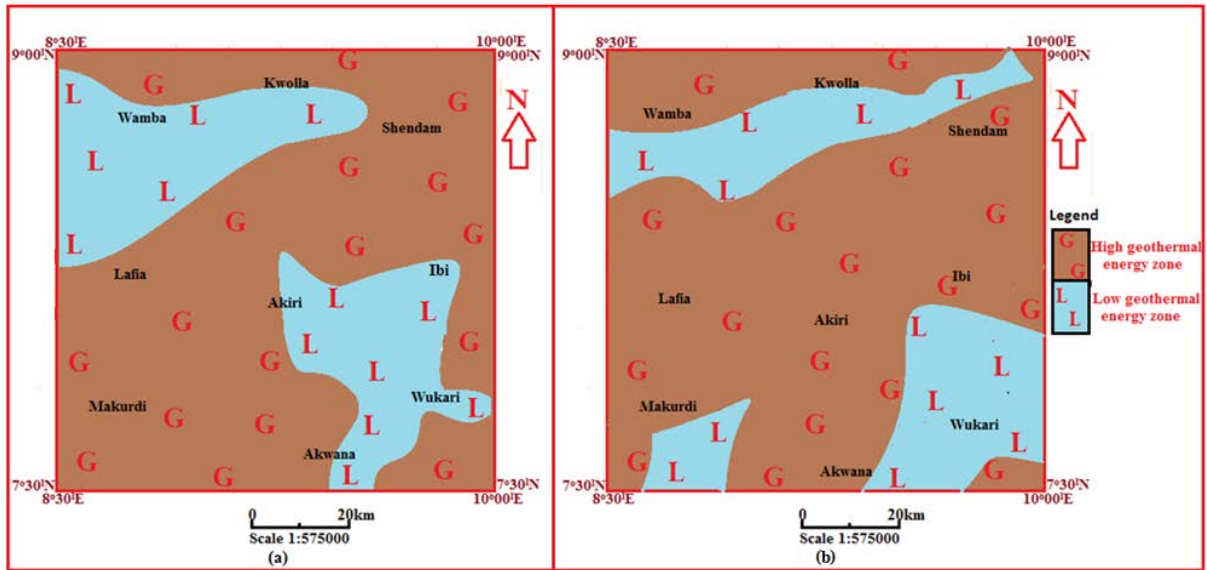
Figure 4.23: Comparism of Geothermal Energy Potential maps deduced from
(a) Aeromagnetic Interpretation and (b) Aeroradiometric Interpretation across the Study Area

From the study, areas around Kwolla, Shendam, Lafia, Akiri, Ibi, Makurdi and Akwana have high geothermal energy potentials, which is almost the same for both aeromagnetic interpretation and aeroradiometric interpretation in the study area (Figures 4.22 (a) and (b)). The study shows that the geothermal energy potential deduced from aeromagnetic data correlates well with the geothermal energy potential deduced from aeroradiometric data (Figure 4.23).

CHAPTER FIVE

SUMMARY, CONCLUSIONS AND RECOMMENDATIONS

5.1 Summary

Information on geothermal gradient and heat flow within the subsurface is critical in the quest for geothermal energy exploration. There had been a rapid increase in the quest for the development of renewable energy resources all over the world, of which geothermal resources is one of them. The present study provides subsurface thermal information that will guide regional geothermal energy exploration in the study area and Nigeria as a whole. The source of geothermal energy used by mankind is the earth's natural heat which is derived primarily from the decay of long-lived radioactive isotopes of uranium, thorium and potassium but probably with a contribution from a slight cooling of the earth (Downing and Gray, 1986). The earth acts as a heat engine and at its surface there is a continuous heat flux comprising the heat flow from the radioactive isotopes which are largely concentrated in the upper crust. As a consequence, a study of subsurface heat flow is a principal technique for the identification and location of geothermal resources as it permits the prediction of temperatures to depths below those reached by shallow drilling.

The application of spectral analysis to the interpretation of potential field data is one method that can be used to determine the basement depth, and is now sufficiently well-established [Spector and Grant, 1970; Fedi *et al.*, 1997]. This present study concerns the evaluation of the total aeromagnetic anomalies for estimation of curie-temperature depth, subsurface heat flow and thermal heat gradient in the Middle Benue Trough of Nigeria, which has in the past received limited attention from geoscientists. Curie-temperature depth combined with heat flow assessment would complement greatly the geophysical information of the area to bridge the gap of absence of crustal temperature information.

Aeromagnetic data have been used in geothermal investigations to estimate basal depths of the Curie point magnetic layer and to assess concealed structure (Abraham *et al.*, 2014). The assessment of variation of the curie isotherm of an area can provide valuable information about the regional temperature distribution at depth and the concentration of subsurface geothermal energy (Tselentis, 1991). One important parameter that determines the relative depth of the curie isotherm with respect to sea level is the local thermal gradient i.e. heat flow (Hisarlis, 1996). Results have shown that a region with significant geothermal energy is characterized by an anomalous high temperature gradient and heat flow (Tselentis, 1991). It is therefore expected that geothermally active areas would be associated with shallow Curie point depth (Nuri *et al.*, 2005).

The Qualitative Interpretation of total magnetic intensity (TMI), residual anomaly map, and lineament maps were done. The total magnetic field from the study area ranges from 7800 to 8240 nanotesla (nT). Higher values (shown in red) are found in the northern, north central, western, south western and southern parts of the study area; while lower magnetic intensity values (shown in blue) are found in the northwest, northeast, central and south-eastern regions. The study area is characterized by closely spaced linear sub-parallel contours which suggest that faults or local fractured zones may possibly pass through such areas. The general trending fabric of the TMI anomalies is northeast to southwest (NE-SW) direction. The residual magnetic field map shows a general trending fabric of NE to SW direction similar to those of the TMI map. The elliptical contour closures seen in the study area suggests the presence of magnetic bodies. These features represent geologic lineaments and their positions are indicated by lines drawn parallel to the elongation and through the centre of the anomalies represented in Figure 4.5.

The residual anomaly map shows that the contour lines are widely spaced in the NW, West and SW parts of the study area which implies that there are thicker sediments in those regions

(Wamba, Lafia, and Makurdi), indicating that the depth to basement is higher in these areas compared to the areas where there are closely spaced contours which suggests shallow sedimentary thickness. Figure 4.2 also shows positive magnetic anomalies in areas like Wamba, Lafia and Makurdi which suggests deeper depths in such areas, while areas around Shendam, Ibi and Akiri show negative anomalies which indicates shallower depths to magnetic bodies.

The Upward Continuation map of the study area shows areas with highest magnetic intensity in blue colour (near Kwolla), Wamba (north), Lafia, Makurdi and Akwana have higher intensity (red colour), while Akiri, Ibi, Wukari and Wamba (south) have lowest intensities (yellow colour). The magnetic lineament map and Rose diagram shows that the main trend of the lineaments is NE-SW, while minor ones trend E-W and NNE-SSW directions.

In the present study, the parameters needed are the depth-to-top of magnetic source, depth to centroid, depth to base (or depth to bottom) of magnetic source which is known as Curie point depth. Curie point depth is the depth at which magnetic minerals lose their magnetism due to the effect of temperature (temperature range of 530^0C to 580^0C is taken as the Curie point temperature). The application of radiometric surveying is useful in geologic mapping because of its ability to detect radioactivity emanating from the natural decay of elements such as uranium, thorium and potassium from the earth material. The product of this decay results in the emission of alpha, beta and gamma radiations which can be detected on the surface using radioactive element detectors. The study of heat production and heat flow is therefore the main tool for the identification and location of geothermal resources.

The study investigating geothermal energy potential of parts of the Middle Benue Trough, Nigeria was carried out using aeromagnetic and aeroradiometric data obtained from the Nigerian Geological Survey Agency (NGSA). The study was aimed at estimating the Curie point depths (CPDs) and geothermal parameters in the study area which include geothermal

gradient and subsurface heat flow. The high resolution aeromagnetic data was analysed through spectral method to obtain depths to top, centroid, and bottom of the magnetic sources. The depth values were then used to assess the Curie point depth (CPD), geothermal gradient, and subsurface geothermal heat flow in the basin.

The results show that the Curie point depth varies between 12.70 and 37.22km, with an average of 26.29km; the geothermal gradient varies between 15.58^0C/km and 45.67^0C/km, with an average of 23.58^0C/km, and the crustal geothermal heat flow varies between 38.96mW/m^2 and 114.17mW/m^2, with an average value of 58.94mW/m^2. The lowest geothermal gradient value (15.58^0C/km) corresponds to the lowest heat flow value (38.96mW/m^2), while the highest geothermal gradient (45.67^0C/km) corresponds to the highest heat flow value (114.17mW/m^2). The lowest heat flow value (38.96mW/m^2) corresponds to the highest Curie point depth (37.22km), while the highest heat flow value corresponds to the lowest Curie point depth (12.70km). This shows that the Curie point depth varies inversely with the geothermal heat flow, and the geothermal gradient varies directly with the heat flow.

The radiometric heat map of the study area was constructed from the values of Potassium (K), Thorium (Th) and Uranium (U) content. The result shows that two-third of the map is covered by high concentration of radiometric heat, with highest occurrence around Wamba north, Kwolla north, Lafia, Akiri and Ibi (in the central region), Makurdi and Akwana (in the south). This corresponds to areas with higher heat flow (calculated). Lineament analysis using the lineament map and rose diagram showed the main structural trend in the study area to be NE-SW, while minor ones trend E-W and NNE-SSW directions.

According to Amadi *et al*; 2012, the uranium and thorium content of rocks generally increases with acidity, with the highest concentrations found in pegmatite's and granites (basement complex) and lowest concentrations found in shale and clay (sedimentary terrain).

In the geologic context, it is observed that those areas covered by crystalline basement rocks, younger granites, and volcanic rocks with areas where magmatic intrusions (such as dykes and sills) occurs within the sedimentary basin have the lowest values of Curie point depths (12.70 to 27.90km) and corresponding higher heat flow values (about 60 to 115mW/m^2) in the study area (also, with high radiometric heat); while the areas covered by the cretaceous sedimentary rocks have high Curie point depths with corresponding lower values of heat flow (and low radiometric heat), where shale and clay are mostly found. It is also found that in areas where there are crustal and mantle uplifts and the Curie point depths are shallow (e.g. on profiles C-C^l, D-D^l and F-F^l), the corresponding geothermal heat flow and radiometric heat is high.

Therefore areas around Kwolla (in the north), Shendam (NE), Akiri (Central), Lafia and Makurdi (SW); and Wukari south (SE) that have low Curie point depths with corresponding high heat flow and high radiometric heat are areas which are geothermally active. These areas have geothermal energy potential which can be utilized. This is manifested at the surface where warm springs occur in Akiri, Awe local government area of Nassarawa State, in the central region of the study area (Ikechukwu, *et al*., 2015). Their temperatures range between 43.5^{0}C and 53.5^{0}C. Two artesian wells are also found in the area. Temperatures of the water flowing freely from the wells are 43.5^{0}C and 34^{0}C respectively.

From the total magnetic field intensity map of the study area, the magnetic intensity ranges from 7800 to 8240 nanotesla (nT). Higher values (shown in red) are found in the northern, north central, western, south western and southern parts of the study area; while lower magnetic intensity values (shown in blue) are found in the northwest, northeast, central and south-eastern regions.

The aeromagnetic data was analysed through spectral method to obtain depths to top, depths to centroid, and depths to bottom of the magnetic sources. The depths to top of magnetic sources indicate the sedimentary thickness in the study area which ranges from 0.76 to 4.46 km, with an average of 2.14 km. The result of depth to basement agrees with the work of previous workers in the Benue Trough. Nwachukwu (1985) estimated the magnetic basement depth of the Middle Benue Trough to be between 2.00 km and 4.00 km, depth to the magnetic basement from the spectral work of Ahmed (1991) vary from 1.513 km and 4.936 km, and Alikali and Kasidi (2016) who obtained depths varying between 0.50 km and 4.80 km in the Middle Benue Trough; while Salako (2014) who worked in the Upper Benue Trough obtained basement depth estimates between 0.96 km and 5.862 km.

The depth values obtained for the study area were then used to compute the Curie point depth (CPD), geothermal gradient, and subsurface geothermal heat flow in the study area. The results show that the Curie point depth varies between 12.70 and 37.22 km, with an average of 26.29 km; the geothermal gradient varies between 15.58 ^{0}C/km and 45.67 ^{0}C/km, with an average of 23.58 ^{0}C/km, and the crustal geothermal heat flow varies between 38.96mW/m^2 and 114.17 mW/m^2, with an average value of 58.94 mW/m^2. The result also shows that the geothermal heat flow in the area increases with a decrease in Curie point depths; while the geothermal heat flow increases with an increase in geothermal gradient. This implies that the Curie point depths vary inversely with the geothermal heat flow values, while the geothermal gradient varies directly with the heat flow.

The radiometric heat map of the study area was constructed from the values of Potassium (K), Thorium (Th) and Uranium (U) content. The result shows high concentration of radiometric heat in the study area, with highest occurrence around Wamba north, Kwolla north, Lafia, Akiri and Ibi (in the central region), Makurdi and Wukari-South. This corresponds to areas with higher geothermal heat flow. Lineament analysis using the

lineament map and rose diagram showed the main structural trend in the study area to be north–east to south-west (NE-SW), while minor ones trend east to west (E-W) and NNE-SSW directions. The major anticline occurs in the study area which coincide with the Keana Anticline, trends NE-SW and extends from northeast of Makurdi via north of Keana to the north of Awe (Akiri). Three minor anticlines close to the major one with axis trending NE-SW also occurs. In addition, the geological structures (magnetic lineaments and dykes) are relatively long suggesting that they are regional structures (Anudu, *et al*., 2014). The main structural trends (NE-SW and E-W) agree with the magnetic trend results. Based on the sedimentary thickness range of 0.76km to 4.46km, the possibility of hydrocarbon generation is feasible.

The study reveals that the region is characterised by shallow Curie point depths and high geothermal heat flow. The Curie point depths estimated, the average depth of magnetic sources and subsurface geothermal heat flow values is concluded to reflect thermal structures in the area. It is also observed that those areas covered by crystalline basement rocks, younger granites and volcanic rocks have the lowest values of Curie point depths (12.70 to 27.90km) and corresponding higher heat flow values (about 60 to 115mW/m^2) in the study area which is attributed to magnetic intrusions at depth combined with volcanic activities; while the areas covered by cretaceous sedimentary rocks have high Curie point depths with corresponding lower values of heat flow, except where there are uplifted crust and mantle, and intrusions like dykes. The average heat flow in "thermally normal" continental regions is around 60mW/m^2. Hence values in excess of about 80-100mW/m^2 indicate anomalous geothermal conditions (Jessop *et al*., 1976). For the present study, anomalous geothermal condition has been assigned to all estimated geothermal heat flow values that are well above 80mW/m^2. Therefore areas around Wamba and Kwolla (in the north), Shendam (NE), Lafia and Akiri (Central), Makurdi (SW) and Wukari south (SE) that have low Curie point depths

with corresponding high heat flow values are areas which are geothermally active. These areas have geothermal energy potential which can be utilized.

High concentration of radiometric heat has the highest occurrence around Kwolla, Shendam, Akiri, Ibi, Makurdi and Akwana. These areas are the hot spots which are potential geothermal areas. The areas of high radiometric heat concentration correspond with the areas with low Curie point depth, high geothermal gradient and high geothermal heat flow.

5.2 Conclusions

The Curie point depths and geothermal parameters in the study area were estimated. The aeromagnetic data was analysed through spectral method to estimate the subsurface geothermal heat flow in the study area, while the aeroradiometric data was analysed by using radiometric heat production equation to estimate the radiometric heat in the study area.

The depth to top of magnetic sources (sedimentary thickness) in the study area ranges from 0.76 to 4.46km. Based on this thickness range, there is an indication that the possibility of hydrocarbon generation is feasible in the study area if all other conditions for hydrocarbon accumulation are favourable. The result of the depth to basement in the study area agrees with the work of previous workers in the Benue Trough. Nwachukwu (1985) estimated the magnetic basement depth of the Middle Benue Trough to be between 2.00 km and 4.00 km, depth to the magnetic basement from the spectral work of Ahmed (1991) vary from 1.513 km and 4.936 km and Alikali and Kasidi (2016) who obtained depths varying between 0.50 km and 4.80 km in the Middle Benue Trough; while Salako (2014) who worked in the Upper Benue Trough obtained basement depth estimates between 0.96 km and 5.862 km.

Areas of low Curie point depths correspond to high geothermal heat and high radiometric heat. Based on these results from the low values of Curie point depth in some areas, there is likelihood that the study area has geothermal potentials. The geothermal heat flow values around Kwolla, Shendam, Lafia, Akiri, Ibi, Makurdi and Wukari South fall between 60 and

100mW/m^2 which is the acceptable standard for geothermal heat flow potentiality. Therefore, areas around Kwolla, Shendam, Lafia, Akiri, Ibi, Makurdi and Wukari South that have low Curie point depths with corresponding high heat flow values and high radiometric heat are areas which are geothermally active and can be utilized for geothermal energy production. Geologically, these areas are those covered by basement complex, volcanic intrusives; and sandstones and shales (in the sedimentary area). The study also shows that the geothermal energy potential deduced from aeromagnetic data correlates well with the geothermal energy potential deduced from aeroradiometric data.

5.3 Contributions to Knowledge

The study has shown several new things derived from aeromagnetic and aeroradiometric methods which in the past have not been adequately utilized.

- **Integration of aeromagnetic and aeroradiometric data to investigate geothermal energy potential:**

  The two data sets used in the study area correlates well.

- **Prediction of geothermal heat from Curie point depths (CPD):**

  A relationship has been established for the study area which shows that as the CPD decreases, the geothermal heat increases (Model equation 1: $Q = 0.1135Z^2 - 8.3879Z + 192.48$).

- **Prediction of geothermal heat from geothermal gradient:**

  A second relationship has been established for the study area which shows that as the geothermal gradient increases, the geothermal heat also increases (Model equation 2: $Q = 2.5Z + 0.0002$).

- **Prediction of radiometric heat from geothermal heat:**

  In the study, the higher the geothermal heat in the area, the higher the radiometric heat.

- **Origin and Source of heat:**

The presence of magmatic intrusions in the crust, uplifted crust and mantle, major faults, volcanic rocks, and high concentration of radiometric elements of K, Th, and U establishes the origin and source of heat in the study area.

- **High geothermal energy:**

The study shows high subsurface heat flow and high concentration of radiometric heat in the study area. These are high enough to cause high geothermal energy which is evident by manifestation of hot springs at the surface.

5.4 Recommendations

The following recommendations are made for further studies based on the results obtained from the analyses of both the aeromagnetic and aeroradiometric data over parts of the Middle Benue Trough, Nigeria.

- The spectral and radiometric heat production methods used in this study should be applied in other areas observed to have geothermal energy potential across Nigeria.

- The geothermal parameters should be further investigated by carrying out borehole temperature logging in the study area.

- In areas where there is high geothermal heat flow and high radiometric heat concentration (around Kwolla, Shendam, Lafia, Akiri, Ibi, Makurdi and Akwana), exploratory wells should be drilled to confirm the depths to heat sources.

REFERENCES

Abdulsalam, N.N, Mallam, A. and Likkason, K.O., 2011. Indication of High Frequency Structures using Derivative Features over Koton Karifi Area, Nigeria, modelled from Aeromagnetic Data, *Academia Arena*, vol. 3, No. 8, pp. 18-25.

Abedi, M., Ghoami, A. and Noronzi, G.H., 2013. A stable downward continuation of airborne magnetic data: A case study for mineral prospectivity mapping in Central Iran, *Computational Geosciences*, vol. 52, pp. 269-280.

Abraham, M.Z., 2013. Challenges and Prospects of Geophysical Exploration of Geothermal System for National Development, *Academic Journal of Interdisciplinary Studies*, MCSER Publishing, Rome, Italy, vol. 2, No. 12, pp. 137-143.

Abraham, E.M., Lawal, K.M., Ekwe, A.C., Alile, O., Murana, K.A. and Lawal, A. A., 2014. Spectral analysis of aeromagnetic data for geothermal energy investigation of Ikogosi Warm Spring–Ekiti State, South-Western Nigeria, *Geothermal Energy*, vol. 2, No. 6, pp. 1-21.

Abraham, E.M., Obande, E.G., Chukwu, M., Chukwu, C.G. and Onwe, M.R., 2015. Estimating depth to the bottom of magnetic sources at Wikki Warm Spring region, N.E. Nigeria, using fractal distribution of sources approach, *Turkish Journal of Earth Sciences*, vol. 24, pp. 1-19.

Abraham, E.M. and Nkitnam, E.E., 2017. Review of Geothermal Energy Research in Nigeria: The Geoscience Front, *International Journal of Earth Science and Geophysics*, vol. 3, No. 15, pp. 1-10.

Abubakar, M.B., 2014. Petroleum Potentials of the Nigerian Benue Trough and Anambra Basin: A Regional Synthesis, *Natural Resources*, vol. 5, pp. 25-58.

Abubakar, Y.I., Umego, M.N., Ojo, S.B., 2010. Evolution of Gongola Basin, Upper Benue Trough, North-Eastern Nigeria, *Asian Journal of Earth Sciences*, vol. 3, pp. 62-72.

Ahmed, N.M., 1991. Spectral Analysis of Aeromagnetic Data over the Middle Benue Trough, Nigeria, Research Publication, M.Sc. Thesis, University of Nigeria Nsukka.

Ajayi, C.O. and Ajakaiye, D.E., 1981. The Origin and Peculiarities of the Benue Trough, Another look from the recent gravity data in the Middle Benue, *Tectonophysics*, vol. 80, pp. 285-303.

Ajibade, A.C. and Fitches, W.R., 1988. The Nigerian Precambrian and Pan-African Orogeny. In: Precambrian Geology of Nigeria, A Publication of the Nigerian Geological Survey Agency, Abuja, pp. 45-53.

Akanbi, E.S. and Udensi, E.E., 2006. Structural trends and spectral depth analysis of the residual field of Pategi Area, Nigeria, using aeromagnetic data, *Nigerian Journal of Physics*, vol. 18, No. 2, pp. 271-176.

Akinsoji, O.O., 2016. The Nigerian Power Sector Investment Opportunities and Guidelines (Draft), Federal Republic of Nigeria, 39p.

Alagbe, O.A. and Sunmonu, L.A., 2014. Interpretation of aeromagnetic data from Upper Benue Basin, Nigeria, using automated techniques, *IOSR Journal of Applied geology and geophysics*, vol. 2, pp. 22-40.

Alikali, S.C. and Kasidi, S., 2016. Determination of Depth to Magnetic Sources using Spectral Analysis of High Resolution Aeromagnetic Data over IBBI and Environs, Middle Benue Trough, North Central Nigeria, *International Journal of Science and Research* (IJSR), ISSN (Online): 2319-7064, vol. 5, Issue 6, pp. 1572-1578.

Amadi, A.N., Okoye, N.O., Olasehinde, P.L., Okunlola, L.A., Alkali, Y.B., Ako, T.A. and Chukwu, J.N., 2012. Radiometric Survey as a useful tool in geological mapping of Western Nigeria, *Journal of Geography and geology*, vol. 4, No. 1, pp. 242-249.

Anakwuba, E.K., Onwuemesi, A.G., Chinwuko, A.I. and Onuba, L.N., 2011. The interpretation of aeromagnetic anomalies over Maiduguri-Dikwa depression, Chad Basin, Nigeria: A structural view. Scholars Research Library, *Archives of Applied Science Research*, vol. 3, No. 4, pp. 499-506.

Anudu, G.K., Stephenson, R.A. and Macdonald, D.I.M., 2014. Using high-resolution aeromagnetic data to recognize and map intra-sedimentary volcanic rocks and geological structures across the Cretaceous Middle Benue Trough, Nigeria, *Journal of African Earth Sciences*, vol. 99, pp. 625-636.

Armstead, H.C., 1983. Geothermal Energy, E. & F. N. Spon, London, U.K., 404p.

Bansal, A.R., Gabriel, G., Dimri, V.P. and Krawezyk, C.M., 2011. Estimation of depth to the bottom of magnetic sources by a modified centroid method for fractal distribution of sources: An application to aeromagnetic data in Germany, *Geophysics*, vol. 76, pp. 11-22.

Bansal, A.R., Anand, S.P., Rajaram, M., Rao, V.K., Dimri, V.P., 2013. Depth to the bottom of magnetic sources (DBMS) from aeromagnetic data of Central India using modified centroid method for fractal distribution of sources, *Tectonophysics*, vol. 603, pp. 155-161.

Baranov, W., 1975. Potential fields and their transformations in applied geophysics, Gebnider publishing Company, Borntenger, Berlin, pp. 1-35.

Bassey, N.E. and Ishaku, J.M., 2012. Conjunctive use of magnetic and radiometric surveys for mapping of ferruginous sandstone horizons in Yola Area, Nigeria, *Journal of Earth Science and Geotechnical Engineering*, vol. 2, No. 1, pp. 39-51.

Bath, M., 1974. Spectral Analysis in Geophysics: Development in Solid Earth Geophysics, Elsevier Publication Company, Amsterdam, 579p.

Beamish, D. and Busby, J., 2016. The Corrubian geothermal province: Heat production and flow in South-Western England: estimates from boreholes and airborne gamma- ray measurements, *Geothermal Energy*, vol. 4, No. 4, pp. 1-25.

Bello, R., Ofoha, C.C. and Wehiuzo, N., 2017. Geothermal Gradient, Curie Point Depth and Heat Flow Determination of some Pats of Lower Benue Trough and Anambra Basin, Nigeria, using High-Resolution Aeromagnetic Data, *Physical Science International Journal*, vol. 15, No. 2, pp. 1-11.

Benkhelil, I., 1989. The origin and evolution of the Cretaceous Benue Trough, Nigeria, *Journal of African Earth Sciences*, vol. 8, pp. 251-282.

Bhattacharyya, B.K. and Leu, L.K., 1975. Analysis of magnetic anomaly over Yellowstone National Park: Mapping of Curie point isothermal surface for geothermal reconnaissance, *Journal of Geophysical Research*, vol. 8, pp. 4461-4465.

Blakely, R.J., 1988. Curie temperature isotherm analysis and tectonic implications of

aeromagnetic data from Nevada, *Journal of Geophysical Research*, vol. 93, pp. 11817-11832.

Blakely, R.J., 1995. Potential theory in gravity and magnetic applications, First Edition, Cambridge University Press, Cambridge, United Kingdom, 441p.

Blodgett, L., 2014. Geothermal 101: Basics of Geothermal Energy, Geothermal Energy Association, 27p.

Boadi, B. Wemegah, D.D. and Preko, K., 2013. Geological and Structural interpretation of the Konongo area of the Ashanti gold belt of Ghana from aeromagnetic and radiometric data, International Research Journal of Geology and Mining, vol. 3, No. 3, pp. 124-135.

Boschetti, F., 2005. Improved edge detection and noise removal in gravity maps via the use of gravity gradients, *Journal of Applied Geophysics*, vol. 57, pp. 213-225.

Bucker, C. and Rybach, L., 1996. A simple method to determine heat production from gamma-ray logs, *Petroleum Geology*, vol. 13, pp. 373-375.

Bullard, E.C., 1965. Historical introduction to terrestrial heat flow, In: Lee, W.H.K., ed., Terrestrial Heat Flow, *American Geophysics*, vol. 8, pp. 1-6.

Burke, K.C., Dessauvagie, T.F.J., Whiteman, A.J., 1972. Geological history of the Benue valley and adjacent areas, In: Dessauvagie, T.F.J, Whiteman, A.J. (Eds), African Geology, University of Ibadan, Ibadan, pp. 181-185.

Burke, K.C. and Whiteman, A.J., 1973. Uplift, rifting and the break-up of Africa, In: Tarling, D.H., Runcorn, S.K. (Eds), Implications on Continental Drift to Earth Sciences, pp. 735-755.

Clark, D.A. and Emerson, D.W., 1991. Notes on rock magnetic characteristic in applied Geophysical Studies, *Exploration Geophysics*, vol. 22, pp. 547-555.

Clark, D.A., 1997. Magnetic properties of rocks and minerals, *AGSO Journal of Australian Geology and Geophysics*, vol. 17, No. 2, pp. 83-103.

Coker, J.O., Mustapha, A.O., Makinde, V. and Adesodun, J.K., 2014. Radiometric Survey to

determine the terrestrial gamma radiation levels: A case study of Sagamu and Abeokuta, South-western Nigeria, *International Journal of Pure and Applied Sciences and Technology*, vol. 21, No.1, pp. 31-38.

Cooley, J.W. and Tukey, J.W., 1965. An algorithm for the machine calculation of complex Fourier Series, *Mathematical Computations*, vol. 19, No. 90, pp. 297-301.

Cratchley, C.R. and Jones, G.P., 1965. An interpretation of geology and gravity anomalies of the Benue Valley, Nigeria, Overseas Geological Survey, London, *Geophysics*, vol.1. pp. 1-26.

Cratchley, C.R., Louis, P., and Ajakaiye, D.E., 1984. Geophysical and geological evidence of the Benue-Chad basin cretaceous rift valley system and its tectonic implications, *Journal of African Earth Science*, vol. 2, pp. 141-150.

Davis, J.C., 2014. Statistics and Data Analysis in Geology, John Wiley and Sons, New Delhi, India, 638p.

Dean, W.C., 1958. Frequency analysis for gravity and magnetic interpretation, *Geophysics*, vol. 23, No. 1, pp. 97-127.

Dickson, B. I. and Scott, K.M., 1997. Interpretation of aerial gamma-ray surveys adding the geothermal factors. *AGSO Journal of Australian Geology and Geophysics*, vol. 17, No. 2, pp. 187-200.

Dickson, M.H. and Fanelli., 2004. What is Geothermal Energy? *Istituto di Geoscienze e Georisorse*, CNR, Piza, Italy, 33p..

Dobrin, M.B., Savit, C.H., 1988. Introduction to geophysical prospecting, Fourth edition, McGraw-Hill, New York, 867p.

Dolmaz, M.N., Ustaomer, T., Hisarli, Z.M. and Orbay, N., 2005. Curie point depth variations to infer thermal structure of the crust at the African Eurasian Convergence zone, S.W. Turkey. *Earth Planets Space*, vol. 57, pp. 373-383.

Downing, R.A. and Gray, D.A., 1986. Geothermal Energy: The Potential in United Kingdom. British Geological Survey Report, pp. 3-7.

Durance, E.M., 2004. Radioactivity in Geology: Principles and Application, Ellis Horwood Limited, Chichester, England, 441p.

ECN, 2012. Energy Commission of Nigeria: Renewable Energy Master Plan, Abuja, Nigeria.

Eletta, B.E. and Udensi, E.E., 2012. Investigation of the Curie Point Isotherm from the Magnetic Fields of the Eastern Sector of Central Nigeria, *Geosciences*, vol. 2, No. 4, pp. 101-106.

Faure, G., 1977. Principles of Isotope Geology, John Willey and Sons Limited, United Kingdom, 608p.

Fedi, M., Quarta and De Santis, A., 1997. Improvements to the Spector and Grant method of source depth estimation using the power law decay of magnetic field power spectra, *Geophysics*, vol. 62, pp. 1143-1150.

Fedi, M. and Florio, G., 2001. Detection of potential fields source boundaries by enhanced horizontal derivative method, *Geophysical Prospecting*, vol. 49, pp. 40-58.

Fedi, M. and Florio, G., 2002. A stable downward continuation by using ISVD method, *Geophysical Journal International*, vol. 151, pp. 146-156.

Fedi, M. and Florio, G., 2013. Determination of the maximum-depth to potential field sources by a maximum structural index method, *Journal of Applied Geophysics*, vol. 88, pp. 154-160.

Fertl, W., 1983. Gamma-ray spectral logging: a new evaluation frontier, World Oil, pp. 79-91.

Garba, M.I., Kurowska, E., Schoeneich, K. and Abdullahi, I., 2012. Rafin Rewa Warm Spring, A New Geothermal Discovery, *American International Journal of Contemporary Research*, vol. 2, No. 9, pp. 231-236.

Grasty, R., 1979. Gamma-ray spectrometric methods in Uranium exploration, Theory and Operational Procedures, *Geophysical and Geochemical search for Metallic Ores*, vol. 31, pp. 147-155.

Gunn, P.J., 1997. Application of aeromagnetic surveys to sedimentary basin studies,

Australian Geological Society Organisation (AGSO), *Journal of Australian Geology and Geophysics*, vol. 17, No. 2, pp. 133-144.

Gunn, P.J., Minty, B.R. and Milligan, P., 1997. The airborne gamma-ray Spectrometric response over arid Australian terrenes, *Exploration*, vol. 97, pp. 733-740.

Hahn, A., 1965. Two dimensional application of Fourier analysis for the interpretation of geomagnetic anomalies, *Journal of Geomagnetism*, vol. 17, pp. 195-225.

Hahn, A., Kind, E. and Mishra, D.C., 1976. Depth estimation of magnetic sources by means of Fourier Amplitude Spectral, *Geophysical Prospecting*, vol. 24, pp. 287-308.

Hisarlis, Z.M., 1995. Determination of the Curie point depths in Edremit-Sururluk region (Turkey), *Jeofisik*, vol. 1, No. 2, pp. 111-117.

Hisarlis, Z.M., 1996. Determination of the Curie point depths in Western Anatolia and related with the Geothermal Areas, PhD Thesis, Istanbul University, Turkey (Unpublished).

Horton, C.W., Hempkins and Hoffman, A.J., 1964. A statistical analysis of some aeromagnetic maps from the North Western Canadian Shield, *Geophysics*, vol. 29, pp. 582-601.

Hsieh, H.H., Chen, C.H. and Lin, P.Y., 2014. Curie point depth from spectral analysis of magnetic data in Taiwan, *Journal of Asian Earth Sciences*, vol. 99, pp. 26-33.

Huttrer, G.W., 2001. The status of World Geothermal Power Generation 1995-2000, *Geothermics*, vol. 30, pp. 7-27.

Ibrahim, A., Halil, I. and Ali, K., 2015. Curie Point Depth map of Turkey, *Geophysical Journal International*, vol. 162, No. 12, pp. 633-640.

Ikechukwu, I.O., Agbidi, D.C. and Olusola, O.B., 2015. Exploration and Application of geothermal energy in Nigeria, *International Journal of Scientific and Engineering Research*, vol. 6, No. 2, pp. 726-732.

Ikumbur, E.B., Onwuemesi, A.G., Anakwuba, E.K., Chinwuko, A.I., Usman, A.O. and Okonkwo, C.C., 2013. Spectral Analysis of Aeromagnetic Data over part of the Southern Bida basin, West-Central Nigeria, International Journal of Fundamental Physical Sciences, vol. 3, No. 2, pp. 27-31.

Inglis, D.R., 1955. Theories of the Earth's Magnetism, Revised Modern Physics, vol. 27, pp. 212-248.

Jessop, A.M., Hobart, M.A. and Schlater, J.G., 1976. The world heat flow data collection 1975, Geothermal services of Canada, Geothermal Services, vol. 50, pp. 55-77.

Jessop, A.M., 1990. Thermal Geophysics, Elsevier, Amsterdam, New York, USA, 306p.

Kasidi, S. and Ndatuwong, L.G., 2008. Spectral analysis of aeromagnetic data over Longuda Plateau and Environs, North-eastern Nigeria, *Continental Journal of Earth Sciences*, vol. 3, pp. 28-32.

Kasidi, S. and Nur, A., 2012. Curie depth Isotherm deduced from spectral analysis of magnetic data over Sarti and environs of North-Eastern Nigeria, *Scholarly Journal of Biotechnology*, vol. 1, pp. 49-56.

Kearey, P., Brook, S.M., Hill, I., 2002. An Introduction to Geophysical Exploration. Third Edition, Blackwell Scientific Publication, Oxford, 262p.

Keating, P.B., 1995. A simple technique to identify magnetic anomalies due to Kimberlite pipes, *Exploration and Mining Geology*, vol. 4, No. 2, pp.121-125.

Khalil, M.H., 2012. Magnetic, geo-electric, and groundwater and soil quality analysis over a landfill from a lead smelter, Cairo, Egypt, *Journal of Applied Geophysics*, vol. 86, pp. 146-159.

Kurowska, E. and Schoeneich, K., 2010. Geothermal exploration in Nigeria, Proceedings of World Geothermal Congress 2010, Bali, Indonesia, pp. 25-29.

Kutasov, I.M. and Eppelbaum, L.V., 2009. Estimation of geothermal gradients from single temperature log-field cases, *Journal of Geophysics and Engineering*, vol. 6, No. 2, pp. 131-135.

Kwaya, M.Y., Kurowska, E. and Arabi, A.S., 2016. Geothermal gradient and heat flow in the Nigeria Sector of the Chad Basin, Nigeria, Computational Water, *Energy and Environmental Engineering*, vol. 5, pp. 70-78.

Li, Y. and Devriese, S.G.R., 2009. Enhancement of magnetic data by stable downward continuation for UXO Applications, *Society of Exploration Geophysics*, Houston, pp. 1464-1468.

Li, Y., Devriese, S.G.R., Krahenbuhi, R.A. and Davis, K., 2013. Enhancement of magnetic data by stable downward continuation for UXO Applications, IEEE Transaction of Geophysical Rem. Sens. Vol. 51, section 6, pp. 3605-3614.

Likkason, O.K., 1993. Application of trend surface analysis of gravity data over the Middle Niger Basin, Nigeria, *Journal of Mining and Geology*, vol. 29, No. 2, pp.11-   19.

Lowrie, W., 1997. Fundamentals of Geophysics, Second Edition, Cambridge University Press, London, United Kingdom, 391p.

Lubimova, E.A., 1968. Thermal history of the Earth, In: The Earth's Crust and Upper Mantle, *American Geophysics*, vol. 13, pp. 63-77.

Lund, J., 2004. "100 Years of Geothermal Power Production", Geo-Heat Centre Quarterly Bulletin (Klamath Falls, Oregon: Oregon Institute of Technology), vol. 25, No. 3, pp. 11-19.

Lund, J.W. and Freeston, D., 2001. World-Wide direct uses of geothermal energy, *Geothermics*, vol. 30, pp. 29-68.

Maus, S. and Dimri, V.P., 1995. Potential field spectrum inversion for scaling geology, *Journal of Geophysical Research*, vol. 200, pp. 12605-12616.

Mishra, D.C. and Naidu, P.S., 1974. Two dimensional power spectrum and analysis of aeromagnetic fields, *Geothermal Prospect*, vol. 22, pp. 345-353.

Megwara, J.U., Udensi, E.E., Olasehinde, P.I., Daniyan, M.A. and Lawal, K.M., 2013. Geothermal and radioactive heat studies of parts of southern Bida basin, Nigeria and surrounding basement rocks, *International Journal of Basic and Applied Sciences*, vol. 2, No. 1, pp. 125-139.

Minty, B.R., 1997. Fundamentals of airborne gamma-ray spectrometry, *AGSO Journal of Australian Geology and Geophysics*, vol. 17, No.2, pp. 39-50.

Myers, K. and Bristow, C., 1989. Detailed Sedimentology and gamma-ray log characteristics of a Namurian Deltaic succession II: Gamma-ray logging, Geological Society, London, Spec. Publication, vol. 136, pp. 1-7.

Negi, J.G., Agrawal, P.K. and Rao, K.N.N., 1983. Three –Dimensional model of the Koyan area of Maharshaitra State, India, based on the spectral analysis of aeromagnetic data, *Geophysics*, vol. 48, No. 7, pp. 964-974.

NERC: Nigerian Electricity Regulatory Commission, 2014. http:// www.nercng.org/index.php/document-library (Accessed 15th July, 2015).

Nettleton, L.L., 1971. Elementary gravity and magnetics for geologists and seismologists, *Society of Exploration Geophysicists*, Monograph Series, vol. 1, 121p.

NGSA, 2009. Nigerian Geological Survey of Agency: Geology of the Benue Trough.

Nur, M.A., Onuoha, K.M. and Ofeogbu, C.O., 1994. Spectral analysis of aeromagnetic data over the Benue Trough, Nigeria, *Journal of Mining and Geology*, vol. 30, No. 2, pp. 211-217.

Nur, A., Ofeogbu, C.O. and Onuoha, K.M., 1999. Estimation of the depth to the Curie point Isotherm in the Upper Benue Trough, Nigeria, *Journal of Mining and Geology*, vol. 35, No. 1, pp. 53-60.

Nuri, D.M., Timur, U.Z., Mumtaz, H. and Naci, O., 2005. Curie Point Depth variations to Infer thermal structure of the Crust at the African-Eurasean Convergence Zone, SW Turkey, *Journal of Earth Planets Space*, vol. 57, No. 20, pp. 373-383.

Nwanchukwu, S.O., 1972. The tectonic evolution of the Southern portion of the Benue Trough, *Nigeria Geological Magazine*, vol. 109, No. 5, pp. 411- 419.

Nwachukwu, J.I., 1985. Petroleum Prospects of Benue Trough, Nigeria, American Association of Petroleum Geologists Bulletin 69, pp. 601-609.

Nwankwo, L.I., Olasehinde, P.I. and Akoshile, C.O., 2008. Spectral analysis of aeromagnetic anomalies of northern Nupe Basin, Central Nigeria, *Global Journal of Pure and Applied Sciences*, vol. 14, pp. 247-252.

Nwankwo, L.I., Olasehinde, P.I. and Akoshile, C.O., 2009. An attempt to estimate the Curie point Isotherm Depths in the Nupe Basin, West Central Nigeria, *Global Journal   of Pure and Applied Sciences*, vol. 15, pp. 427-433.

Nwankwo, C.N. and Ekine, A.S., 2009. Geothermal gradients in the Chad Basin, Nigeria, from bottom hole temperature logs, *International Journal of the Physical Sciences*, vol. 4, No. 12, pp. 777-783.

Nwankwo, L.I., Olasehinde, P.I. and Akoshile, C.O., 2011. Heat flow anomalies from the Spectral analysis of Airborne Magnetic data of Nupe Basin, Nigeria, *Asian Journal of Earth Sciences*, vol. 1, No. 1, pp. 1-6.

Nwankwo, L.I., 2015. Estimation of depths to the bottom of magnetic sources and ensuing geothermal parameters from aeromagnetic data of Upper Sokoto Basin,   Nigeria, *Geothermics*, vol. 54, pp. 76-81.

Nwankwo, L.I. and Shehu, A.T., 2015. Evaluation of Curie-point depths, geothermal gradients and near–surface heat flow from high-resolution aeromagnetic (HRAM) data of the entire Sokoto Basin, Nigeria, *Journal of Volcanology, Geothermal Research*, vol. 305, pp. 45-55.

Nwankwo, L.I. and Abayomi, J.S., 2017. Regional estimation of Curie-point depths and succeeding geothermal parameters from recently acquired high-resolution aeromagnetic data of the entire Bida Basin, North-Central Nigeria, *Geothermal Energy Science*, vol. 5, pp. 1-9.

Nwosu, O.B. and Onuba, L.N., 2013. Evaluation of the magnetic basement depth over parts of Middle Benue Trough, Nigeria by empirical depth Rule based on slope techniques using High Resolution Aeromagnetic Data, *International Journal of Scientific and Technology Research*, vol. 2, No. 11, pp. 19-29.

Nyabeze, P.K. and Gwavava, O., 2016. Investigating heat and magnetic source depths in the Soutpansberg Basin, South Africa: explore the Soutpansberg Basin Geothermal Field, *Nyabeze and Gwavava Geothermal Energy*, vol. 4, No. 8, pp. 1-20.

Obaje, N.G., Wehner, H., Hamza, H. and Scheeder, G., 2004. New Geothermal data from the Nigerian sector of the Chad Basin: Implications on hydrocarbon Prospectivity, *Journal of African Earth Sciences*, vol. 38, No.5, pp. 477- 487.

Obaje, N.G., 2009. Geology and Mineral Resources of Nigeria, Lecture Notes in Earth Sciences, Springer, Berlin Heidelberg.

Obande, G.E., Lawal, K.M., Ahmed, L.A., 2014. Spectral Analysis of Aeromagnetic data for geothermal investigation of Wikki Warm Spring, North-East Nigeria, *Geothermics*, vol. 50, pp. 85-90.

Ochieng, L., 2013. Overview of geothermal surface exploration methods, presented at short course VIII on exploration for geothermal resources, organised by UNU-GTP, GDC and Ken-Gen, at lake Naivasha, Kenya, October 31-November 22, 2013.

Odegard, M.E., and Berg, W., 1975. Gravity interpretation using Fourier integral, *Geophysics*, vol. 32, No. 4, pp. 1-4.

Offodile, M.E., 1976. The geology of Middle Benue Trough, Nigeria, Special volume of Paleontological Institute, University of Uppsala, vol. 4, pp. 1-66.

Offodile, M.E., 1980. A mineral survey of the cretaceous of the Benue Valley, Nigeria, *Cretaceous Resource*, vol.1, pp.101-124.

Offodile, M.E., 1989. A Review of the geology of the Cretaceous of the Benue Valley. In: Kogbe, C.A. (Ed), Geology of Nigeria (Second Revised Edition), Rock View Nigeria Limited, Jos, 538p.

Ofoegbu, C.O., 1984. Aeromagnetic anomalies over the Lower and Middle Benue Trough, *Nigerian Journal of Mining and Geology*, vol. 21, pp. 103-108.

Ofoegbu, C.O., 1985. Long wave magnetic anomaly and crustal structure underneath the Benue Trough and surrounding regions, *Nigerian Journal of Mining and Geology*, vol. 2, pp. 45-50.

Ofoegbu, C.O., 1988. An aeromagnetic study of part of the Upper Benue Trough, Nigeria, *Journal of African Earth Sciences*, vol. 7, pp. 77-90.

Ofoegbu, C.O. and Odigi, M.I., 1989. Basement structures and ore mineralization in the Benue Trough: Structure and Evolution (ed. Ofoegbu, C.O.), *Earth Evolution Science*, pp. 239-248.

Ofoegbu, C.O. and Onuoha, K.M., 1991. Analysis of magnetic data over the Abakiliki Anticlinorium of the Lower Benue Trough, Nigeria, *Marine and Petroleum Geology*, vol. 8, pp. 174-183.

Ofor, N. and Udensi, E.E., 2014. Determination of heat flow in the Sokoto Basin, Nigeria using Spectral Analysis of Aeromagnetic Data, *Journal of Natural Sciences Research*, vol. 4, No.6, pp. 83-93.

Okubo, Y., Graff, R.G., Hansen, R.O., Ogawa, K. and Tsu, H., 1985. Curie point depths of the Island of Kyushu and Surrounding areas, *Geophysics*, vol. 53, pp.481- 494.

Okubo, Y., Tsu, H. and Ogawa, K., 1989. Estimation of Curie point temperature and geothermal structure of Island Arcs of Japan, *Tectonophysics*, vol. 159, pp. 279-290.

Okubo, Y. and Matsunaga T., 1994. Curie point depth in North-East Japan and its correlation with regional thermal structure and seismicity, *Journal of Geophysical Research*, vol. 99, pp. 363-371.

Olade, M.A., 1975. Evolution of Nigeria's Benue Trough (Aulacogen): A tectonic model, *Geologic Magazine*, vol. 112, No. 6, pp. 575-583.

Olasehinde, P.I., 1991. A Spectral evaluation of the aeromagnetic anomaly map over part of the Nigerian Basement Complex, Unpublished PhD Thesis, University of Ilorin.

Olorunsola, K. And Aigbogun, C., 2017. Correlation and Mapping of geothermal and radioactive heat production from the Anambra Basin, Nigeria, *African Journal of Environmental Sciences and Technology*, vol.11, No. 10, pp. 517-531.

Olusola, O.B., 2014. A Review of Solar Chimney Technology: Its application to desert prone villages and regions in northern Nigeria, *International Journal of Scientific and Engineering Research*, vol. 5, No. 12, pp. 1210-1216.

Omanga, U.S.A., Abaa, S.I. and Najime T., 2001. Radiometric determination of the source of heat of Wikki spring in Yankari, Bauchi State of Nigeria, *Nigerian Journal of Pure and Applied Sciences*, vol. 1, pp. 70-71.

Onuba, L.O., Chinwuko, A.I., Onwuemesi, A.G., Anakwuba, E.K. and Nwokeaba, N.C., 2012. Interpretation of aeromagnetic anomalies over parts of Upper Benue Trough

and Southern Chad basin, Nigeria, *Advances in Applied Science Research*, vol. 3, pp. 1757-1766.

Onwuemesi, A.G., 1997. One-dimensional spectral analysis of aeromagnetic anomalies and Curie depth isotherm in the Anambra Basin of Nigeria, *Journal of Geodynamics*, vol. 23, No. 2, pp. 95-107.

Osazuwa, I.B., Ajakaiye, D.E. and Verheijen, P.J.T., 1981. Analysis of the structure of part of the Upper Benue Rift Valley on the basis of new geophysical data, *Earth Evolution Sciences*, vol. 2, pp. 126-133.

Pal, P.G., Khurana, K.K. and Unnikrishnan, P., 1978. Two examples of spectral approach to source depth estimation in gravity and magnetic, *Pure and Applied Geophysics*, vol. 117, No. 4, pp. 772-783.

Ravat, D., Pignatelli, A., Nicolosi,I. And Chiappini, M., 2007. A study of spectral methods of estimating the depth to the bottom of magnetic sources from near–surface magnetic anomaly data, *International Journal of Geophysics*, vol. 169, pp. 42-434.

Reeve, W.D., 2010. Geomagnetism Tutorial, Reeve Observatory Anchorage, Alaska, U.S.A., 35p.

Reeves, C.V., 1989. Aeromagnetic interpretation and rock magnetism. First Break, vol. 7, pp. 275-286.

Reeves, C.V., 2005. Aeromagnetic Surveys: Principles, Practice and Interpretation, Geosoft Publication, Earthworks, 155p.

Reeves, C., Reford, S. and Millingan, P., 1997. Airborne geophysics: Old methods, new images. In A. Gubins (Ed.), Proceedings of the Fourth Decennial International Conference on Mineral Exploration, Australia, pp. 13-30.

Remke, L., Jan, M.H., Bruce, H., Brian, B., David, N., Samuel, N., Chris, J., Patrick, N., Robert, N., David, V., Lucas C. and Simms, J.E., 2004. Spatial Variability of magnetic soil properties, The International Society for Optical Engineering, vol. 5415, Part 1, pp. 665-675.

REPP Mission, 2010: http://www.repp.org/geothermal-brief-geothermal-resources.html (Accessed: 15th July, 2018).

Reynolds, L.R., Rosebaum, J.G.. Hudson, M.R. and Fishman, N.S., 1990. Rock magnetism, the distribution of magnetic minerals in the earth crust and aeromagnetic anomalies, U.S. Geological Survey. Bulletin 1924, pp. 24-45.

Reynolds, J.M., 1997. An Introduction to Applied and Environmental Geophysics, John Wiley and Sons Limited, Bans Lane, Chichester, pp. 124-132.

Reynolds, J.M., 2011. An Introduction to Applied and Environmental Geophysics, Second Edition, Wiley-Blackwell, West Sussex, 696p.

Richardson, K.A. and Killeen, P.G., 1980. Regional radiometric heat production mapping by airborne gamma-ray spectrometry, in Current Research, Part B, Geological Survey of Canada, Paper 80-1B, pp. 227-232.

Rivas, J., 2009. Gravity and Magnetic Methods, jarivas@loger.com.sv.

Rybach,L. and Schwarz, G.F., 1995. Ground gamma radiation maps: Processing of airborne, Laboratory, and in situ spectrometry data, *First Break*, vol. 13, pp. 97-104.

Saibi, H, Aboud, E. and Azizi, M., 2015. Curie point depth map for Western Afghanistan deduced from the analysis of aeromagnetic data, Proceedings World Geothermal Congress 2015, Melbourne, Australia, pp.19-25.

Salako, K. A., 2014. Depth to Basement Determination Using Source Parameter Imaging (SPI) of Aeromagnetic Data: An Application to Upper Benue Trough and Borno Basin, Northeast, Nigeria, Academic Research International, vol. 5, No. 3, pp. 74-86.

Salem, A., Ushijima, K., Elshiraft, A. And Mizunaga, H., 2000. Spectral analysis of aeromagnetic data for geothermal reconnaissance of Quseir area, Northern Red Sea, Egypt. In: Proceedings of the World Geothermal Congress, Tohoku, Japan, pp. 1669-1674.

Salem, A. and Fairhead, D., 2011. Geothermal reconnaissance of Gebel Duwi Area, Northern Red Sea, Egypt, using airborne magnetic and spectral gamma ray data, Getech, pp. 1-22.

Salem, A., Abouelhoda, E.A., Aref, A.I., Sachio, E. and Keisuke, U., 2005. Mapping radiometric heat production from airborne spectral gamma-ray data of Gebel Duwi

Area, Egypt, Proceedings of World Geothermal Congress, 2005, Antalya, Turkey, pp. 24-29.

Sanderson, D., East, B., and Scott, E., 1989. Aerial radiometric surveys of parts of North Wales in July 1989, Scottish Universities Research and Reactor Centre, Glasgow, United Kingdom.

Sedara, S.O. and Joshua, E.O., 2013. Evaluation of the Existing State of Geothermal Exploration and Development in Nigeria, *Journal of Advances in Physics*, vol. 2, No. 2, pp. 118-123.

Selemo, A.O.I. and Akaolisa, C.Z., 2010. Tectonic features interpreted from aeromagnetic maps of Okigwe-Oguta Axis, South of Benue Trough, Nigeria, *International Journal of the Physical Sciences*, vol. 5, No. 16, pp. 2450-2457.

Sheriff, R.E., 2002. Encyclopaedic Dictionary of Applied Geophysics, Fourth Edition, No. 13, Geophysical Reference Series, Society of Exploration Geophysicists, Tulsa, U.S.A., 429p.

Spector, A. and Grant, F.S., 1970. Statistical models for interpreting aeromagnetic data, *Geophysics*, vol. 35, pp. 293-302.

Stacey, F.D. and Loper, D.E., 1988. Thermal history of the earth: A corollary concerning non-linear mantle rheology, *Physics of the Earth Planet International*, vol. 53, pp. 167-174.

Stampolidis, A. and Tsokas, G.N., 2002. Curie point depths of Macedonia and Thrace, Northern Greece, *Pure and Applied Geophysics*, vol. 159, pp. 1-13.

Stampolidis, A., Kane, I., Tsokas, G.N. and Tsourlos, P., 2005. Curie point depths of Albania inferred from ground total field magnetic data, *Surveys in Geophysics*, vol. 26,   pp. 461-480.

Tanaka, A.Y., Okubo, Y. and Matsubayashi, O., 1999. Curie point depth based on spectrum analysis of the magnetic anomaly data in East and Southeast Asia, *Tectonophysics*, vol. 396, pp. 461-470.

Telford, W.M., Geldart, I.P. and Sheriff, R.E., 1990. Applied Geophysics, Second Edition, Springer, Berlin, 770p.

Thompson, P.H., Judge, A.S., Charbonneau, B.W., Carson, J.M. and Thomas, M.D., 1996. Thermal Regimes and Diamond Stability in the Archean Slave Province, North-western Canadian Shield, District of Mackenzie, North West Territories, in Current Research, 96-1E, Geological Survey of Canada, pp. 135-146.

Thorarinsson, F., Magnsson, S.G. and Bjornsson, A., 1998. Directional spectral analysis and filtering of geophysical maps, *Geophysics*, vol. 53, No. 12, pp. 1587-1591.

Tiwari, G.N. and Ghosal, M.K., 2005. Renewable Energy Resources: Basic Principles and Application, Alpha Science International Ltd, Oxford, United Kingdom, 649p.

Tselentis, G.A., 1991. An attempt to define Curie Depth in Greece from Aeromagnetic and Heat Flow Data, *Pageoph*, vol. 136, No. 1, pp. 87-101.

Udensi, E.E. and Osazua, I.B., 2004. Spectral determination of depth to buried magnetic rocks under the Nupe Basin, Nigeria, Nigeria Association of Petroleum Explorationists, Bulletin, vol. 17, No. 1, pp. 22-27.

Umeanoh, D.C., 2015. Structural interpretation of aeromagnetic data over parts of Lower Benue Trough, Nigeria, MSc Thesis, University of Port-Harcourt, Nigeria (Unpublished).

Urquhart, E.E.S., 1988. Airborne gamma-ray Spectrometer Surveys, Paper Presented at The 55th Annual Meeting of SEG, Anaheim, October, 1988.

Uysal, T., 2009. Tracing the origin of heat anomalies in hot sedimentary aquifer system in Australia. http://Geothermalenergy centre of excellence.org (Accessed: 14th October, 2014).

Wemegah, D., Menyeh, B. and Danuor, S., 2009. Magnetic Susceptibility Characterization of Mineralized and Non-mineralized rocks of the Subenso Concession of Newmont, Ghana Gold Limited, Ghana Science Association Biennial Conference, Accra, University of Cape Coast, 4th-9th July, 2009.

World Energy Council (WEC), 2014. Benchmarking the sustainability of national energy systems, Energy Trilemma Index, World Energy Council, London, United Kingdom, 155p. http://www.worldenergy.org/data/trilemma-index/country/Nigeria/2014 (Accessed: 20th June, 2015).

Wright, J.B., 1981. Review of origins and evolution of the Benue Trough in Nigeria, *Earth Evolution Science*, vol. 2, pp. 98-103.

Wright, J.B., 1989. Volcanic rocks in Nigeria. In: Kogbe, C.A. (Ed.), Geology of Nigeria, Second Revised Edition, Rock View Nigeria Limited, Jos, pp. 125-174.

Yamano, M., 1995. Recent heat flow studies in and around Japan. In: Gupta, M.L. and Yamano, M. (eds), Terrestrial Heat Flow and Geothermal Energy in Asia, A.A. Balkema, Rotterdam, pp. 173–200.

Zaborski, P., Ugodulunwa, F., Idornigie, A., Nnabo, P. and Ibe, K., 1997. Stratigraphy and structure of the Cretaceous Gongola basin, Northeast Nigeria, *Bulletin du Centre de Recherches* Elf Exploration Production, vol. 21, No. 1, pp. 153-185.

Zira, A.M., 2013. Challenges and prospects of geophysical exploration of geothermal system for National Development, *Academic Journal of Interdisciplinary Studies*, MCSER Publishing, Rome, Italy, vol. 2, No. 12, pp. 137-143.